Integrated Sulphate Removal from Ion Exchange Brine Using Chemical Precipitation and Ceramic Nanofiltration

Master Thesis

Floriana Ayumurti Kukuh

Water Management
Faculty of Civil Engineering and Geoscience
TU Deft

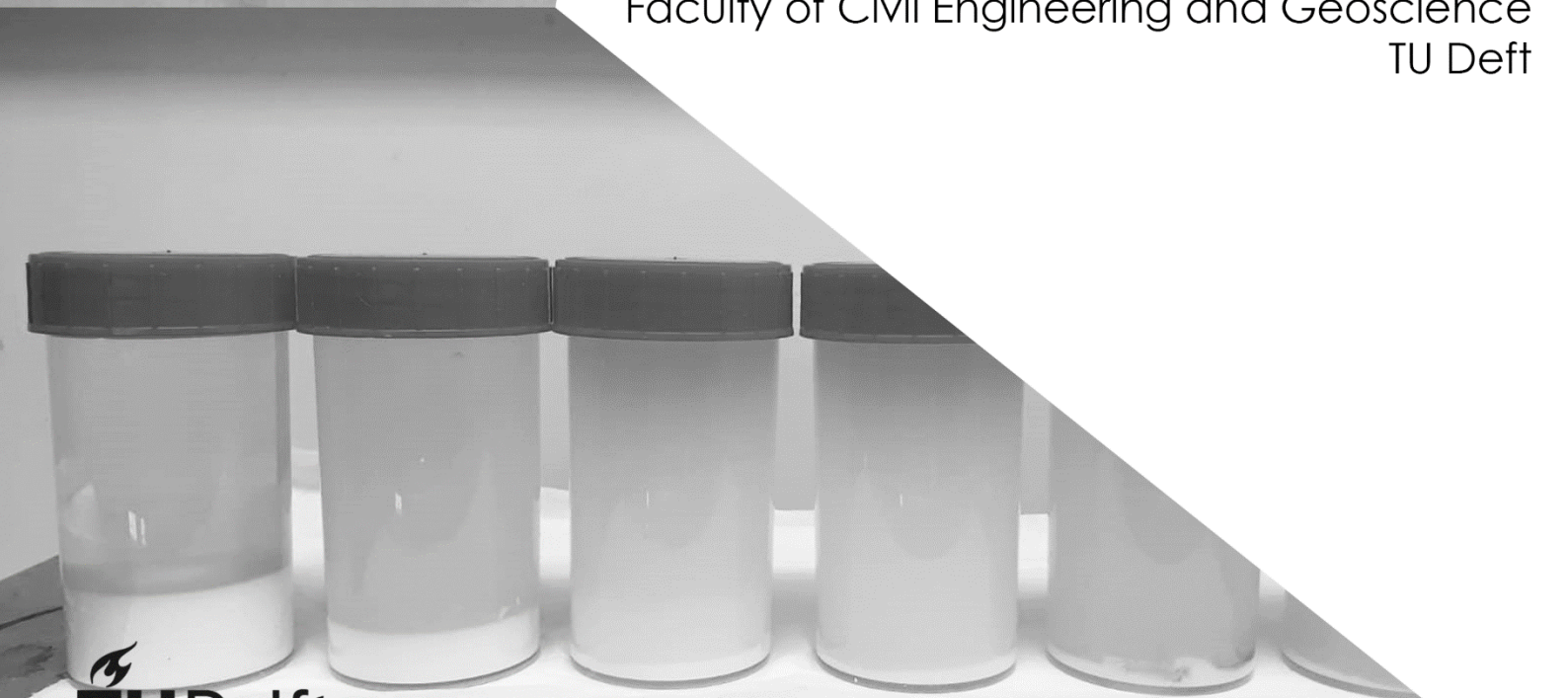

TU Delft

Integrated Sulphate Removal from Ion Exchange Brine Using Chemical Precipitation and Ceramic Nanofiltration

By

Floriana Ayumurti Kukuh

in partial fulfilment of the requirements for the degree of

Master of Science
in Civil Engineering

at the Delft University of Technology,
to be defended publicly on August 27, 2019 at 10:00

Thesis committee:	Prof. dr. ir. L.C. Rietveld	TU Delft
	Dr. ir. S.G.J. Heijman	TU Delft
	Dr. ir. Ralph Lindeboom	TU Delft
	Ir. Irene Caltran	TU Delft

TU Delft

Preface

This master thesis is a remark of my 2 years of master education in Water Management of TU Delft which full of challenges. Three years ago, I decided to pursue a higher education in TU Delft because of my deep interest in water treatment and the Netherlands has been well known for long time as the expert in water management. That decision was the best decision to make, that every experience during the educational period in TU Delft has brought me to the higher standards of myself. I would like to appreciate all the people who has support me to go through for these past 2 years.

For the last eight months, I was drowned into the intensive laboratory research on combination of chemical precipitation and ceramic nanofiltration, which was a new field for me. Often, I met some confusion and frustration moments during the research, but I always got the light from my thesis committee. Therefore, I would like to gratitude their guidance and support.

First, to Luuk Rietveld as the committee chairman, who always gave me a lot of constructive feedback and guided me to improve the report. Bas Heijman, who shared his ideas and knowledge to assist, guide, and supervise my experiment and analysis. Irene Caltran as my daily supervisor, who introduce me to the project, thank you for all the support and assistance to arrange the experiment set-ups and improving my analysis, also for always listening to my story during the research. Ralph Lindeboom who gave me fruitful insight to improve my analysis of the result of my experiments.

I would also like to thank my friends from Hydraulic Engineering: Felix, Ryan, Catra, and Acha whom I have passed all the shine or rain of my thesis and life with. Also, Fajar, who always willing to discuss my thesis even though we are million kilometres away. Cristo, who always listened and gave me supports from Germany. Sasongko and Bela, who assisted me for all the presentations I had to prepare. Pandji and Grace Kastanya, where I can share my frustration on bad experiment results and clueless moments during my thesis. Lastly, I would like to give the biggest gratitude to my parents and family who encouraged me to come to TU Delft and always give endless supports and prays for my success.

Floriana Ayumurti Kukuh

Delft, August 2019

Abstract

In drinking water production, natural organic matter (NOM) is sometimes removed using ion exchange (IEX) resin. This treatment method has a limitation based on the exchanging capacity on the resin. Therefore, the resin needs to be regenerated when it is saturated with adsorbed NOM which leads to the production of brine. In general, NaCl is used to regenerate the resin, hence, the brine will contain NOM, high sodium and chloride concentrations. Moreover, some other anions are also found in the IEX brine, such as sulphate that is usually present in surface water and ground water. Because of its salinity, the disposal of IEX brine is not possible to be done conventionally due to its impact on the environment and high cost. Therefore, separating chloride from the brine is an interesting alternative that can be reused for the regeneration of the IEX in the later process.

Ceramic nanofiltration (NF) emerges to be an interesting alternative for water treatment. Compared to polymeric membranes, this type of membrane offers great mechanical robustness and can be operated under extreme conditions, and tolerates high-pressure backwash, chemical cleaning, and high-temperature sterilization, which leads to longer periods of reliable performance. Moreover, ceramic NF membranes are potentially capable to separate multivalent ions from monovalent ions. Hence, this method could be applicable to treat IEX brine. Alternatively, chemical precipitation using barium and calcium is widely used to remove sulphate from water which is more straight forward than membrane filtration. The precipitates can be mechanically separated from the supernatant for further treatment or use.

Combination of chemical precipitation and ceramic NF membrane (later called as integrated sulphate removal) was investigated to remove sulphate from IEX brine. Along with that, investigation using synthetic brines consisting of Na_2SO_4 and NaCl for a binary salt solution and only Na_2SO_4 for a single salt solution was also conducted to build the understanding in treating the IEX brine. Barium salt was proved to efficiently remove sulphate due to its very low solubility. However, calcium salt was not as effective as barium salt. The treatment was followed by NF using a ceramic membrane with MWCO of 900 Da. In the end, the integrated approach was able to remove 86% of the sulphate and 85% of NOM from IEX brine. Furthermore, the precipitation stage was also modelled in PhreeqC by using Pitzer database.

Barium salt ($BaCl_2.2H_2O$) was preferred in this research for precipitating the sulphate. However, due to its toxicity, alternative precipitation was desired. Ettringite (calcium sulfoaluminate) precipitation was considered since the involving salts were not toxic. The efficacy of this method was predicted through modelling in PhreeqC to give some insight to alternatively removing sulphate from IEX brine. Eventually, a comparison using cost estimation and Life Cycle Assessment (LCA) were performed to obtain some considerations to implement the treatment alternative in a full-scale application.

Content

List of Figures

List of Tables

1 Introduction

1.1 Natural Organic Matter Treatment Using Ion Exchange

In drinking water production, usually fresh surface water and/or ground water are used as the water source. The quality of the water source determines the required treatment processes to produce water that complies with drinking water standards. Surface water quality is determined by the topography and vegetation of the catchment area so that minerals, organic material, salt, and other soluble substances are taken into the solution (Shammas & Wang, 2016). Whilst, many processes affect the quality of the ground water, such as rainwater composition, evaporation and transpiration, oxidation/reduction processes and dissolution of minerals (Appelo & Postma, 2010).

Natural organic matter (NOM) is naturally present in the water sources because it originates from microbial exudate, animal waste, and products of degraded tissue (Hendricks, 2006). The concentration of NOM is increasing in many surface waters, which are used as the source for drinking water production and affect the treatment process due to higher organic load (Finkbeiner, et al., 2018). The removal of NOM in drinking water production is crucial since it is responsible for e.g. the color of water (Hendricks, 2006) and biological instability in the drinking water network (Croué, et al., 1999; Hendricks, 2006). Ion exchange (IEX) is considered to be able to remove NOM effectively (Croué, et al., 1999), since the majority of NOM carry a charge (Finkbeiner, et al., 2018; Galjaard & Koreman, 2015). These organic compounds are exchanged with a counter ion, commonly chloride, from the resin surface (Finkbeiner, et al., 2018).

The resin of IEX has the capacity to replace the original ions by the adsorbed ions. Further, this capacity decreases during the operation, therefore the resin needs to be regenerated periodically using concentrated salt. However, the regeneration process, using salt, leads to brine production (Galjaard & Koreman, 2015). Frequently, NaCl is used to regenerate the anion IEX resin (Shammas & Wang, 2016). Hence, in this case, the brine will contain NOM, high sodium and chloride concentrations. Moreover, some other anions are also found in the IEX brine, such as sulphate, nitrate and bicarbonate. This is because the surface water and ground water also contain these anions (Calmon, 1986; Appelo & Postma, 2010) that are also removed by IEX.

Because of high concentration of desorbed salts and NOM, the disposal of IEX brine is not possible to be done conventionally which will lead to high costs for large volume disposal (Vaudevire, et al., 2012) and harmful impact to the environment (Salehi, et al., 2011). Improper disposal of waste brine can result in ground water pollution, damaging agriculture due to airborne deposition, harm the municipal sewage effluent by increasing the dissolved solids' content (Almasri, et al., 2015). Usually, brines are preferred to be disposed to the sea through a pipeline if the treatment plant is located on a coastal area (Vaudevire, et al., 2012). However, this disposal way is not always economical. Therefore, a good management in treating the brine is needed. The option of salt (chloride) recovery from the regenerant brine is interesting in order to minimise the disposal of waste brine. The recovered chloride can be reused as IEX regenerant in a later regeneration process.

1.2 Brine Treatment Technologies

To recover the desorbed chloride ions from the anion IEX brine, these adsorbed anions and NOM are required to be separated from the IEX brine. Separating monovalent ions from multivalent ions is still a recurrent problem in industrial application, especially when the salinity is the crucial parameter (van der Bruggen, et al., 2004). NF becomes important in industrial application as it is widely used in several fields, for example water softening, pharmaceutic synthesis, and water purification (Chen, et al., 2017). A previous study had found that NF membranes are capable to reject up to more than 90% of sulphate, while chloride is able to pass the membrane (Krieg, et al., 2004). Also, NF is able to reject organic solutes in aqueous solution with molecular weigth between 100 and 1000 Da (Salehi, et al., 2011). These NF capabilities are beneficial for the purpose of the recovering of chloride ions from the IEX brine.

There are two types of membrane based on the materials: polymeric (e.g. polyamide and polysulphone) and inorganic membranes (e.g. ceramic, zeolite) (Singh & Hankins, 2016). Ceramic membranes emerge to be an interesting treatment technology for drinking water and industrial water treatment (Metcalfe, et al., 2016). This type of membrane offers great advantages over polymeric membranes, which are mechanical robust (high pressure backwash and sterilization at high temperature), and can be chemically cleaned which gives longer periods of reliable performance (Lee, et al., 2015; Metcalfe, et al., 2016; Shang, et al., 2014).

The interaction between the ions and ion rejection on NF membranes are predicted based on electrostatic repulsion, size exclusion, and Donnan exclusion on the membrane surface (Salehi, et al., 2011). Furthermore, the rejection of ions on the membrane is a function of concentration. According to a previous study by He, et al. (2009), the rejection of NaCl and Na_2SO_4 decreased as the concentration of the salt increased. The increase of salt permeation is related to the weakened electrostatic interaction between the dissolved ions and membrane charge (He, et al., 2009). Therefore, the use of a NF membrane alone might not be sufficient to obtain salt with the desired purity when the brine has a very high salinity.

Alternatively, applying a conventional chemical precipitation is considered to enhance the sulphate removal. Addition of barium or calcium salts are the other options in removing soluble sulphate from water. $BaSO_4$ (barite) will be formed by reacting SO_4^{2-} ions with barium salt due to its extremely low solubility (Akinwekomi, et al., 2017), while, in the presence of excess Ca^{2+} ion, sulphate will form $CaSO_4$ precipitate (Benatti, et al., 2009). Compared to membrane filtration, this treatment method is more straightforward. Once the solid precipitate is formed, it can be mechanically separated from the supernatant.

Similar to ion rejection of NF, the precipitation of sulphate using barium and calcium salts are affected by other dissolved consistuent in water. Ionic strength is proven to have an effect in $BaSO_4$ precipitation by changing the solubility of the mineral (Ronquim, et al., 2018). Besides, organic matter present in the water might also have a profound effect to inhibit the precipitation (Boerlage, et al., 2000). However, precipitation using barium and calcuim salts are insensitive to pH (MacAdam & Jarvis, 2015) so that it can avoid the change of ionic composition in water due to pH adjustment prior to the precipitation.

1.3 Problem Statement

Considering the harmful effect of improper brine disposal, minimizing the volume of the brine is preferred. Therefore, salt recovery is a possible way to limit the waste volume. To recover a clean solution with the regeneration salt (NaCl), the other salts and the NOM needs to be removed from the brine. In particular, Na_2SO_4 is present in the waste brine. NF membranes are expected to be able to separate monovalent ions (e.g., Cl^-) and divalent ions (e.g., SO_4^{2-}) in low ionic strength solutions. This capability is important to ensure the purity of the recovered salts. Furthermore, ceramic NF membrane is chosen for ion separation over polymeric membranes due to its advantages. With its properties, the ceramic NF membrane is expected to be able to avoid membrane fouling and have a longer reliable performance. However, the ion rejection performance of ceramic NF depends on the ionic strength of the brine. A previous study found that ceramic membranes are uncharged in a high ionic strength environment, whilst, it is found to be negatively charged in common conditions (Feng, 2018). As the membrane is uncharged, the electrostatic repulsion on the membrane surface is no longer available and the ions can pass through the membrane. Consequently, the sulphate rejection is significantly decreased in treating high ionic strength brine.

Salt recovery desires a high purity of the salt, in this case the salt is sodium chloride, for the purpose of salt reuse. In order to reach a high purity of sodium chloride from the brine, good sulphate removal is required. As a result of the membrane limitation in treating high ionic strength solution, an additional step is needed prior to ceramic NF, so that the sulphate concentration has been lowered in the beginning of the filtration process. Chemical precipitation is one of the alternatives to enhance the removal of sulphate. The combined methods of chemical precipitation and ceramic NF membrane is expected to have a synergetic effect in removing sulphate from the brine.

1.4 Research Objectives

In an attempt to minimise the waste brine disposal, salt recovery is preferred to be applied for the purpose of reuse. Due to the purpose of brine treatment, the recovered salts need to have a high purity that leads to the formulation of the objective as:

"Removal of sulphate from IEX brine using the treatment combination of chemical precipitation and ceramic NF, aiming for 95% removal"

1.5 Research Questions

To achieve the objective of this research, several research questions and methods to answer the questions were constructed as follows:

1. What are the effects of ionic strength on sulphate rejection on ceramic NF membrane?

   Method: NF process without chemical precipitation was conducted by using brines with different ionic strengths. The composition of contributing salts were varied (single/binary salt solution) in the same ionic strength.

2. To what extent the barium salts and calcium salts are able to remove sulphate from the brine through chemical precipitation?

   Method: A model was built prior to the chemical precipitation experiment with the designated experimental setup. Synthetic brines with different ionic strength and NOM-rich IEX brine were used to perform the experiment. The dosage of barium and calcium salt were adjusted from the results of the modelling.

3. What is the result of the application of chemical precipitation and ceramic NF membrane on the NOM-rich IEX brine?

   Method: Synthetic brines with different ionic strength and NOM-rich IEX brine were used to investigate the synergic of combined treatment.

4. How can calcium salts precipitation for sulphate removal be improved?

   Method: Further modelling in PhreeqC will be performed to improve the precipitation using calcium salt through ettringite precipitation

5. How large are the cost and the environemntal impact in implementing the sulphate removal methods?

   Method: Cost estimation and environmental impact assessment using LCA are used to consider the implementation of the treatment methods.

To answer the research questions, this research is structured into several steps:

1. Literature review
   Background theories from various literatures were reviewed to understand ceramic NF membrane, ion rejection mechanisms of NF membranes, and chemical precipitation. These theories were summarised in chapter 2.

2. Experimental design
   Laboratory experiments were designed considering the knowledge that has been found during the literature review stage. The experiments were divided into three parts: ceramic NF membranes characterisation (including the ability of ceramic NF membrane to remove ions from brine), batch-chemical precipitation, and combined treatment of chemical precipitation and ceramic NF. The methodologies and procedures of conducting each experiment are described in chapter 3.

3. Modelling of sulphate precipitation
   Estimations on sulphate removal using precipitation were modelled in PhreeqC. The results were made as the reference to perform the laboratory experiment for chemical precipitation. At the end, the model was used to create a new alternative by improving the removal of sulphate using additional precipitation step. The setup of the model are explained in chapter 3, while the improvements of the precipitation process are described in chapter 6.

4. Sulphate removal experiments
   Experiments were conducted based on the methodologies and procedures that are explained in chapter 3. Salt rejection experiments with nanofiltration were conducted under constant flux operation. Whilst, the chemical precipitation experiments were

performed with batch tests using stoichiometric dosage of barium and/or calcium salts. In the end, the combination of nanofiltration and chemical precipitation was tested on the NOM-rich brine to investigate the efficacy of both treatment methods in removing sulphate from IEX brine. During these experiments, various parameters were observed. The results of the experiments are shown in chapter 4.

5. Cost estimation and environmental impact assessment
   After obtaining the experiment results and modelling results for sulphate removal improvement, some considerations are made to predict the implementation of the treatment in the real practice. The suggestions for the implementation of the treatment method are described in chapter 6.

6. Analyses
   The result of integrated treatment methods were analysed based on the variables that were set in the experiment design stage. From this analysis, evaluations were made to conclude the feasibility of combination treatment methods (chemical precipitation and ceramic NF) in removing sulphate from the brine. Some recommendations were also suggested for experiment in the future to have a better picture on the experiment which are presented in chapter 4 through chapter 6.

2 Background Theory

2.1 Ceramic membranes

2.1.1 Ceramic filtration in water treatment

Ceramic membrane filtration was used the first time in the 1940s and it has been developing for the last two decades (Gitis & Gadi, 2016). Ceramic membranes are usually made from inorganic materials, for example aluminum oxide (Al_2O_3), zirconium oxide (ZrO_3) or titanium oxide (TiO_2); these inorganic materials are resistant to mechanical, chemical, and thermal stress, also have a high porosity and a hydrophilic surface (Qiu, et al., 2017). Due to their chemical, mechanical, and thermal properties, ceramic membranes can be used for application under harsh and extreme operating conditions (Song, et al., 2016) and offer a reability on performance over long periods of time (Lee, et al., 2015; Qiu, et al., 2017).

In the field of liquid treatment, the microfiltration (MF, pore size 50 nm-1µm), ultrafiltration (UF, pore size 2-50 nm), and nanofiltration (NF, pore size less than 2 nm) are the most application of the ceramic membrane (Qiu, et al., 2017). Among those types of membrane, according to (Weber, et al., 2003), ceramic NF has proven to successfully treat various waste stream in a full scale (Shang, et al., 2017). Typically, the ceramic NF membranes have a molecular weight cut-off between 200 and 1000 Dalton (Da). The sol-gel method is used for the fabrication of ceramic NF membrane because through this method, the separation precision of membrane layers can be controlled by adjusting the colloid particles size in sols (Qiu, et al., 2017). Ceramic NF membranes are further divided into tight ceramic NF membrane, with MWCO less than 400 Da, and loose ceramic NF membrane, with MWCO higher than 400 Da. The later type of ceramic NF membrane is the majority of commercially available membrane (Shang, et al., 2017). In the operation, the performance of ceramic membrane is greatly dependent on its micro structural properties, material properties, and operational parameters (Qiu, et al., 2017).

The micro structural properties of the ceramic membrane, according to Qiu, et al. (2017), are determined by average pore size, pore size distribution, membrane thickness, porosity, pore shape, and tortuosity. All of the abovementioned parameters affect the permeability, flux, and separation performance of the ceramic membrane. The permeability is mainly affected by pore size, pore size distribution, and membrane thickness. If the thickness of the membrane increases, the permeability will decrease due to longer transport path of the liquid.

Looking from the material of the membranes, the properties of the common materials that compose ceramic membrane, namely alumina, zirconia, titania give different advantages for the membrane: high thermal and electrical resistance, stable separation performances at high temperature, and excellent chemical resistance in a broad pH range (da Silva Biron, et al., 2018).

In addition, operational parameters and the properties of the solution, such as the properties of the solution (i.e. pressure, pH, and temperature) can affect the performance of ceramic membrane. The pH of the solution can affect the charge of membrane surface, while a higher temperature tends to increase the solubility of the solution, which might increase the permeate flux (Qiu, et al., 2017).

2.1.2 Membrane characterization

Ceramic membranes are produced with specific properties from the manufacturer that are adjusted to the specific application. However, membrane characterization is still an important step to compare the information from the manufacturer and the information gathered for research. This step is useful to choose the suitable membrane for certain application and to give better understanding on the selectivity and fouling mechanisms (Causserand & Aimar, 2010).

The characterization is divided into two main aspects, which are physical and chemical aspects. The physical aspect includes the membrane morphology, pore structure, mechanical strength, and charge, while the chemical aspect considers the membrane surface layers and its composition (Gitis & Gadi, 2016). There are many methods available to perform ceramic membrane characterization. Gitis & Gadi (2016) summaries the methods into five sections:

1) Pore size and pore size distribution detection
2) Microscopy methods for membrane surface images
3) Chemical methods using radiation and vibrational spectroscopy
4) Physical methods for characterizing porosity, tortuosity, surface roughness and mechanical strength
5) Other methods to characterize the hydrophilicity and surface charge

For ceramic membranes, permeability and selectivity are the most important characteristics because they give the information on the expected permeate flow and the size of rejected molecules (Causserand & Aimar, 2010). In terms of retention, the pore size and the pore size distribution determine the performance of a ceramic membrane (Combe, et al., 1997; Gitis & Gadi, 2016). Moreover, pore size and pore size distribution can be analysed in many ways. Permeability and tracer retention techniques are two common ways use in practice.

Permeability is defined as the quantity of mass or volume of fluid which goes through the membrane (da Silva Biron, et al., 2018). This parameter is simple, yet the test can give a comprehensive overview regarding the membrane feature (Gitis & Gadi, 2016). The test will give the membrane initial permeability, which is crucial to be taken as the reference to the possibility of fouling occurrence on the membrane. Later, the membrane permeability during the operation can be compared with the initial permeability and the determination whether the membrane needs to be cleaned can be made. In addition, other membrane characteristics such as pore tortuosity, porosity, and amount of effective pores can be predicted because they play a role in determining the permeability (da Silva Biron, et al., 2018). On the other hand, temperature during the permeability test is important because the key parameter for permeability is liquid viscosity (Marchetti, et al., 2012) which is affected by temperature (Causserand & Aimar, 2010).

Tracer retention techniques use macromolecules or calibrated particles (tracers). The principle of this method is to measure the retention of the tracers to obtain a graph between selectivity and molar mass/size of the tracer molecule (Causserand & Aimar, 2010). Based on Gitis & Gadi (2016), the choice of the type of tracers depends on the tested membrane, required result, test frequency, test sensitivity, tracer availability, and testing equipment. Organics (i.e. organic acids, polysaccharides, polyethylene glycols), gases (i.e. oxygen and nitrogen), and ions (i.e. Na^{+}, Mg^{2+}, and Ca^{2+}) are the popular tracers (Gitis & Gadi, 2016). Furthermore, characterisation using polyethylene glycols (PEG) is widely chosen since it is a very reliable and easily reproducible method (Puhlfürβ, et al., 2000).

The selectivity of the membrane is represented as molecular weight cut off (MWCO). The MWCO represents the 90% retention of the tracers according to the molecular mass selectivity, as indicated in Figure 2.1 as the example. The correlation between the solute/tracer retention and radius of the tracer molecules gives the pore size distribution of the membrane. A log normal distribution is the most frequently chosen approach in determining the MWCO (Causserand &

Aimar, 2010; Pera-Titus & Llorens, 2007), based on the retention and molecular mass relationship. Because of this relationship, the unit for MWCO is expressed as Dalton (Da). Nevertheless, this method underestimates the enlarged pore sizes and potential cracks or gaps on the membrane (Kramer, et al., 2019).

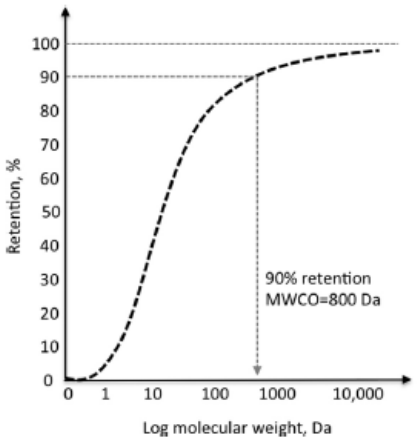

Figure 2.1. Retention graph indicating membrane MWCO (Gitis & Gadi, 2016)

2.1.3 Separation mechanisms of ceramic NF membrane

NF is a pressure driven filtration because it uses pressure as the applied driving force to transfer the fluid to the permeate side (Gitis & Gadi, 2016). The separation on ceramic membrane indicates similar behavior to the polymeric membrane (Puhlfürβ, et al., 2000). Therefore, transport mechanisms of molecules within the solution through the ceramic membrane can be explained by the mechanisms on polymeric NF membranes. Size exclusion and electrostatic effect (charge effect) are the major mechanisms for ion separation on ceramic NF membrane (Chen, et al., 2017; Ortiz-Albo, et al., 2019). Also, dielectric exclusion is found to contribute in separation process in NF (Lanteri, et al., 2009), as well as diffusion and convection (Ortiz-Albo, et al., 2019) and hydration (Tansel, 2012). However, since the main separation mechanisms on ceramic membrane are size exclusion and charge effect and not the diffusion process (Chen, et al., 2017), the diffusion effect can be neglected in ceramic membrane.

The components inside the solution might be able to pass the membrane through the membrane pores and the membrane channels, or they are rejected by the membrane, and this can depend on size exclusion. This separation mechanism is based on the size of the components within the solution. If the size of the compounds is bigger than the size of the membrane pores, these compounds will be rejected. If the molecules have smaller size than the membrane pores, the molecules will permeate through the membrane pores.

The interaction between water molecules and ions in the solution should not be neglected as the ions have hydration potential, which indicates the ability of the ions to attract water molecules (Tansel, 2012). Water is a polar molecule which can be rearranged around the charged ions (Tansel, et al., 2006) as depicted in Figure 2.2. Therefore, the hydration potential affects the ionic size since the ionic radius equals to hydrated radius in aqueous environment (Tansel, 2012). According to that, hydration effect is also taken into account as size exclusion mechanism in membrane filtration.

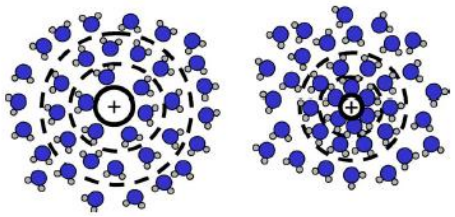

Figure 2.2. Hydration shells around a large ion (left) and a small ion (right) (Source: Tansel, et al., 2006)

Furthermore, cations and anions have relatively different potential for hydration that anions bind the hydration shells more strongly than cations (Tansel, et al., 2006). This might be correlated with the ionic radius, that monovalent anions show smaller ionic radius at the transition from strong to weak hydration. Moreover, the ionic characteristics of the solution, such as ionic strength, pH, and temperature play a significant role in determining the hydration strength (Tansel, 2012).

Besides size exclusion, electrostatic effect also influences rejection in NF. Especially for ionic rejection, the charge interaction between the ions and the membrane surface also determines the rejection. This electric effect exclusion is also known as Donnan exclusion since the transport of the ions follows the Donnan equilibrium theory. The electric exclusion serves as a rejection for co-ions (ions with similar charge) of a charged membrane and as an attraction for counter ions (ions with opposite charge) (Epsztein, et al., 2018).

NF membranes are typically negatively charged at natural pH (Yan, et al., 2016). The origin of the membrane surface charge is from the dissociation of the ionic group on the membrane surface, including the pores wall (Nicolini, et al., 2016). In addition, the membrane surface charge can be modified from the adsorption of the contacting ions onto the membrane surface (Nicolini, et al., 2016; Ortiz-Albo, Ibañez, et al., 2019), which makes the the membrane surface charge is related to the bulk concentration of the charged compound (Ortiz-Albo, et al., 2019).

The charge presents on the membrane surface results an electrical double layer of ions (Figure 2.3). In electrical double layer, there are three parts: a) surface charge; b) Stern layer, which consists of the counter-ions of the surface charge; and c) Diffuse layer, a layer of the solution adjacent to the particle and contains free ions with higher concentration of the counter-ions of the Stern layer (Park & Seo, 2011). This electrical layer acts as a boundary between the stationary layer and the mobile layer of the charge, called as slipping plane (shear plane) where the potential in this boundary is expressed as zeta potential (Ortiz-Albo, et al., 2019; Park & Seo, 2011). This potential is dependent on pH, ionic strength, and the composition of the solution in contact with the membrane (Ortiz-Albo, et al., 2019).

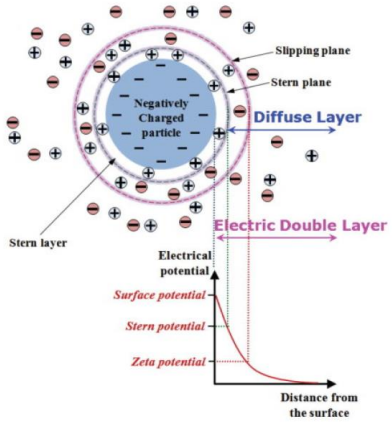

Figure 2.3. Diagram of electric double layer (Park & Seo, 2011)

With dielectric exclusion, ion rejection is affected by the confined solution inside the membrane pores. This mechanism consists of two phenomena, namely the Born effect and the production of image force. Born effect relates to the lower dielectric constant of the solution that is trapped in nanopores due to modified equilibrium. In confined situation, the molecules of the solution show an ordered structure which reducing the solution dielectric constant. The production of image phenomenon is caused by the different dielectric constant between the membrane material and the solution (Lanteri, et al., 2009). This phenomenon might be able to increase the electrostatic interaction between the ions and the polarization charges. Since the sign of the polarization charges is similar to the sign of ions of the solution, this increases the rejection. Dielectric exclusion is considered as the reason of the unexplained divalent ions rejection solely using Donnan exclusion theory (Vezzani & Bandini, 2002).

2.1.4 Sulphate and chloride separation by nanofiltration

As NF membranes surface are charged, the selectivity for ions is different, depending on charge densities. Hence, NF membrane is suitable for fractionation of the salts (Yan, et al., 2016), particularly effective for the rejection of the multivalent anions, such as sulphate (Ortiz-Albo, et al., 2019) since NF membare are usually negatively charged. According to the experiments of Choi et al., (2001), NF membrane is also able to reject monovalent ions as long as there is no other influencing ions in the solution. However, the rejection of the divalent ions can be higher than the monovalent ions, solely due to the higher charge interaction (van der Bruggen, et al., 2004).

In the case of sulphate and chloride separation, the separation on NF membrane is found to be dependent on the membrane type, permeate flux, total salt concentration, and salt concentration ratio (Yan, et al., 2016). A study by Krieg, et al. (2004), revealed that the higher rejection of chloride occurrs when its concentration is low. This behavior is typical for NF membrane. In the case of increasing salt concentration, it is found that the increase of sulphate concentration causes a decrease in chloride rejection, even a negative rejection (Yan, et al., 2016). At the same time, the increase of chloride concentration will decrease the rejection of the sulphate. This can be said that as the concentration of the anions decrease (sulphate or chloride), the rejection of that anion decreases (Krieg, et al., 2004). In addition, pH is considered to have influence in separation of the ions (Mazzoni, et al., 2009). This is related to the isoelectric point (IEP) of the membrane, where the charge effect due zeta potential of the membrane equals to zero at a certain pH. When the pH is higher than IEP, the membrane will have negative charge.

2.2 Chemical precipitation

2.2.1 Precipitation mechanisms

Precipitation is the process of adding one or more chemicals to remove specific cations or anions that may impair the use of water. Calcium and magnesium are examples of cations that are likely to be an issue in water treatment; therefore, chemical precipitation has been traditionally used for softening (Hendricks, 2006). Precipitation also has an important role in industrial process, metallurgy, geology, physiology, and other science (Mullin, 2001). Furthermore, precipitation is becoming one of the alternatives for removal of metals, inorganic compounds, suspended solids, fats, oils, greases, and part of organic substances (Bennati, et al., 2009) from the water.

Precipitation is considered as a fast crystallization and implies an irreversible process; the process goes through three basic step: supersaturation, nucleation and growth (Mullin, 2001). According to a previous study, precipitation kinetics is determined by nucleation and cyrstal

growth, while the supersaturation is the driving force for both steps (Boerlage, et al., 2000). In general, the steps involving in precipitation can be briefly describe as follows:

- Supersaturation
  Crystallization processrequires supersaturation state to proceed. Precipitation is defined as a process that generally initiated at high supersaturation (Mullin, 2001). This stage is usually quantified as a supersaturation ratio, which is calculated as the product of the concentration of the involving ions and their activity divided by the thermodynamic solubility product (Ksp). In the case of $BaSO_4$ precipitation, for instance, the supersaturation ratio is calculated using Eq. (1) (Boerlage, et al., 2000).

$$S_r = \sqrt{\frac{\gamma + [Ba^{2+}]\gamma - [SO_4{}^{2-}]}{Ksp}} \quad (1)$$

- Nucleation
  A number of solid bodies, nuclei or seeds must be present in the solution to start crystallization. Nuclei acts as the center of the crystallization (Mullin, 2001). In other words, nucleation can be considered as the early stage of crystal solid formation or the birth of the crystal. There are several nucleation mechanisms understood in the crystallization process as depicted in Figure 2.4.

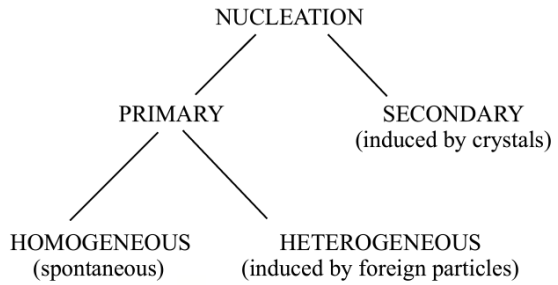

Figure 2.4. Nucleation mechanisms (Mullin, 2001)

Primary nucleation occurs in solutions that are free from crystal or solid matter, in which supersaturation plays the important role in generating the nuclei. Once the ion product of the involved ions exceeds the Ksp value, precipitation will occur spontaneously (Brady & Humiston, 1986). This condition is considered as homogeneous nucleation which it is dominant at high supersaturation conditions. Heterogeneous nucleation takes place when foreign particles or dissolved system impurities are added to the solution system. This heterogeneous nucleation mechanism is effective at low supersaturation conditions (Boerlage, et al., 2000). In the case of secondary nucleation, this mechanism is triggered by pre-existing crystalline solids that are formed in the solution, leading to catalysing effect on nucleation (Boerlage, et al., 2000), mostly at moderate supersaturation (Mullin, 2001) .

The time needed for the nuclei to form is known as induction time/period. This period is described as the gap time between supersaturation state until the appearance of the next phase (Boerlage, et al., 2000), which can be indicated by several ways, for example: solution turbidity and ion bulk concentration.

- Crystal growth
  After the nuclei are stable, the crystal particles will grow larger by addition of crystal ion from the supersaturated solution until the solution reaches its equilibrium. Until then, the concentration of precipitating ions will change as the function of time as depicted in Figure 2.5 (Boerlage, et al., 2000). There are two phases that involve in the crystal growth steps: 1) movement of the solute to the crystal/water interface through advection and diffusion, and 2) adsorption of the solute on to the solid surface, then incorporated into the crystal lattice (Hendricks, 2006).

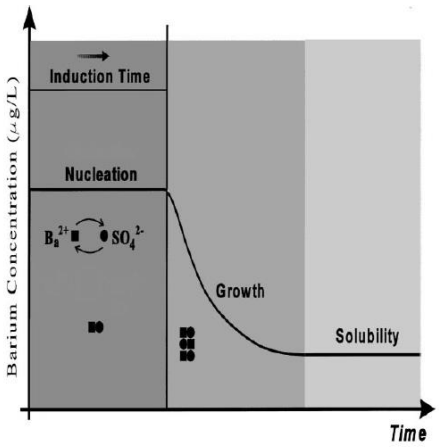

Figure 2.5. Decreasing bulk concentration in solution during precipitation process

In the precipitation process, there are two secondary steps that have profound effect on the final product, which are agglomeration and ageing. Agglomeration is the tendency to cluster together between the particles in the solution. Most of the time, agglomeration is also called as coagulation and/or flocculation. This step generally occurs soon after the nucleation is achieved. Whilst, ageing is a term that covers all the irreversible changes after the formation of the precipitate (Mullin, 2001).

Solubility product, temperature, particle charge, and retention time play a major role in general precipitation process (Hendricks, 2006). Also, molar ion concentration ratio (later discussed as lattice ion ratio) is important in determining the precipitate/crystal morphology (Kucher, et al., 2006). Moreover, according to the classical nucleation theory, there is another important parameter affects the nucleation and induction time known as interfacial tension (He, et al., 1994b). The interfacial tension between the crystal and the aqueous solution is a fundamental parameter to understand the rate of nucleation and crystal growth and is emperically correlated to solubility (He, et al., 1994a). As the solubility increases, the interfacial tension decreseas.

2.2.2 Sulphate precipitation

Precipitation for sulphate removal is mostly used to treat acid mine drainage. Addition of calcium or barium salt is an alternative to remove the sulphate chemically by forming $CaSO_4$ or $BaSO_4$ (barite) precipitates, respectively. Precipitation using barium is potentially more effective due to the very low solubility product of $BaSO_4$ (Akinwekomi, et al., 2017). The difference between the solubility products of $BaSO_4$ and $CaSO_4$ is in the order of 10^5, which indicates that the required concentration for barium salts is considerably lower than calcium salt to form precipitate. Moreover, barite is a highly insoluble salt in water; hence, barium salt is more suitable and more efficient to be used for removing sulphate from water (Benatti, et al., 2009; Špaldon, et al., 2017). However, barium is a very toxic compound compared to calcium, even at

low concentration (Benatti, et al., 2009; Swanepoel, et al., 2012). Therefore, the dosing should be done carefully to avoid the undesirable effect on the generated waste from the precipitation.

The rate of precipation using barium salts depends on the concentration of the barium and sulphate ions, and the inorganic species of $BaSO_4$ is produced stoichiometrically (1 mole of SO_4^{2-} per 1 mole of Ba^{2+}) (Benatti, et al., 2009). Akinwekomi, et al., (2017) revealed that complete sulphate removal is achieved faster when the stochiometric ratio between barium and sulphate is 2. On the contrary, the $CaSO_4$ precipitation is limited by its solubility; the experiment of Almasri, et al. (2015) showed that addition of calcium salt with a stochiometric ratio between calcium and sulphate is 2 was able to reduce the sulphate concentration only by 87.6% (from 97 mM to 12 mM). On the other hand, both $BaSO_4$ and $CaSO_4$ precipitation are not sensitive to pH (Almasri, et al., 2015; MacAdam & Jarvis, 2015; Xu, et al., 2019).

2.2.3 Barite and gypsum precipitation

Generally, barite precipitation is not desired because it potentially forms adherent and hard scale on the equipment surface, hence; removing the barite scale is extremely difficult (MacAdam & Jarvis, 2015). Barite precipitation can cause damages on pumps, membrane, and clog the pipelines (Ronquim, et al., 2018). In the contrary, in some cases, the formation of barite precipitates is desired for the quantitative analysis of barium or sulphate concentration, for example a quantitative analysis using a test kit.

In case of $CaSO_4$ precipitation, several types of $CaSO_4$ can form, depending on the water molecule that attaches to the precipitate. $CaSO_4$ exists in the form of $CaSO_4.nH_2O$, where n=0 is known as anhydrite, n=0.5 is hemihydrate, and n=2 is gypsum (MacAdam & Jarvis, 2015). Gypsum is thus the highest form of hydration for $CaSO_4$ (Cowan & Weintritt, 1976). The transition of these three forms is a function of the temperature (Lu, et al., 2012); however, the temperature transition point between gypsum and anhydrate is still uncertain (He, et al., 1994a). Precipitation using calcium salt is attractive because the $CaSO_4$ solids are non-toxic and they can potentially be reused for many purposes, for example as a mixture combination with Portland cement (Cowan & Weintritt, 1976).

3 Materials and Methods

3.1 Materials

3.1.1 Experimental setup

The laboratory experiments were performed using three experimental set-ups: membrane NF, batch-sulphate precipitation, and integrated sulphate removal. The membrane NF experiment set-up consisted of feed tank, feed pump (Getriebebau NORD GmbH & Co. KG, type SK 180E-550-340-B), pressure meter (ESI USB Transducer), membrane housing, valve, weight balance (Kern, type EWJ), and flow meter (Sea Zhongjiang, type ZJ-LCD-M). The setup was set to provide a crossflow membrane filtration and the membrane concentrate was recirculated to the feed tank during the experiment. The scheme of the set-up is depicted in Figure 3.1.

In this set-up, the transmembrane pressure is the average pressure of feed and concentrate that are shown on the pressure meter, and it was controlled by opening or closing the valve and by regulating the rotations per minute of the pump. The flow of the permeate was measured based on the weight of the water using a balance, that was subsequently converted to volume unit based on the density of water. Permeate was collected in another container for further analyses of the dissolved ions and dissolved organic carbon (DOC) concentration. The recirculation flow of the brine was measured using flow meter, while the pH and temperature are monitored using portable multimeter (WTW, Multi 3630 IDS).

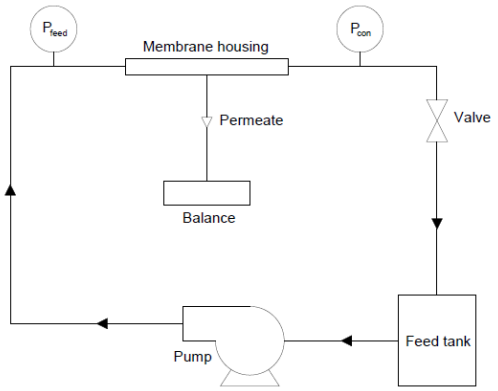

Figure 3.1. Membrane filtration scheme

The batch-sulphate precipitation experiment aimed to analyse the removal of sulphate using precipitation by adding salt that reacts with sulphate to form precipitate. The precipitation process took place in plastic beakers with the volume of 180 ml. Magnetic stirrers were used to mix the brine and the salt solution to create precipitate that contains sulphate. To operate the stirrer, a stirring plate (Labinco) with 6 points was used.

The integrated NF and sulphate precipitation experimental setup consisted of a mixing mechanism that was added prior to the membrane filtration. The scheme of the integrated experimental setup is depicted by Figure 3.2. A stirrer from Heldolph Instrument (type RZR 1) with a 3-blade propeller with diameter of 14 cm (blade dimension: length 7 cm, width 2.5 cm, thickness 0.1 cm) was used as the stirrer of the solution. The mixing of the solution was performed in a 9 L tank. After the precipitation step was done, a tube was used to convey the

supernatant to the feed tank of the membrane filtration system. From this point, the operation of the experiment continued to the membrane filtration mechanism.

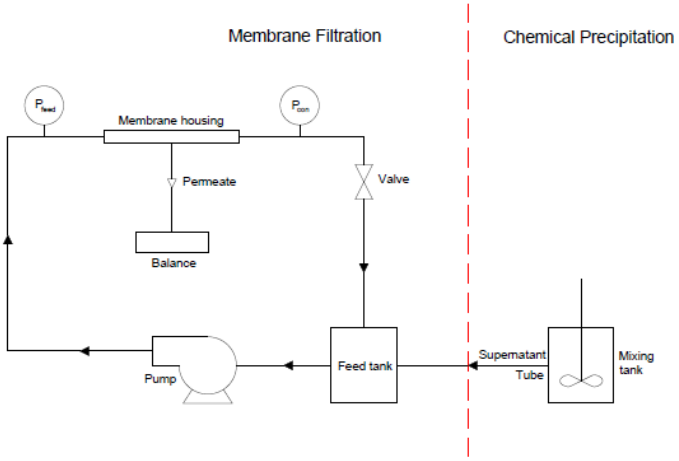

Figure 3.2. Integrated sulphate removal scheme

3.1.2 Ceramic NF membranes

Ceramic nanofiltration membranes used in this research were provided by Inopor GmbH, Germany. Based on the information from the manufacturer, the separation membrane layer is made of TiO_2 and the support layers made of Al_2O_3, while the front-side of the membrane sealing is made of silica glass. The membranes have a mean pore size of 0.9 nm with a porosity of 30-40%. The given molecular weight cut-off (MWCO) of the membrane used in this research was 450 Da.

Tubular membranes with single channel were used, as shown in Figure 3.3. The membranes have an inner diameter of 7 mm and outside diameter of 10 mm with a filtration length of 75 mm. With this dimension, the effective filtration area of the membrane is 0.00163 m^3. The membranes were held by a PVC module (shown in Figure 3.3) during the filtration experiments. This PVC module has a maximum operating pressure of 10 bar.

Figure 3.3. Ceramic NF membranes (left) and PVC module as the membrane housing (right)

3.1.3 Polyethylene glycol solutions

A tracer molecule was used to determine the effective MWCO of the membrane. In this research, polyethylene glycols (PEG) from Sigma-Aldrich was used as tracer molecules with various molecular weights. PEG was chosen because the molecules are not charged, therefore, the rejection of the PEG is purely based on size exclusion (Shang, et al., 2017). The concentration of PEG of each different size for this research was 0.6 g/L. The selection of the range size of the PEG depended on the membrane purchased cut off size. For this research, the rule of thumb for the maximum PEG size was twice the membrane purchased cut-off pore size. In the

characterization for 450 Da membranes, the PEG molecular sizes that were used were 200 Da, 300 Da, 400 Da, 600 Da, and 1000 Da.

3.1.4 Synthetic brines

The synthetic brines were made using Na_2SO_4 and NaCl dissolved in demineralized water. Na_2SO_4 salt was obtained from Carl Roth GmbH for the salt rejection test and Sigma-Aldrich for the batch-sulphate precipitation experiment. Whilst, NaCl salt was used in two forms, in powder from (Sigma Aldrich) and granular form (Poolsel). The granular NaCl was used to make synthetic brine in a large volume (salt rejection and integrated sulphate removal experiments).

3.1.5 IEX brine

NOM-rich IEX brine used in this research was SIX brine from Sweden treatment plant and the brine was diluted with dilution factor of 100.

3.1.6 Barium and calcium salts

Sulphate was precipitated into barite ($BaSO_4$) using $BaCl_2.2H_2O$ obtained from Sigma-Aldrich and into $CaSO_4$ using $CaCl_2.2H_2O$ from Merck. The concentration of the salts was determined according to the desired ratio between barium and/or calcium and sulphate. All salts for precipitation experiment were added to the brine in the solution form, which they were dissolved in ultrapure water. The volume of barium and calcium solution were adjusted to the working volume of the experiment. The detailed preparation of barium and calcium solution will be explained in the next section.

3.2 Methods for Analysis

3.2.1 MWCO analysis

In determining the MWCO of the membranes, High-performance Liquid Chromatography (HPLC) from Shimadzu, Japan equipped with a size exclusive chromatography columns (SEC) 5 µm 30 Å (PSS Polymer Standards Service GmbH, Germany). SEC, also known as gel permeation chromatography (GPC) was used to measure the distribution of molecular weights based on the elution time. The principle is the size exclusion by adsorption of molecules into the solid adsorbent materials inside the chromatogram column. Small molecules will be easily adsorbed, while the bigger molecules will pass the adsorbent and leave the column in shorter time. Therefore, the big molecules can be detected by short retention time.

3.2.2 Ion analysis

For determining the concentration of ions (except barium) in the samples, ion chromatography (IC) from Metrohm Instrument, Swiss was used. The analysis of cation and anion were conducted independently in different systems, 818 Compact IC pro for anion analyses while the cations were analysed in the 883 Basic IC plus system. Each system was equipped with a specific column where the ion can pass through and analysed based on the retention time. Suppressor 5 150/4.0 was used as the anion column and C4 Cation 150/4.0 was the column used for cation analysis.

IC is able to detect accurately for the concentration of the ions in between 1-100 mg/L. Therefore, the samples were diluted to have the ion concentration in that range. The samples were required to be particle-free, hence, the samples were filtered using 0.45 μm filter (Macherey-Nagel GmbH& Co. KG, Germany) before the dilution. To compute the concentration of the ions, a calibration curve was made in the beginning of the analysis by using a series of standard containing desired ions to be analysed. The concentrations used for the standard were

1, 10, 25, 50, and 100 mg/L. The acquisition time depends on the ions to be analysed. In this research, the acquisition time is 35 minutes due to the presence of calcium in the sample which the calcium's retention time was around 30 minutes.

The rejection of the ions was calculated based on the difference of the ion concentration between the feed and the permeate, as indicated in Eq. (2).

$$R\ (\%) = \frac{(C_{feed} - C_{permeate})}{C_{feed}} x\ 100 \qquad (2)$$

Where C_{feed} is certain ion concentration in the feed sample and $C_{permeate}$ is concentration of the similar ion in permeate sample.

3.2.3 Barium analysis

Barium was analysed using inductively coupled plasma-optical emission spectrophotometry (ICP-OES) from Spectro, Arcos EOP (end of plasma) with deviation of ±2.5% from the reading. The analysis was performed in collaboration with the Faculty of 3ME of TU Delft.

3.2.4 Test kits

Several samples were analysed using sulphate and barium test kits to confirm the concentration and estimate the dilution factor before the samples were analysed with IC and ICP-OES. Sulphate concentration was analysed using test kit from Hach (LCK 153) with analysis range of 40-150 mg/L as SO_4^{2-}, and barium was analysed using test kit from Hach Lange GmbH (BariVer 4 Barium Reagent) with analysis range of 2-100 mg/L. The samples were diluted prior the analysis using test kit with the dilution factor adjusting to the analysis range for each test kit. Both test kits provided a reagent to be added to the samples with the provided tube. After the reaction between the samples and reagent finished (reaction time is indicated in the manual of the test kit), the concentrations were analysed using turbidimetric method in spectrophotometer (Hach, D3900).

3.2.5 DOC analysis

Natural organic matter (NOM) was measured as dissolved organic carbon (DOC) in the feed, permeate, and supernatant samples. The samples were measured after 0.45 µm filtration by a total organic carbon (TOC) analyzer (TOC-VCPH, Shimadzu, Japan). The rejection of DOC was calculated in the same way as the rejection of ions (Eq (2)). For further characterisation of the NOM, the percentage on total organic matter (TOC) of biopolymers, humic substances, building blocks, low molecular weight acids and low molecular weight neutrals, were measured by Het Water Laboratorium (the Netherlands), using liquid chromatography-organic carbon detection (LC-OCD) analyses as described in Huber, et al. (2011).

3.3 Methods for membrane characterization and cleaning

3.3.1 Membrane characterisation

The properties of the membranes should be known to select a suitable membrane based on the pore size and the absence of defects. In the characterization phase, permeability and MWCO of the membranes were determined.

The permeability of the membranes was examined using ultrapure water filtration under a constant pressure 3 bar. Permeability is the flux of the membrane, divided by the trans-membrane pressure (TMP). However, since the temperature varied during the experiments due

to heat conductance from the pump, the permeability was calculated using the temperature correction at 20°C which the equation shown in Eq. (3) (Shang, et al., 2017).

$$L_{p,20°C} = \frac{J}{\Delta P}, \frac{\eta_T}{\eta_{20}} = \frac{J\ x\ e^{-0.0239(T-20)}}{\Delta P} \quad (3)$$

Where $L_{P,20°C}$ is permeability at 20°C (L/m²h.bar), J is membrane flux (L/m²h), ΔP is TMP (bar) and T is temperature of the water (°C).

The size of the membrane pores is stated as MWCO with the unit of Dalton (Da). MWCO was determined by passing PEG solutions with different MWCO through the membrane under constant pressure of 3 bar. During the experiment the membrane cross flow was kept at about 1.3 m/s, experiment, to guarantee turbulent flow through the membrane channel (the Reynolds number was >9000, calculation is explained). Creating turbulent flow inside the membrane was intended to avoid stagnant layer on the membrane surface that can affect the permeation of the solution through the membrane. Reynolds number (Re) is a unitless term that is used to define the turbulence of the flow. Re<1000 is considered as laminar flow (White, 2011) and this research expects Re>3000. Re value is determined using Eq. (4).

$$Re = \frac{\rho V L}{\mu} \quad (4)$$

Where ρ is fluid density (kg/m³), V is fluid velocity (m/s), L is hydraulic diameter (m), and μ is dynamic viscosity (kg/ms).

In this research, experiments were conducted at room temperature, hence the density and viscosity of water were based on room temperature, velocity was 1.3 m/s, and the hydraulic diameter equal to the membrane diameter since the flow is considered in full-filled condition.

$$Re = \frac{1000\ kg/m^3\ x\ 1.3\ m/s\ x\ 0.007\ m}{0.001\ kg/m.s}$$

$$Re = 9095$$

Based on the Re calculation, the cross-flow is applicable for the experiments of this research.

MWCO was calculated based on the analysed samples of the permeate and feed using HPLC. One hour of stabilization was needed before the samples of the brine were collected. The samples were taken within 1 hour with 30 minutes interval. Therefore, there were 3 samples (0, 30, and 60 minutes), yet, the feed was only sampled in the beginning and the end of experiment. The samples were filtered using 0.45 µm filter before being analysed in HPLC. During the sample collection, temperature of the feed was measured using a multimeter.

During the sample analysis in HPLC, different PEG molecular weight passed the column in different elution time. Each molecular weight corresponds to a specific elution time and showed as a signal, depicted in the example of Figure 3.4 This signal showed in HPLC is proportional to the concentration of PEG in the samples.

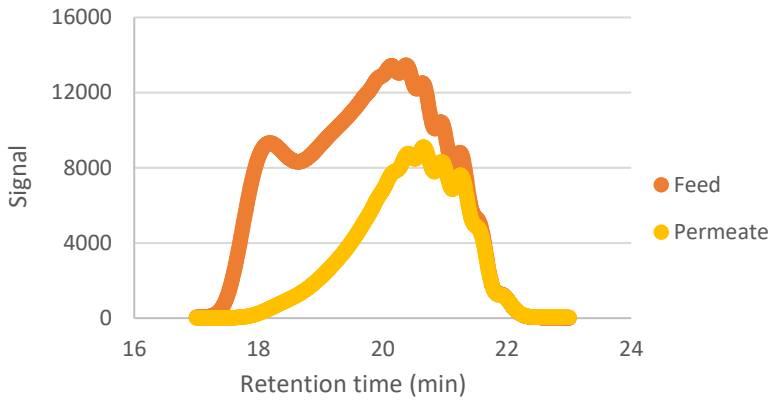

Figure 3.4. PEG signal from HPLC

The molecular weight of PEG was converted from the retention time to molecular weight size using Eq. (5) obtained from the calibration curve showed in Figure 3.5. This calibration curve was made by a set of PEG standards with known molecular sizes that were analysed in the HPLC before the samples were analysed.

$$MW = 13761096.8280462e^{-0.524944t} \quad (5)$$

Where MW is molecular weight (Da) and t is the retention time (min).

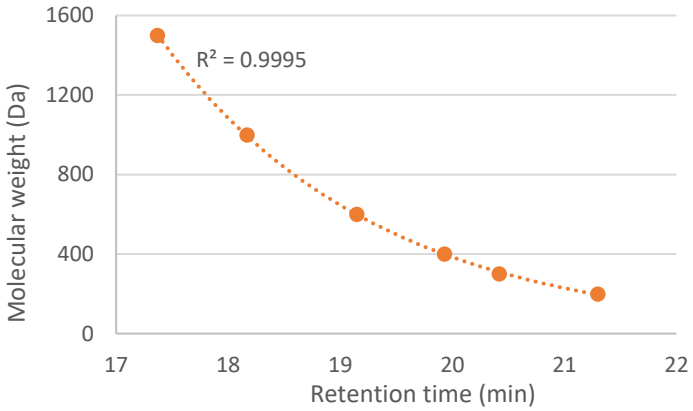

Figure 3.5. Molecular weight calibration curve from PEG analysis

Furthermore, MWCO of the membrane was determined by the 90% PEG rejection efficiency which was calculated based on Eq. (6). The example of the retention curved is showed in the example of Figure 3.6.

$$R\ (\%) = \frac{(C_{feed} - C_{permeate})}{C_{feed}} x\ 100 \quad (6)$$

Where C_{feed} is PEG concentration in the feed sample and $C_{permeate}$ is PEG concentration in permeate sample.

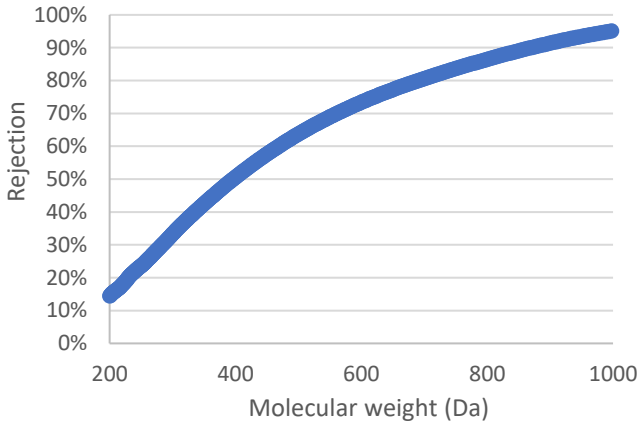

Figure 3.6. Retention curve of PEG for MWCO determination

3.3.2 Membrane cleaning

After MWCO analysis, the membrane needed to be cleaned to remove the PEG that might still be attached to the membrane and to recover the permeability. In this research, chemical cleaning with acid was used. The cleaning was performed by immersing the membrane into 0.2% (w/v) active chloride sodium hypochlorite (NaClO) solution of 2 hours and subsequent immersion with ultrapure water for 2 times 30 minutes. The permeability of the membrane was expected to be close to the initial permeability after the cleaning. If the recovery of the permeability was too low, additional cleaning step was needed until the permeability of the membrane close to the initial permeability. Moreover, the cleaning of the membrane was also performed after the salt rejection experiment and the integrated sulphate removal experiment.

3.4 Methods for the brine and salts experiments

3.4.1 Salt rejection experiment

To understand the removal of sulphate by ceramic NF membrane, salt rejection experiments were conducted with synthetic brine solutions with different ionic strengths. The synthetic brines were made as single solutions (with Na_2SO_4 only) and as binary solutions (with Na_2SO_4 and NaCl). The variation of the ionic strength of the brines is shown in Table 3.1. IEX brine was also used for the salt rejection experiment and the estimated ionic strength of the brine is 0.3 M (based on the calculation from IC analysis).

Table 3.1. Variation of ionic strength in the synthetic brines for salt rejection experiment

Total Ionic Strength (M)	**Ionic Strength Contribution Binary (M)**		**Ionic Strength Single (M)**
	Na_2SO_4	**NaCl**	**Na_2SO_4**
0.1	0.05	0.05	0.1
0.5	0.28	0.22	-
1	0.5	0.5	1

The filtration mechanism was operated according to constant flux at around 30 L/m²h. Therefore, the pressure was adjusted during the first hour of the experiment (stabilisation period) to ensure the flux stayed around 30 L/m²h during the sample collection period. During the experiment the membrane cross flow was kept at about 1.3 m/s, to guarantee turbulent flow through the membrane channel. In addition, the pH of the brines was adjusted to around 8 before the experiment begins, in order to have the similar pH condition with the IEX brine.

The sample collection period for salt rejection experiment followed the sample collection period for the MWCO experiment, both for permeate and feed samples. The samples were filtered using 0.45 μm filter and transferred to new sample tubes before being analyzed.

3.4.2 Batch-sulphate precipitation model and experiments for model validation

Since the removal of the sulphate depends on the amount of the barium or calcium added to the brine, some modelling was performed in PhreeqC to predict the dosage of the barium and calcium salt. To model the solution with high salinity, the Pitzer database was able to estimate the concentration more accurately than the default Phreeqc database. For this research, the Pitzer database was obtained from the supplementary data of Appelo (2015).

In the purpose of investigating the result of various ratio between barium or calcium and sulphate, several $Ba:SO_4$ and $Ca:SO_4$ ratios were simulated in the model. The conditions in the model are shown in Table 3.2, and they were roughly similar to the conditions in the laboratory where the experiment took place.

Table 3.2. Condition set for precipitation modelling

Parameter	**$BaCl_2.2H_2O$**	**$CaCl_2.2H_2O$**
$Ba:SO_4$ or $Ca:SO_4$	0.90-1.10	0.90-1.30
pH	~8	
Temperature (°C)	20	

The results of the model needed to be validated to determine whether the model represented the actual conditions. The experiments were set to have the similar conditions as described in the model as shown in Table 3.2. All the experiments were performed with the working volume of 160 ml. This working volume was the total volume of the brine and barium or calcium salt solution. Prior to salt addition, all the beakers were mixed for a few minutes to ensure all the beakers had approximately the same agitation.

As mentioned in the previous section, barium and calcium salts were added in the solution form, and the salts were dissolved in 10 ml of ultrapure water. Since $BaCl_2.2H_2O$ is less soluble than $CaCl_2.2H_2O$, 20 ml of ultrapure water was needed to dissolve the required $BaCl_22H_2O$ for removing sulphate in 1 M brine solution. After the salts were added, the solutions were mixed for 30 minutes. Subsequently, the mixing was terminated, and the solutions were kept for another 30 minutes to settle the precipitate. Samples were taken from each beaker after the 30 minutes of precipitation settling using a 10 ml syringe and filtered using 0.45 μm filter before it was transferred to the sample bottles.

3.4.3 Batch-sulphate precipitation experiment

After the salt rejection analysis on ceramic membrane, experiments with sulphate precipitation were also conducted to understand the sulphate removal mechanisms in each step of the integrated sulphate removal approach. As explained in the previous section, modelling with PhreeqC was used to estimate the dosing of chemicals and removal efficacy using chemical precipitation. Afterwards, the sulphate precipitation batch experiments with brines were performed. The result was used as the reference to continue to the integrated approach.

Different ionic strength solutions were used in this research to broaden the view of sulphate removal from the brine considering the quality of the real brine is not the same all the time. The variation of the ionic strength was made in synthetic brines by mixing Na_2SO_4 and NaCl with around the same ratio of 50:50. Table 3.3 provides the variation of the ionic strength for the synthetic brines.

Table 3.3. Ionic strength variation on synthetic brine for sulphate removal experiment

Total Ionic Strength	Ionic Strength		Concentration (g/L)	
	Na_2SO_4	NaCl	SO_4^{2-}	Cl^-
0.01 M	0.005	0.005	0.16	0.18
0.1 M	0.05	0.05	1.6	1.8
0.5 M	0.28	0.22	9	8
1 M	0.5	0.5	16	18

Similar to the salt rejection experiments with ceramic NF membrane, the pH of the solution was adjusted to be around 8 by adding 0.1 N NaOH. The conditions and the settings for the precipitation experiments for sulphate removal were similar to the model validation experiment. Both salts, $BaCl_2.2H_2O$ and $CaCl_2.2H_2O$ were added for concentration ratio of 1 ($Ba:SO_4$ or $Ca:SO_4$ equals to 1).

3.4.4 Integrated sulphate removal experiment

In this experiment, sulphate was removed using the combination between chemical precipitation and ceramic NF. The experiment was performed based on the scheme in Figure 3.2. To deepen the understanding of sulphate removal in the IEX brine, experiments with synthetic brines were also performed. Synthetic brines were varied according to the variation of the ionic strength solution for the sulphate removal experiment, yet, the 0.01 M solution was excluded.

For the chemical precipitation step, the brines were prepared with a volume of 8 L. Whilst, the barium salt was prepared in 1 L ultrapure water for experiments with synthetic brines, and 120 mL for the experiment using IEX brine. This approach was taken to avoid too large volume of the treated brine. The concentration of the barium salt was set to be equimolar between barium and sulphate ($Ba:SO_4$ = 1). Table 3.4 shows the variation of solution ionic strength and the amount of $BaCl_2.2H_2O$ added for each variation.

Table 3.4. Brine variation for integrated sulphate removal experiment

Solution	SO_4^{2-} concentration		Barium Concentration (g/L)
	g/L	mol/L	
0.1 M	1.6	0.017	4.07
0.5 M	9	0.094	22.89
1 M	16	0.17	40.7
IEX Brine	2.24	0.023	5.61

Prior to the precipitation step, the pH of the solution was adjusted by using 0.1 N NaOH until it reached the pH around 8. Subsequently, the brines were mixed with the prepared barium salt solutions for 10 minutes. After the mixing finished, a retention time of 30 minutes was set to let the precipitate to settle. A tube was used to transfer the supernatant (liquid part of the mixed solution) from the mixing tank to the feed tank. From this point, the mechanism of sulphate removal followed the procedure of the salt rejection experiment.

4 Results and Discussions

4.1 Membrane characterization

4.1.1 Membrane permeability and MWCO

Even when the pore size is similar between two different membranes, the permeability of the membranes might be different since the permeability is not solely determined by the pore size. Other factors such as membrane thickness and pore tortuosity can affect the permeation of the liquid through the membrane (Lee, et al., 2015; Shang, et al., 2017; da Silva Biron, et al., 2018). Figure 4.1. shows the ultrapure water permeability of the tested membranes.

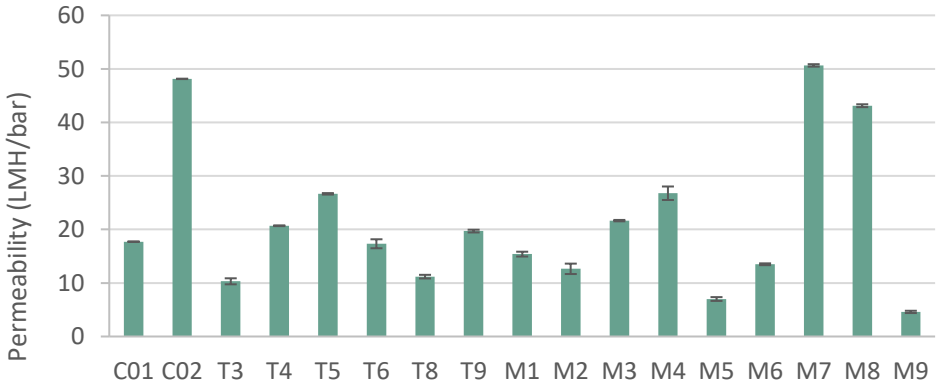

Figure 4.1. Ultrapure water permeability of the tested membranes

In the beginning, 17 ceramic NF membranes were characterized. However, only membranes with permeability between 10 and 30 L/m²h.bar were further tested for MWCO. Based on a previous study, the operation of NF membranes at a very low flux (approximately 10 kg/m²h) showed lower retentions than when it was operated at a higher flux (Bargerman, et al., 2015). Assuming the density of the water was 1000 kg/m³, the estimated low flux equals to 10 L/m²h. Therefore, this value was set to be the lower bound of the permeability. Whilst, the upper bound considered the desired flux during the salt rejection (30 L/m²h). The results of the MWCO experiments is indicated in Table 4.1.

Table 4.1. Results of membrane characterization

Membrane	Ultrapure water permeability (L/m²h.bar)	MWCO (Da)
C01	17.72	867
T3	10.31	715
T4	20.69	818
T5	26.65	1004
T6	17.33	696
T8	11.18	720
T9	19.70	864
M1	15.39	917
M2	12.64	*Defect 40%**
M3	21.65	*Defect 15%**
M4	26.77	997
M6	13.49	876

**defect: membranes were unable to reject 1000 Da PEG up to 90%. The number represents the difference between the 1000 Da PEG rejection from 90% rejection.*

According to Table 4.1, the MWCO of the membranes are greater than 450 Da, although the manufacturer stated that the MWCO of the membranes is 450 Da.

There were two membranes stated as defect membranes, since these membranes could not reject the 1000 Da PEG up to 90% due to the cracks or gaps that caused short-circuiting of feed water to the permeate side (Kramer, et al., 2019). Whilst, the percentage of defect represents the difference of the rejection of the membrane at the highest molecular weight of PEG from 90% rejection. The percentage of the defect can be observed from the pore size distribution as depicted in Figure 4.2.

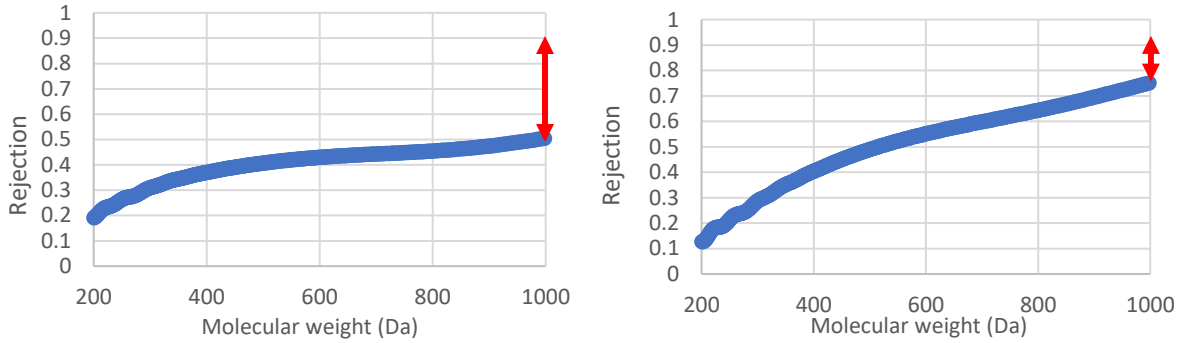

Figure 4.2. Defect on tested membrane M2 (left) and M3 (right). The arrow indicates the gap where the rejection does not reach 90% at the highest PEG size.

Considering the results of membrane characterisation, membrane C01 and M6 were chosen for further experiments. These membranes have a similar MWCO and were expected to give quite similar results. Further, the MWCO of these membranes was determined as 900 Da. Even though the MWCO of these membranes were higher than the purchased cut-off, the MWCO was still in the range of NF membrane MWCO, which was in between 200-1000 Da (Bargerman, et al., 2015; Chen, et al., 2015; Puhlfürβ, et al., 2000; van Gestel, et al., 2002).

4.2 Salt rejection experiment

To investigate the salts rejection by NF of the two selected membranes, filtration using the artificial and IEX brines was performed without precipitation step prior to the NF step. In addition, NF using the NOM-rich IEX brine was tested to understand the role of NOM on salt rejection. The effect of ionic strength and NOM presence on salt rejection on ceramic NF membranes is shown in Figure 4.3

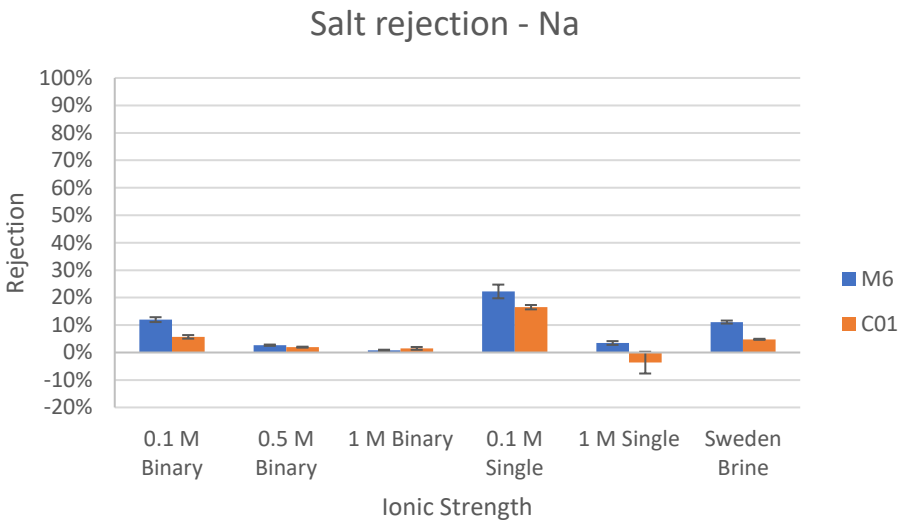

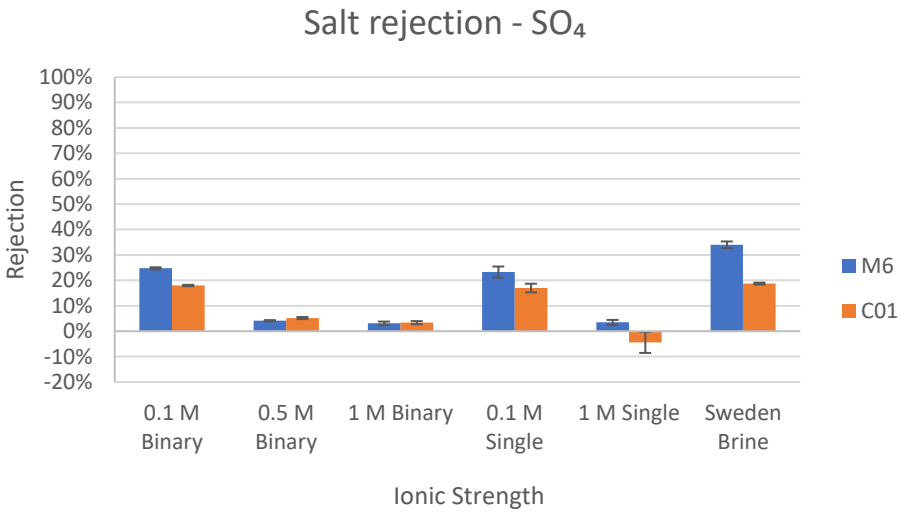

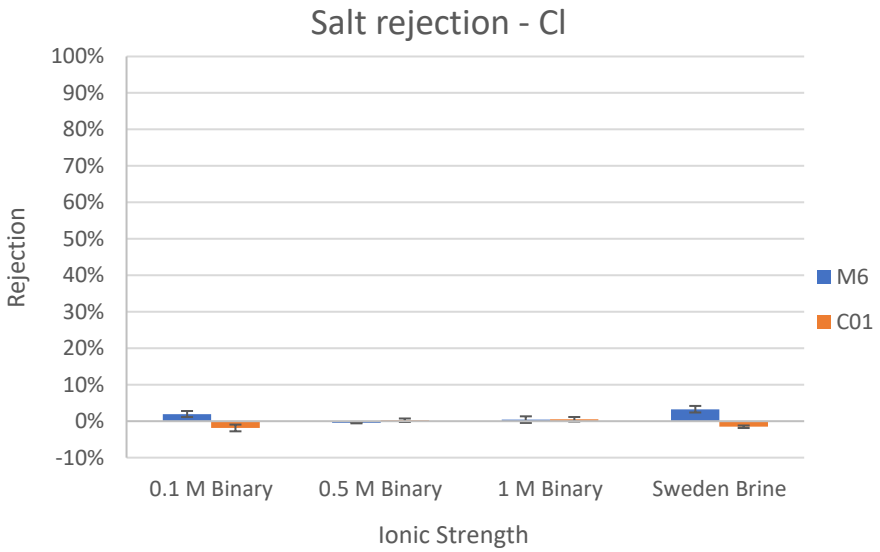

Figure 4.3. Salt rejection on ceramic NF membranes without precipitation step

The results show that M6 rejected salts more than C01, but both membranes had low permeation of chloride, with less than 5 %. Based on Figure 4.3, the rejection of salts in synthetic brine decreased as the ionic strength increased and it occurred in all ion rejections. Even though the rejection of sulphate was higher than chloride, the rejection was still low, from around 30% to no rejection. However, when NOM was present in the IEX brine, the removal of sulphate was higher than what has been expected based on the results of synthetic brines. In the next sections, these results will be discussed further.

4.2.1 Difference salts removal by membranes with the same MWCO

Membrane M6 had a higher rejection than C01 for every ion at the different ionic strengths of the brines (except for the sulphate in 0.5 M binary solution and chloride in 0.1 M single solution). The separation ability of ceramic membranes was not only determined by the MWCO, but it also depended on the pore size distribution (Pera-Titus & Llorens, 2007; Nicolini, et al., 2016). Figure 4.4 shows that the pore size distribution of the two membranes was different, the pore size distribution of M6 was narrower than C01. This means that M6 has more smaller pores than C01 that might help to reject the ions.

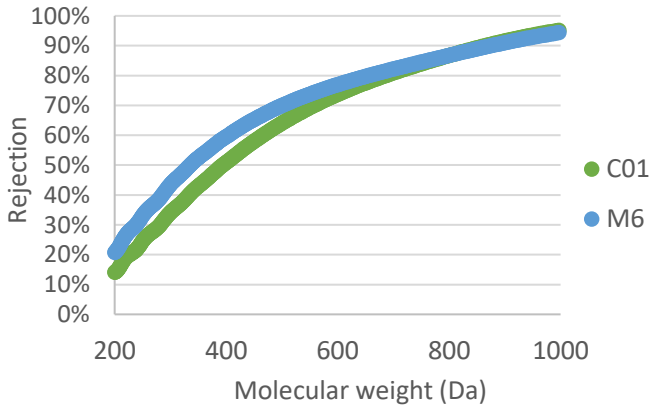

Figure 4.4. Pore size distribution of the selected membranes

These results agreed with a previous study where it was found that higher salt retention could be obtained with narrower membrane pores with TiO_2 top layer (van Gestel, et al., 2002). Furthermore, the study from Fane, et al. (1992) explained that charge (electrostatic) effect dominated the separation mechanism in smaller pore sizes. This mechanism was characterised by the increase of membrane's co-ion rejection, while the counter-ion rejection stayed the same. Moreover, the divalent ions would have higher rejection than the monovalent ion. Figure 4.1 shows that this theory applies to the results of the salt rejection experiment because among all ions, sulphate has the highest removal when the membranes are negatively charged at operating pH of 8 (based on the previous study of Feng, 2018).

4.2.2 Lower rejection of ions at higher ionic strength

As shown in Figure 4.3, the rejections of the salts were rather low (maximum 34%). This is probably due to the high ionic strength of the brines. Moreover, the rejection of sulphate and sodium were decreasing as the ionic strength increased for all type of brines, while the chloride tended to permeate through the membrane. In NF membranes, electrostatic interaction was considered as the major factor that could explain the separation mechanism (Wang, et al., 2005) which was represented as an electrical double layer. Hence, the phenomena of lower salt rejections could be explained by the change of the electrical double layer on the membrane surface.

At higher salt concentrations, thus, at higher ionic strength, the thickness of double layer on the membrane surface will be compressed, and the overlapping electrical layers between ion and the membrane surface will be less; this leads to the passage of the ion through the membrane (Puhlfürβ, Voigt, et al.; van Gestel, et al., 2002). This happens because, when the feed water contains high concentrations of salt, more counterions will present on the layer of the membrane surface (Puhlfürβ, et al., 2000). Consequently, this counter-ions will shield the free charge area, and this will cause a decrease in the zeta potential of the membrane (Chen, et al., 2017; Nicolini, et al., 2016). Therefore, the charge effect becomes less important in rejecting the ions as the effective area of the membrane pore is larger when the electrical double layer is thinner (Wang, et al., 2005). As a result, the ions can easily permeate through the membrane.

Furthermore, the radius in the membrane pores where the influence of electrical potential still takes place is known as Debye length (Eq. (7)) also has a role. Based on Eq. (7), the magnitude of Debye length strongly depends on the ionic strength of the solution which it has an inverse relationship with the solution ionic strength. Hence, it explicitly indicates that high ionic strength of the solution decreases the Debye length.

$$\kappa^{-1} = \sqrt{\frac{\varepsilon_0 \, \varepsilon_r \, K_B \, T}{2000 \, N_A \, e^2 \, I}} \tag{7}$$

Where, ε_0 is vacuum permittivity (8.85 x 10^{-12} C/V.m), ε_r is relative permittivity of the background solution (80 for water at 20°C), K_B is Boltzmann constant (1.38 x 10^{-23} J/K), T is temperature (K), N_A is Avogadro number (6 x 10^{23} /mol), e is the elementary charge (1.6 x 10^{-19} C), and I is ionic strength of the solution.

The constants for each element in Eq. (7) are obtained from Shang, et al. (2014b). Based on the known constants, the Debye length for the synthetic brines of this research with the ionic strength of 0.1 M, 0.5 M, and 1 M were 0.97 nm, 0.43 nm, and 0.31 nm, respectively. The reduction of the Debye length looks proportional to the reduction of sulphate rejection. Debye length decreased by 56% from 0.1 M to 0.5 M, and the sulphate rejection decreased by 21 percent point for M6 and 13 percent point for C01. While, the reduction of Debye length from 0.5 M to 1 M is 28% and the reduction of sulphate rejection for M6 and C01 were 1 percent point and 2 percent point, respectively.

4.2.3 Lower rejection of chloride compared to sulphate

Similar to the ionic strength effect on ion rejection, lower rejection on chloride could also be explained by the electrostatic effect of the NF membrane surface. Further, this was explained by the Donnan equilibrium theory, where the electrochemical equilibrium was reached between the solution and membrane by repelling and attracting ions. The equilibrium was dependent on: a) salt concentration; b) fixed charge concentration on the membrane; c) valence of co-ion; and d) valence of the counter-ion (Peeters, et al., 1998).

According to Figure 4.3, almost no chloride rejection occurred, compared to sulphate and sodium. This was also observed by Puhlfürβ, et al. (2000). The rejection was even negative in the synthetic brine with the ionic strength of 0.1 M. Negative rejection of chloride was often observed in mixed salt solution filtration using NF membranes (Pérez-González, et al., 2015; Yan, et al., 2016). The higher rejection of sulphate was due to the higher valence of sulphate (Wang, et al., 2018). While, the permeation of chloride through the membrane was influenced by the presence of sodium in the brine. Sodium, the counter-ion of the membrane surface charge, was attracted to the membrane and was able to pass the membrane, leading to excessive positive charges in the permeate side. Consequently, electrostatic forces were generated between the solution and the membrane (Yan, et al., 2016). Due to its lower valence and smaller

radius, chloride was able to pass the membrane through facilitated transport phenomena, where chloride was dragged by sodium ions to achieve the electroneutrality for both feed and permeate sides (Déon, et al., 2009; Pérez-González, et al., 2015).

4.2.4 Enhanced ions rejection by NOM presence

The rejection of sulphate was the highest in IEX brine, which was 34% for M6 and 19% for C01. The IEX brine used for this research had an ionic strength of around 0.3 M. The ionic strength of the brine was calculated based on the average results of IC analysis using Eq. (8) and the result is summarised in Table 4.2.

$$I = \frac{1}{2} \sum m_i {z_i}^2 \tag{8}$$

Where m_i is the molality of the i^{th} ion and z_i it the ion charge of i^{th} ion.

Table 4.2. Ionic strength calculation for IEX brine

Parameter	SO_4^{2-}	Cl^-	Na^+	I
Concentration (mg/L)	1944	9982	6232	0.3
MW (mol/g)	96.056	35.45	22.99	
Molality (mol/kg)	0.02	0.28	0.27	
Ion charge/z	-2	-1	+1	

In accordance with the results of salt rejection on synthetic brine, expected rejection of ions from IEX brine should be between the rejection of the 0.1 M and 0.5 M of the synthetic brines. However, the salt removal in the IEX brine was more similar to the salt removal of the synthetic 0.1 M brine.

Improved salts retention in the presence of NOM has also been observed in the literature. Previous research showed that salt rejection could be improved by an additional "NOM filtration layer" (Shang, et al., 2014b). The presence of NOM fouling could also modify the membrane surface charge in terms of its zeta potential (Comerton, et al., 2009; Shim, et al., 2002). Also Jarusutthirak, et al., (2007) observed that NOM deposition on the membrane surface was able to increase the salt rejection (Jarusutthirak, et al., 2007). Because the majority of NOM was negatively charged at natural pH, the membrane surface could exhibit a higher negative charge (Shim, et al., 2002) which enhanced the rejection of anions.

In our case, the improved rejection of sulphate might be due to NOM fouling. Generally, NOM fouling causes flux decline (Jarusutthirak, et al., 2007; Lee, et al., 2005). Moreoever, Winter, et al. (2017) indicated that the fouling-dominant of flux decline could be predicted from the recovery of the flux of clean water after treating NOM-containing solution. Based on the flux graph during the experiment (Appendix B), the flux recovery after treating brine (ultrapure water flux post-brine filtration) was the lowest for both membranes. Besides, the study from Winter, et al. (2017) revealed that fouling was found to be dominant (over concentration polarization) to increase the resistance to the permeate flow when the recovery after treating the NOM-containing water was low. This suggests that the increase of sulphate rejection in our experiment was due to the NOM fouling.

Furthermore, the removal of NOM during our IEX brine rejection experiments was high, above 90% for both membranes. Besides increasing the salt rejection, NOM presence was also able to enhance the NOM removal itself. Higher NOM rejection with increasing NOM concentrations was also observed Jarusutthirak, et al. (2007); the increasing NOM concentration altered the NOM rejection up to 13%. Thus, the high NOM rejection in our experiment might be the result of

enhanced removal from the presence of a high NOM concentration in the brine (compared to the concentration of NOM in surface water, which is 0.1-20 mg/L) (Volk, et al., 2002).

4.3 Batch-sulphate precipitation experiment

4.3.1 Sulphate removal model

To model the high salinity solution, the Pitzer database was used instead of the default PhreeqC database. Pitzer database origins from Pitzer modelling which provides more accurate calculation by measuring the activity coefficients that affect the solubilities in concentrated solutions (Appelo, 2015). This model proposes an approach of ion-interaction which relies on empirical coefficients in describing the ion complexation at high ionic strength (Dudal & Gérard, 2004). All manuscripts of PhreeqC modelling of this research can be found in Appendix C.

In order to estimate the right dosage of chemicals to be added to the brine, several barium and calcium salt ($BaCl_2.2H_2O$ and $CaCl_2.2H_2O$) concentrations are modelled to see the removal efficacy. The results of the modelling are shown in Figure 4.5 and Figure 4.6. The model shows that sulphate removal is very effective using barium salt, almost 100% removal with a molar dose ratio $Ba:SO_4$ of 1. The calcium salt is less effective, with 75% sulphate removal with a molar dose ratio $Ca:SO_4$ of 1.

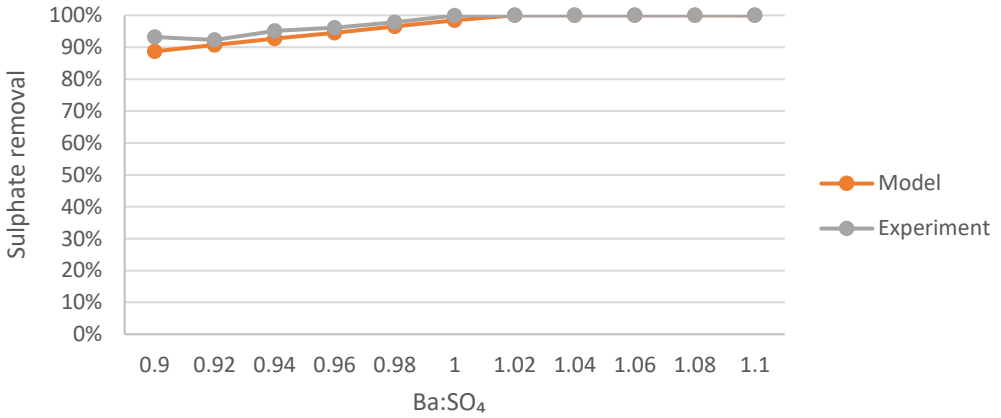

Figure 4.5. Modelling result of sulphate removal efficacy using barium salt

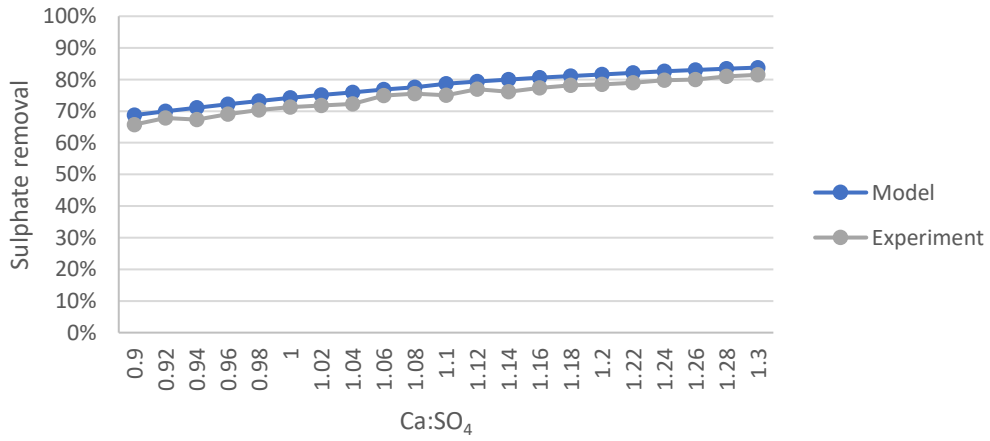

Figure 4.6. Modelling result of sulphate removal efficacy using calcium salt

The results of the modelling were confirmed by validating the modelling through experiments and the results of the experiments were almost the same as the prediction from the model.

Although not all the experimental results perfectly fitted to the model results, the maximum deviation for both models was only 3%.

Calcium sulphate precipitate exists in different forms, but in this case, it was considered as gypsum, due to the temperature of the experiment. Based on a previous study, the transition temperature between gypsum and anhydrate is 58°C in pure water and decreases to 25°C in NaCl electrolyte of 6 molal (He, et al., 1994b). The composition of NaCl in the synthetic brine in the experiment was way lower than 6 molar, therefore, at room temperature, it can be assumed that only gypsum was generated in the precipitation process. Consequently, the properties of gypsum were used to compare the sulphate removal from the brine over the properties of barite precipitation.

Based on Figure 4.7 and Figure 4.8, the differences in the removal efficacy between barium and calcium salt addition are evident. In the precipitation process, solubility product is the key for removing the sulphate through chemical precipitation. The solubility product of gypsum is 4.9 x 10^{-5}, while the solubility product of barite is 1.1 x 10^{-10} (Hendricks, 2006). Gypsum solubility is 10^{5} higher than barite which means the required molar ratio between calcium and sulphate will be higher compared to barium and sulphate ratio to have similar sulphate removal. The remaining ions concentration in the brine is also interesting to be considered for the choice of the chemical to remove the sulphate. The concentration of the remaining calcium, sulphate and barium in the brines were modelled with PhreeqC and validated through experiment as shown in Figure 4.7 and Figure 4.8.

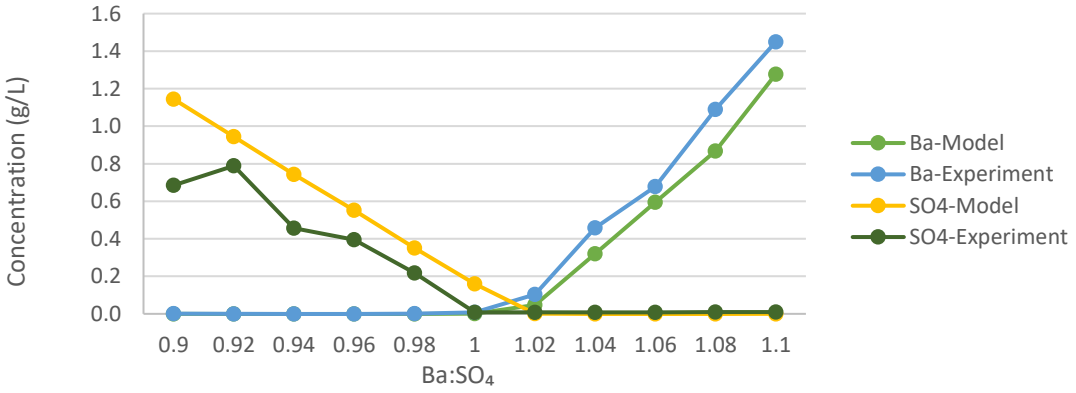

Figure 4.7. Remaining concentration of sulphate and barium in the brine

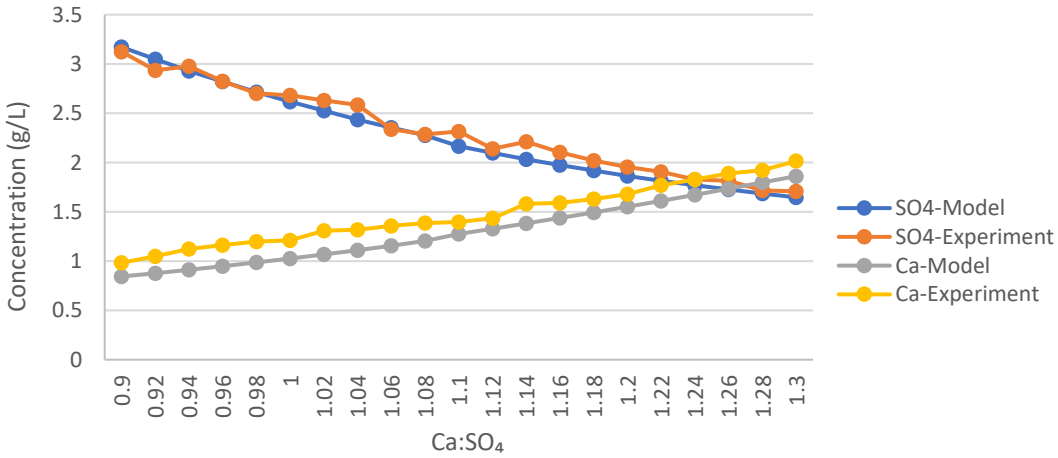

Figure 4.8. Remaining concentration of sulphate and calcium in the brine

Figure 4.7 and Figure 4.8 show that the addition of barium salt was effective to completely remove the sulphate from the brine. When $Ba:SO_4=1$, all sulphate was completely removed based on the result of the experiment. In the case of calcium salt addition, the remaining sulphate concentration was still above 1 g/L even with lattice ion ratio 1.3. In order to achieve very low sulphate concentration with calcium salt, an overdose was thus required. Yet, based on Figure 4.8, once the sulphate concentration was very low, there would be an excess of calcium ions which might lead to scaling problems in further treatment.

Barium and calcium salt have their advantages and disadvantages in removing the sulphate through precipitation. Barium was obviously very effective in removing the sulphate, yet it was toxic even in small concentrations. Calcium was not toxic, but to remove sulphate completely, extremely high overdose was required. Since the aim of sulphate removal in this research is 95%, an additional model was made to estimate how high the dosage of calcium salt should be added to achieve this goal, as shown in Figure 4.9. According to the model, the target was never achieved even with an ion concentration ratio up to 10. Therefore, barium salt was preferred to be used for further experiments.

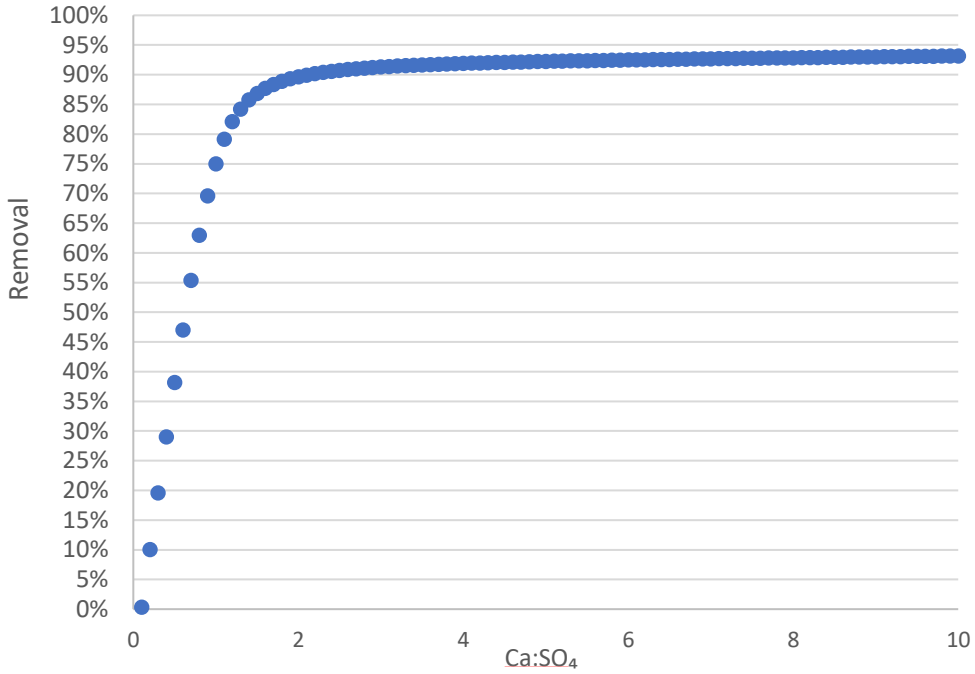

Figure 4.9. Overdosed calcium salt for sulphate removal

4.3.2 Sulphate removal experiment in synthetic brines

The initial sulphate concentration of the brines used for modelling and the sulphate concentration in synthetic brines for the sulphate removal experiments were different. For the modelling, the initial sulphate concentration was set to be 10 g/L, while the initial concentration of sulphate for sulphate removal experiment was adjusted to the desired final ionic strength of the brine (e.g. 0.1 M, 0.5 M). Because of that, modelling of sulphate removal at different ionic strengths was done before the experiments with IEX brine were performed. The result of the model and the experiments on sulphate removal in different ionic strength solutions is depicted in Figure 4.10

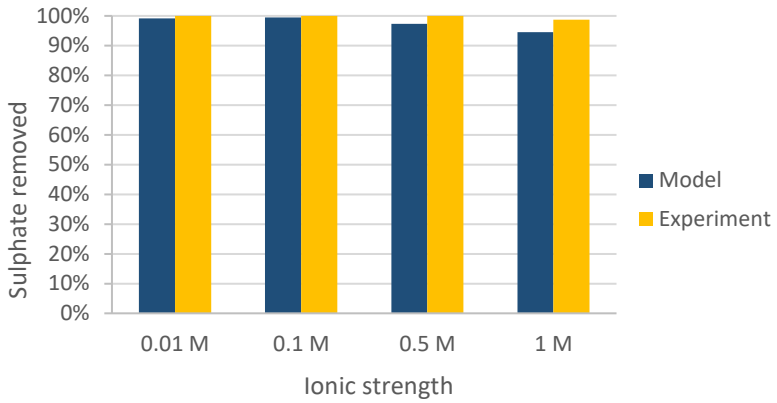

Figure 4.10. Result of sulphate removal using chemical precipitation in batch experiment

The experimental results confirm that barium salt was effective to remove the sulphate at different ionic strengths of the brine. However, there was a very slight decrease in sulphate removal from lower (0.01 M) to higher (1 M) ionic strength, of 5% for the model and 1% for the batch experiment. A possible cause of this slight decrease of sulphate removal is the decreasing activity of barium and sulphate under higher ionic strength environment (Azaza, et al., 2017; Risthaus, et al., 2001).

From Eq. (1), it is clear that ion activity affects the supersaturation, and the relationship is proportional. Supersaturation decreases as ion activity decreases. Hence, in high ionic strength condition, where the ion activity is lower, the supersaturation will also lower. As a result, the driving force for precipitation is less, and this might affect the nucleation stage in precipitating sulphate with barium salt. Furthermore, Debye-Hückel theory can be used in describing the relationship between ion activity and ionic strength of the solution. However, this theory is only valid for the dilute solutions (I < 0.01 M), while for higher ionic strength, equations from Davies (Eq.(9)) and Truesdell and Jones (Eq (10)) are commonly used (Appelo & Postma, 2010).

$$\log \gamma = -Az^2 \left(\frac{\sqrt{I}}{1 + \sqrt{I}} - 0.3I \right) \tag{9}$$

Where γ denotes ion activity, A is temperature dependent constant, z is ion charge, and I is ionic strength.

$$\log \gamma = -\frac{Az^2\sqrt{I}}{1 + Ba\sqrt{I}} + bI \tag{10}$$

Where parameter γ, A, z, and I are similar to Eq.(9), while a and b are ion-specific fit parameters.

Ionic strength is defined as the combined effects of the activities of several ionic species in a solution (Davies & Collins, 1971). Davies equation and Truesdell and Jones equation are often used to calculation solution with ionic strength up to 0.5 M and 2 M, respectively. To prove the decreasing ion activity in this research, both equations are used, as the Davies equation represents the divalent ions (Ba^{2+} and SO_4^{2-}), while, Truesdell and Jones equation represents specific ion activity. However, barium ion activity is not possible to be calculated here due to the scarcity of the data resource for the ion-specific fit parameters (a and b from Eq. (10)) of barium ion. Table 4.3 indicates the values of the parameters used for calculating the ion activity and the results are shown in Table 4.4.

Table 4.3. Parameter values for ion activity calculation (Appelo C. A., 2015)

Parameter	Davies	Truesdell and Jones
A	0.5085	0.5085
B	-	0.3285×10^{10} /m
a (SO_4^{2-})	-	5×10^{-10} m
b (SO_4^{2-})	-	-0.04

Table 4.4. Ion activity for synthetic brines

Ionic strength	Davies	Truesdell and Jones
0.01 M	0.66	0.67
0.1 M	0.37	0.38
0.5 M	0.29	0.21
1 M	-	0.15

Table 4.4 shows the decrease of ion activity due to the increase of the ionic strength. Moreover, even though the ion activity of barium ions were not calculated, it can be seen from the ion activity of the sulphate that decreased as the ionic strength increased. Therefore, a similar trend is also expected for barium ion activity. However, it seems that the lowering of the activity coefficient did not match with the actual sulphate removal since the reduction of the removal was not as much as the reduction of the ion activity.

In addition, ionic strength can also contribute in decreasing the interfacial tension between solution and solid surface which leads to increasing solubility (Boerlage, et al., 2000; Risthaus, et al., 2001). This is substantial in the nucleation phase because surface nucleation depends on the number of growth sites available initially and the degree of saturation (Nancollas & Purdie, 1963). It is clear that, with higher solubility, ions tend to dissolve than to form nuclei which reduce the growth site to initiate the precipitation.

4.3.3 Sulphate removal in IEX brine

A sulphate removal experiment was conducted using the IEX brine as well. However, the modelling was not performed due to the complexity of the brine composition which contains NOM, compared to a brine that only contains inorganic salts. Sulphate was removed by 84% by precipitation using barium salt with a dosage of 5.7 g/L. With the estimated ionic strength of the IEX brine, the removal of the sulphate was expected to be higher than 90% according to Figure 4.10. This precipitation was retarded, and it can be accounted to the presence of NOM in IEX brine. In this research, using the LC-OCD analysis, NOM was represented as total organic carbon (TOC). The LC-OCD characterization for the IEX brine used in this research indicated that 76.3% of TOC was detected as humic substances (Table 4.5), which comprised of humic acid and fulvic acid. Both compounds were known to be able to form complexes with metals, such as barium (Boerlage, et al., 1999) since they have a high complexation affinity (Kim, et al., 1990). A study from Schäfer, et al. (1998) revealed that organics were able to inhibit inorganic precipitation, yet, in a high degree of uncertainty due to the complex mixture of compounds in NOM. Furthermore, humic substances could be adsorbed onto freshly formed nuclei and inhibit the crystal growth which led to a slower bulk concentration reduction (Boerlage, et al., 2000), which was the sulphate concentration in our case.

Table 4.5. LC-OCD fractionation for IEX brine (Het Waterlaboratorium, 2019)

Fraction	Concentration (% TOC)
Biopolymer (>20,000 Da)	0.3
Humic substances (1000 Da)	76.3
Building blocks (350-500 Da)	16.4
Low molecular neutral (< 350 Da)	9.2
Low molecular acids (< 350 Da)	0

4.3.4 NOM removal through chemical precipitation

Along with sulphate removal, NOM was also removed during the precipitation in IEX brine by 23%. This has been previously explained regarding retarded barite precipitation (section 4.3.3). Further, the removed NOM would be mainly humic substances (humic and fulvic acid) since it was the biggest fraction of TOC in IEX brine used for this research (Table 4.5).

The removal of NOM during precipitation was difficult to estimate because the solubility product of NOM is largely unknown due to the complexity of the compounds present in NOM. Yet, some components may form insoluble complexes with multivalent ions and precipitate subsequently (Schäfer, et al., 1998). The ability of NOM, especially humic substances, to interact with ion is caused by the different functional groups where the ion can bind (Benedetti, et al., 1996). These functional groups are carboxylic and phenolic groups, which exhibit negative charge (Kinniburgh, et al., 1999; Ritchie & Perdue, 2003). Specifically for fulvic acids, these functional groups are commonly associated with alkaline earth metals and transition metals (Saar & Weber, 1982). These two explanations suggest that humic substances reacted with barium ions, as barium is a positively charged ion and one of the alkaline earth metals. In addition, humic substances adsorption onto barite precipitates, as explained in section 4.3.3, enhanced NOM removal.

4.4 Integrated sulphate removal

For the integrated sulphate removal with NF and precipitation, we tested one membrane, C01. The combination of chemical precipitation using barium salt and ceramic NF membrane resulted in a high removal of sulphate (Figure 4.11). For synthetic brines, the removal was 100% (Figure 4.12) because the sulphate had been completely removed during the chemical precipitation step. Whilst, for the IEX brine, the removal of the sulphate (86%) did not reach the target (95%). Similar to the salt rejection experiment, the rejections of chloride and sodium were near zero or even negative. The concentration of sodium and chloride in each step of the integrated approach are depicted in Figure 4.13 and Figure 4.14, respectively. Besides sulphate and sodium, some NOM were also removed and the NOM concentration in each step within the integrated treatment is depicted in Figure 4.15. In the following sections, the results of the chemical precipitation step and the ceramic NF step are discussed separately for the IEX brine.

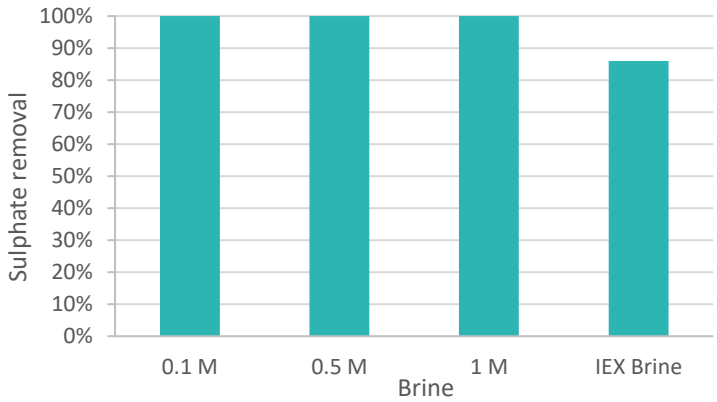

Figure 4.11. The overall result of integrated sulphate removal for the synthetic brines and in the IEX brine

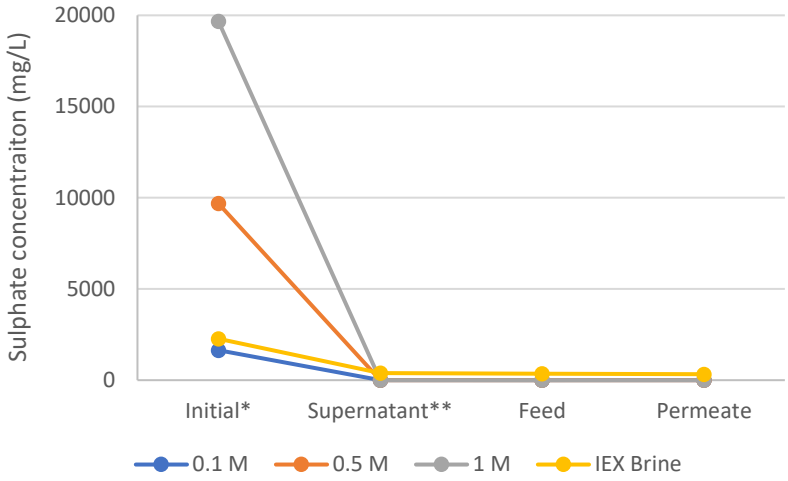

Figure 4.12. Sulphate concentration in integrated sulphate removal

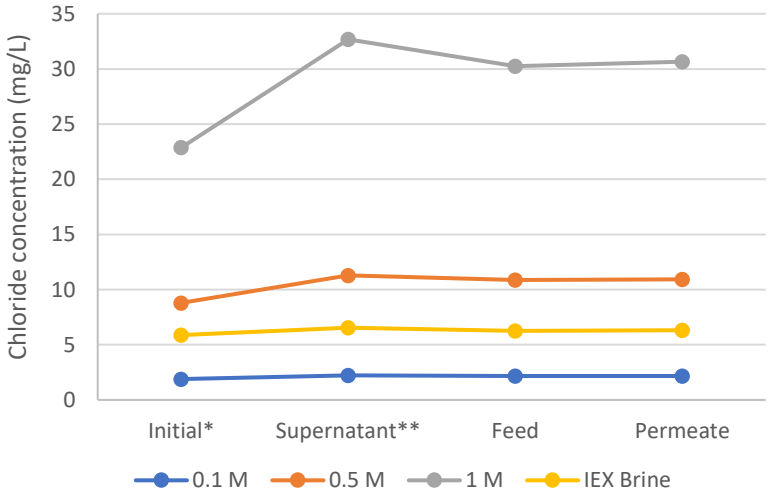

Figure 4.13. Chloride concentration in integrated sulphate removal

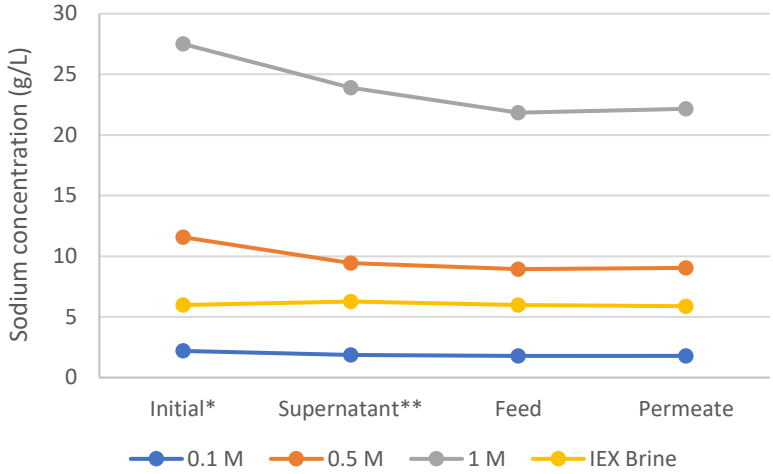

Figure 4.14. Sodium concentration in integrated sulphate removal

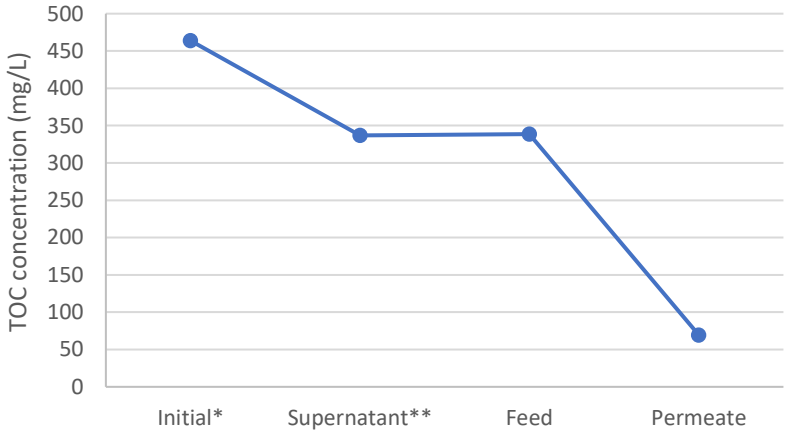

Figure 4.15. TOC concentration in each step of integrated sulphate removal

**initial: untreated brine (before barium salt addition)*
***supernatant: liquid part of the solution after precipitation*

4.4.1 Chemical precipitation

With chemical precipitation, 83% of sulphate and 27% of NOM were removed, similar to the results of the batch experiment. These results can be explained in the same way as the explanation in the batch experiment results. The supernatant from this step was used as the feed for the ceramic NF step. To compare the results of the NF step with the salts rejection tests of section 4.2, the ionic strength of the supernatants was calculated in Table 4.6.

Table 4.6. Ionic strength of supernatant

Ionic strength	Concentration (mol/L)			Calculated ionic strength
	SO_4^{2-}	Cl^-	Na^+	
0.1 M	0	0.064	0.081	0.07
0.5 M	0	0.318	0.41	0.36
1 M	0	0.922	1.039	0.98
IEX Brine	0.003	0.18	0.26	0.23

The ionic strength of the feed from the supernatant after precipitation was already altered with the additional chloride from $BaCl_2.2H_2O$ salt addition. Table 4.7 shows the increase of chloride concentration in the brine after precipitation in comparison with the expected increase based on stoichiometry calculation.

Table 4.7. Chloride concentration after precipitation step

Solution		Cl (mg/L)	Cl increase (mg/L)	Expectation (mg/L)
0.1 M	Initial	1891.4	335.2	1181.5
	Supernatant	2226.6		
0.5 M	Initial	8794.2	2493.8	6643
	Supernatant	11288		
1 M	Initial	22869	9811.8	11814.9
	Supernatant	32680.8		
Brine	Initial	5879.4	668	1628.9
	Supernatant	6547.4		

Based on Table 4.7, the increase in chloride concentration does not meet the expectation. However, this result is still unexplainable considering that the sulphate in the synthetic brines was completely removed (Table 4.6). Therefore, the effect of mixed ions' presence in the brine during the precipitation process needs to be further investigated.

4.4.2 Ceramic NF membrane

The changes in the ionic strength between untreated brines and supernatant after precipitation were low, as shown by the change of electrical conductivity (Table 4.8). This explains the reason why the results of chloride and sodium rejection, as depicted in Figure 4.13 and Figure 4.14, were similar to the results from the salt rejection experiment.

Table 4.8. Conductivity of the brine after precipitation

Initial ionic strength	Conductivity (mS/cm)	
	Initial	Supernatant
0.1 M	9.3	8.6
0.5 M	40.3	37.3
1 M	69.2	66.8
IEX Brine	23.2	23.5

Most of the NOM or DOC was removed by NF by 80%, while the sulphate was rejected by only 7%. The overall rejection with the combination of precipitation and NF was 85% for TOC and 86% for sulphate. The overall rejection gave different results from the NF experiment of section 4.2, where NF removed more than 90% of DOC and 19% of sulphate. This lower rejection rate might be attributed to the precipitation step. It is assumed that humic substances were the part of DOC that precipitated with barite. As mentioned in the previous explanation, 76.3% of TOC was comprised as humic substances, while the remaining part consisted of 16% building blocks and 9% low molecular weight neutral compounds based on the NOM characterisation (Table 4.5).

Humic substances have a relatively high molecular weight with the size around 1000 Da, while building blocks size is in the range of 300-500 Da and low molecular weight neutral size is less than 350 Da. By assuming that only humic substances were precipitated, it can be assumed that 27% of the large compounds were precipitated, hence the fouled TOC layer on the membrane surface might be not as dense as in the salt rejection experiment. As the results, smaller organic compounds can pass the membrane due to their smaller size than membrane MWCO, and more sulphate can permeate through the membrane.

5 Improvement of Sulphate Removal

5.1 Ettringite precipitation

This research has proven that barium salt was able to effectively remove sulphate from IEX brine. However, the use of barium in drinking water treatment may give some concerns due to its toxicity. We also studied sulphate precipitation using calcium salt, which is not toxic, but it has a drawback, i.e. the solubility of calcium sulphate is high, which gave a low efficacy in sulphate removal. An alternative precipitation method is given by a co-precipitation reaction that forms ettringite mineral. A previous study mentioned that ettringite precipitation was able to remove 99.5% of sulphate from dye effluent (Kabdaşli, et al., 2016). This method has been also studied to treat industrial wastewater, such as aluminium anodizing, textile wastewater, and mine water (Fang, et al., 2018).

Ettringite consists of calcium, aluminium and sulphate, and has a very low solubility (log Ksp = -43.13) (Almasri, et al., 2015). This mineral is naturally occuring as a secondary fracture-lining mineral in calcium-rich igneous rocks (Perkins, 2000). Ettringite is also commonly found in concrete as an important hydration product of Portland and super-sulphated cement, together with monosulphate (another calcium sulfoaluminate mineral), and is also used as a coating for paper (Clark & Brown, 1999; Perkins, 2000). The formation of ettringite is given by Eq. (11).

$$6\ Ca^{2+} + 2\ Al(OH)_4^- + 3\ SO_4^{2-} + 4\ OH^- + 26\ H_2O \rightarrow Ca_6[Al(OH)_6]_2(SO_4)_3.26H_2O \qquad (11)$$

In spite of its very low solubility, ettringite formation requires certain conditions. Ettringite precipitation is pH-dependent and not favourable at around a near-neutral pH. At near-neutral pH, ettringite will completely dissolve, even with excessive aluminium salt addition at mild pH (5-9) (Germishuizen, et al., 2018; Tait, et al., 2009). Some studies found that ettringite is stable at alkaline pH with the optimum to be at around pH 12, as depicted in Figure 5.1.

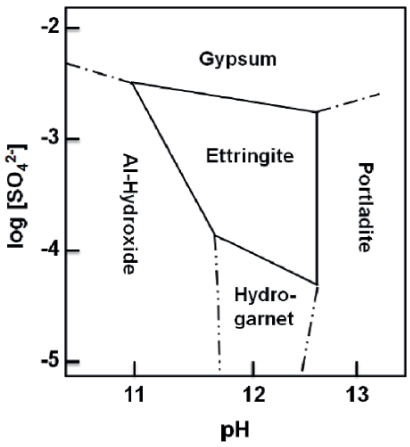

Figure 5.1. Ettringite stability in alkaline pH (Germishuizen, et al., 2018)

Also, high concentrations of anions in the solution affects the sulphate removal through ettringite precipitation due to the competition between anions and sulphate to bind with calcium and aluminium ions (Fang, et al., 2018).

5.2 Theoretical analysis: PhreeqC modelling of ettringite precipitation

For modelling ettringite precipitation, the Pitzer database had to be modified because the speciation of aluminium and ettringite phase were not available in the database. The additional data were extracted from llnl.dat, which was a large database containing minerals in a large range which can be found in Appendix D. Additional data, calculation, and manuscript for Ettringite modellingdix D. To validate the initial model with the modified database, the model was compared to the results of the experimental work of Almasri, et al. (2015). The description and the result of the model is indicated in Table 5.1 and Table 5.2.

Table 5.1. Initial ettringite model description (Almasri, et al., 2015)

Model description	Sulphate removal from synthetic NF rejected brine using calcium salt and ettringite precipitation in 2 stages.
Stage 1	Reducing initial sulphate concentration from 97 mM to 12.1 mM using $CaCl_2$ with lattice ion ratio of 2. In this stage, $CaSO_4$ formed.
Stage 2	Subsequent ettringite precipitation by adding lime ($Ca(OH)_2$) and sodium aluminate ($NaAlO_2$). Lattice ion ratio between lime and sulphate was 100% and between sodium aluminate and sulphate is 67%. Final sulphate concentration was 4 mM.

Table 5.2. Comparison of initial model and previous experiment

Stage	**Almasri, et al. (2015)**		**Initial Model**	
	SO_4^{2-} (mmol/L)	**SO_4^{2-} removal**	**SO_4^{2-} (mmol/L)**	**SO_4^{2-} removal**
Initial	97		97	
Stage 1	12.1	87.5%	11.3	88.3%
Stage 2	4	66.9%	3.5	69%
Overall	95.9%		96.3%	

The difference between the results of the initial model and the previous study was small, therefore the model was used for further modelling of ettringite precipitation. As previously mentioned, ettringite precipitation is pH-dependent. Ettringite is stable at pH above 10.7 (Germishuizen, et al., 2018), but Almasri, et al. (2015) found that the optimum pH is between 11 and 12.5, which is also supported by a study from Fang, et al. (2018). Besides pH, ion concentration ratio between sulphate, lime, and sodium aluminate are also important. The experiment of Almasri, et al. (2015) used 100% and 67% of remaining sulphate concentration (from first stage) for lime and sodium aluminate dosage, respectively, was due to the stoichiometry of the ettringite empirical formula. Adding the salts above these number will not give significant sulphate removal.

These optimum conditions for ettringite precipitation were used to improve the previous model of sulphate removal using calcium salt addition. The conditions used for improving the sulphate removal are indicated in Table 5.3. Figure 5.2. depicts the improvement of sulphate removal by enhancing the model with ettringite precipitation.

Table 5.3. Setup of sulphate removal modelling with ettringite

Parameter	**Value**
Initial pH	8
Initial sulphate concentration	104 mmol/L (10 g/L)
$Ca:SO_4$ (Stage 1)	0.90-1.30
Lime ratio (Stage 2)	100%
Sodium aluminate ration (Stage 2)	67%
Working temperature	23°C

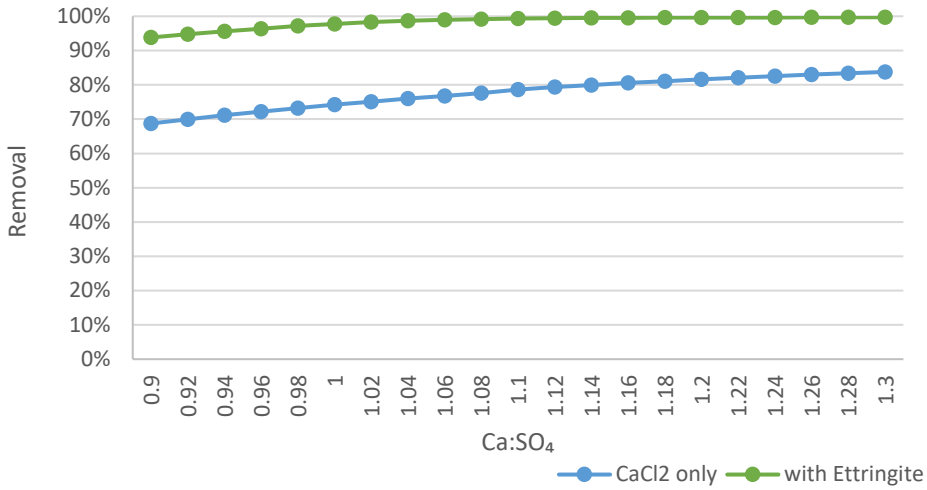

Figure 5.2. Improvement on sulphate removal using ettringite precipitation

The sulphate removal was improved by applying ettringite precipitation after gypsum precipitation. Therefore, this method can be an alternative to remove sulphate from the brine to prevent the possibility of using barium in drinking water treatment. For this purpose, further modelling with IEX brine was performed. However, the modelling only used the known composition of the brine from the result of IC analysis and was not including NOM. The setup of this model is shown in Appendix D.Appendix D. Additional data, calculation, and manuscript for Ettringite modelling

In this modelling, $CaCl_2$ was chosen instead of lime because the hydroxide from the lime would increase the pH, however, the final pH for this modelling was intended to be as close as the initial pH. This is because NOM can act as a solution buffer and the pH increase by lime will be uncertain. Therefore, the pH in this system was set to be controlled by NaOH (see Appendix D). Results of the modelling IEX brine with ettringite precipitation are shown in Table 5.4.

Table 5.4. Result of ettringite precipitation model in IEX brine

Simulation	Ca:SO_4	Remaining SO_4 (mmol/L) (Stage 1)	$NaAlO_2$ (mmol/L)	$CaCl_2$ (mmol/L)	SO_4 Final (mmol/L)	SI Ettringite	pH Final	SO_4 Removal
1	1	23.95	16.05	-	23.96	-7.70	8.8	0%
2	1	23.95	16.05	23.95	23.96	-6.15	8.8	0%
3	2	19.84	13.29	-	19.85	-6.69	8.8	16%
4	2	19.84	13.29	19.84	19.85	-6.69	8.8	16%
5	2	19.84	13.29	19.84	19.85	-6.69	9.0	16%
6	2	19.84	13.29	19.84	19.85	-6.69	10.0	16%
7	2	19.84	13.29	19.84	15.12	0	10.5	36%
8	2	19.84	13.29	19.84	7.85	0	11	67%
9	2	19.84	13.29	19.84	3.83	0	11.5	84%
10	2	19.84	13.29	19.84	1.74	0	12	93%
11	2	19.84	13.29	19.84	0.75	0	12.5	97%
12	3	15.63	10.47	-	15.6	-6.40	8.8	34%
13	3	15.63	10.47	15.63	15.6	-5.99	8.8	34%
14	3	15.63	10.47	15.63	11.6	0	10.5	51%
15	3	15.63	10.47	15.63	0.94	0	12	96%

Based on the results of the modelling, it can be concluded that the important factors to remove sulphate from the brine were the initial ion concentration ratio between calcium and sulphate, and the pH condition where ettringite precipitation takes place. Excess of calcium alone did not improve the removal of the sulphate, relatively high $Ca:SO_4$ (4:1 according to Fang, et al., (2018)) in the second stage was also important. It is clear that the pH determined whether the ettringite was able to precipitate or not, and it determined how much sulphate can be removed. To remove sulphate as much as targeted (95%), the pH should be adjusted to at least 12 with the concentration of calcium in the first stage was three times of the initial sulphate concentration. However, this result might differ in real application due to NOM presence that, based on experiments with barium salt, can retard the precipitation process.

6 Implementation of Sulphate Removal Alternatives

In the end, this research shows there are two alternatives in removing sulphate from the brine: integrated approach (combination of chemical precipitation and ceramic NF) and ettringite precipitation. Each option has its own advantages and disadvantages. To predict the suitable alternative for the full-scale implementation, some considerations need to be reviewed. Cost estimation and assessment of environmental impact using LCA are used to consider the economic and environmental burden of the treatment methods. The overall analysis of the assessment would be explained in the next sections.

6.1 Cost estimation

In order to make the treatment alternatives comparable to one another, a similar unit reference is required. In this case, the treatment alternatives were compared based on the cost estimation to treat 1 m^3 of IEX brine. Then, the cost for each treatment method was calculated by breaking down the component for each treatment alternative, followed by determining the unit cost of each component, and finally calculating the final cost for every treatment alternative.

Breaking down the component of the treatment alternative was intended to identify the important components (e.g. chemicals, process) of each treatment which would be considered in estimating the treatment cost. The reference for the ceramic NF and integrated sulphate removal is from the experiment of our research (e.g. materials, chemical concentration), while the alternative of ettringite precipitation is based on the modelling setup and assumptions of additional material that might be needed. All components are divided based on the treatment method as shown in Table 6.1 and Table 6.2.

Table 6.1. Integrated sulphate removal treatment component

Component	Unit	Value
Chemical precipitation		
Barium concentration	g/L	5.77
Brine volume	m^3	1
Barium consumption	g	5772
Stirring machine	kWh	4
Mixing duration	min	10
Ceramic NF		
Pump energy	kWh	0.55
Flowmeter energy	kWh	0.006
Filtration duration	hours	5.6
Membrane cleaning		
Sodium hypochlorite	%	0.2
	mL/L	12.5
Solution volume	L	0.3

Table 6.2. Ettringite precipitation treatment component

Component	Unit	Value
Precipitation Stage 1		
Calcium concentration	g/L	10.42
Brine volume	m^3	1
Calcium consumption	g	10423
Stirring machine	kWh	4
Mixing duration	min	10
Precipitation Stage 2		
Calcium concentration	g/L	1.73
Sodium aluminate concentration	g/L	0.86
NaOH concentration	mL/L	4.11
Brine volume	m^3	1
Calcium consumption	g	1731
Sodium aluminate consumption	g	858
NaOH consumption	mL	4107
Stirring machine	kWh	4
Mixing duration	min	10
Ceramic NF		
Pump energy	kWh	0.55
Flowmeter energy	kWh	0.006
Filtration duration	hours	5.6
Membrane cleaning		
Sodium hypochlorite	%	0.2
	mL/L	12.5
Solution volume	L	0.3

Based on Table 6.1 and Table 6.2, filtration duration was longer than the duration in the experiment (section 3.4.1). The duration for this calculation has been adjusted to treat 1 m^3 of the brine using the same membrane in the experiment. Also, the concentration of the chemical was calculated based on the sulphate concentration in integrated sulphate removal experiment. After identifying the component of each treatment method, the unit cost for every component was determined. Then, the total cost of each treatment method could be calculated. The unit cost and total cost of all treatment alternatives can be found in Appendix E. In general, capital expenditure (CAPEX) was also considered to estimate the cost of an item. However, the calculation in this section only considered the operational cost to treat 1 m^3 IEX brine.

Based on the calculation of the operational cost, the two options have different cost due to the chemicals required for precipitation. The treatment using integrated approach costs €175.20/m^3, while the ettringite precipitation approach has an extreme cost of €653.08/m^3. If the comparison only considers the cost, integrated sulphate removal could be an option. However, it has a drawback in toxicity. Further explanation regarding the toxicity and impact of each chemical (barium and calcium salt) will be provided in the next section (section 6.2).

6.2 Environmental impact assessment

One way to assess the potential environmental impact of utilizing certain chemicals is by using Life Cycle Assessment (LCA). LCA is a tool to assess environmental impact of a product associating with all stages of product's life from raw material extraction to material usage (cradle-to-grave) (Muralikrishna & Manickam, 2017) by identifying and describing the required energy and materials, as well as the emission and the waste released to the environment, qualitatively and quantitatively (Rentizelas & Georgakellos, 2014). In this case, both treatment alternatives were analysed using LCA to assess the potential environmental burden of the chemical used to remove the sulphate from the IEX brine. However, this LCA analysis only considers the impact of the chemical production, not the toxicity of calcium and barium salt themselves.

LCA is standardized in ISO 14040 and based on the standard, the steps of performing LCA consists of 4 stages (Muralikrishna & Manickam, 2017; Thannimalay, Yusof, & Zawawi, 2013):
a) Goal definition and scoping
b) Life cycle inventory
c) Impact assessment
d) Intepretation

The detailed explanation regarding the LCA stages of this research are discussed in the following sections.

6.2.1 Goal definition and scoping

This stage determines the boundaries, process scope (how far the of the product life cycle will be taken to account on the assessment), and functional unit of process alternatives (Muralikrishna & Manickam, 2017; Pillay, et al., 2002). Functional unit is defined as a quantitative description or service to be assessed (i.e. 1 m^3 of groundwater, 1 L of crude oil) (Bjørn, et al., 2018). This forms a basis for comparison.

For this research, LCA was conducted on the chemicals used for the treatments of IEX brine to produce 1 m^3 of permeate using ceramic NF membrane. As the first step, the treatment processes were expressed in flow diagrams to define the input and output of each process as depicted in Figure 6.1 and Figure 6.2.

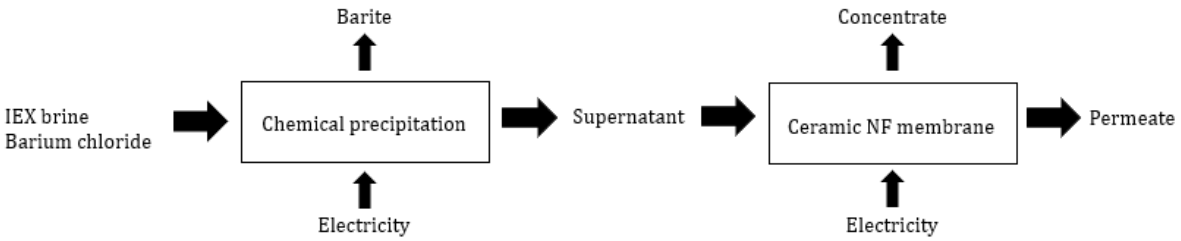

Figure 6.1. Flow diagram of integrated sulphate removal treatment

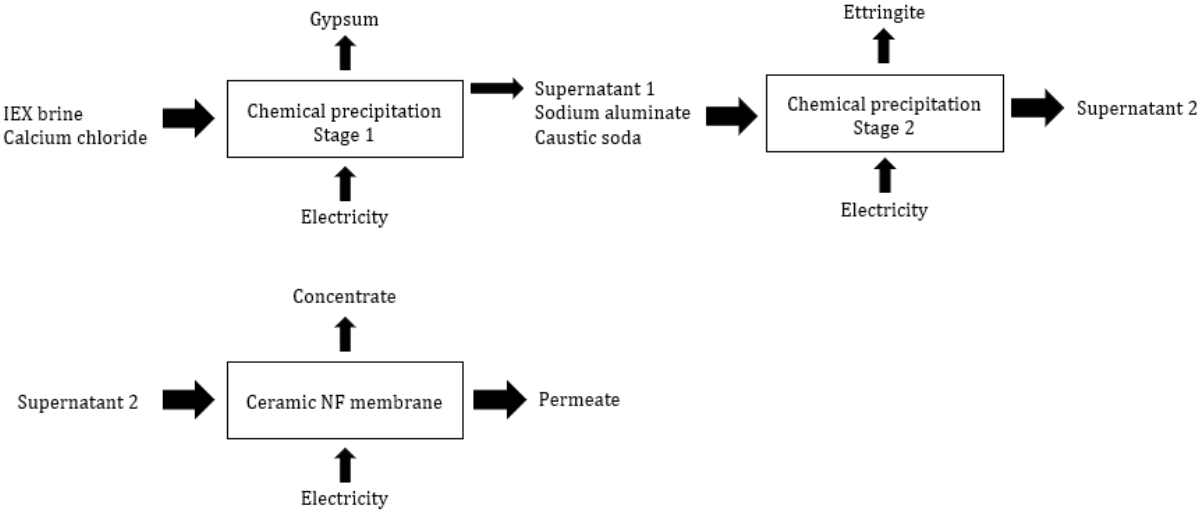

Figure 6.2. Flow diagram of ettringite precipitation treatment

The output of the LCA in our research was intended to give a general estimation on which chemical utilization would give higher potential environmental impact. Thus, a recommendation on the choice of treatment could be provided.

6.2.2 Life cycle inventory

Inventory at this stage means to collect and analyse the quantification of the product, materials, and output emissions that have been defined in the previous stage. Based on the aim of this LCA, the input and emission material of the chemical involved in the IEX brine were collected, including the production of electricity. The inventories of the chemicals were obtained from Ecoinvent database (Althaus, et al., 2007), while the electricity inventory was referred to Rentizelas & Georgakellos (2014). However, there were some chemicals that were not included in the database. For those missing chemicals from the database, the inventory was analysed based on the reaction equation as explained in Hischier, et al., (2005). In chemical precipitation stage, the loss of the solution is assumed to be zero (volume input = volume output), while the ceramic NF membrane is assumed to have recovery of 70%. Thus, the initial IEX brine volume is 1.43 m^3 to produce 1 m^3 ceramic NF permeate. The detailed inventory input for the calculation are provided in Appendix F.

6.2.3 Impact assessment

The flows summarized in the inventory stage were evaluated for the potential impacts from the input and the output. At the end, this stage will give an outcome in a form of certain scores for potential environmental impacts. These certain scores are generated from the assessment of relevant impact categories from the available impact indicator. Based on previous study, this stage consists of four steps: 1) selecting impact categories; 2) classification of impact and resource stream (assigning inventory results to the selected impact categories); 3) characterisation of the impact magnitude (calculation of indicator result); and 4) valuation of the charaterisation – normalisation and weighting methods are usually applied to generate a single potential impact score (Muñoz & Fernández-Alba, 2008; Pillay, et al., 2002).

There are several impact indicators published, such as Eco-Indicator 99, EPS 2000, CML 2001, and IMPACT 2002+ (Muralikrishna & Manickam, 2017). Each impact indicator serves different values and impact categories; therefore, the choice of the indicator should consider the goal of the LCA (Goedkoop & Spriensma, 2001). For our research, Eco-Indicator (EI-99) is used to assess the potential environmental impact of barium and calcium addition for IEX brine treatment.

EI-99 is chosen because the indicator assumes that the damages occurred in Europe (Goedkoop & Spriensma, 2001). The damages are further classified to midpoint and endpoint categories. Midpoint represents the mechanisms where several substances can contribute to a similar impact, while endpoint indicates the issues that can be appeared or experienced in daily life (Ahlroth, 2014). This impact indicator has three endpoints: human health, ecosystem quality, and resources; in which each endpoint has several midpoints categories. Every endpoint is expressed by different unit. The description of the endpoints, midpoints, and the unit of each endpoints are described in Table 6.3.

Table 6.3. Impact categories of EI-99 (Goedkoop & Spriensma, 2001)

Endpoint	Midpoint	Unit	Unit description
Human health	Carcinogenic	DALY (Disability-Adjusted Life Years)	The unit measures the average of total amount of healthy life loss due to illness, disability, or premature death from the standard living years.
	Respiratory effect		
	Climate change		
	Ionising radiation		
	Ozone layer depletion		
Ecosystem quality	Ecotoxicity	PDF x m^2 x y (Potential Disappeared Fraction per area per time)	This unit considers all species that might be affected by the damage. The area and time included in the unit indicate that the damage is spatial and temporal dependent.
	Acidification and eutrophication		
	Land-use		
Resources	Mineral	MJ surplus	The unit represents the increase of extraction energy to extract the material. The higher the energy, the lower the remaining resources in the earth.
	Fossil fuel		

The calculation of impact assessment for this research was conducted using CMLCA (an LCA software established by Leiden University). All the input data (from life cycle inventory stage) and characterisation factors obtained from van Oers (2016) were added in the software and the results are shown in Table 6.4 and Table 6.5.

Table 6.4. Impact assessment of integrated sulphate removal

Endpoints	Midpoints		Total impact assessment
Human health	Respiratory effect (inorganic)	1.1 x 10^{-5} DALY	1.542 x 10^{-5} DALY
	Damage due to climate change	3.92 x 10^{-6} DALY	
Ecosystem quality	Acidification and eutrophication	0.21 PDF*m^2*y	0.21 PDF*m^2*y
Resources	Fossil fuel extraction	25.6 MJ	25.6 MJ

Table 6.5. Impact assessment of ettringite precipitation

Endpoints	Midpoints		Total impact assessment
Human health	Respiratory effect (inorganic)	2.01 x 10^{-6} DALY	4.49 x 10^{-6} DALY
	Damage due to climate change	2.48 x 10^{-6} DALY	
Ecosystem quality	Acidification and eutrophication	0.0384 PDF*m^2*y	0.0349 PDF*m^2*y
Resources	Mineral extraction	1.09 MJ	6.45 MJ
	Fossil fuel extraction	5.36 MJ	

In most assessments, the impact values are normalised and weighted to produce a final single index. However, normalisation and weighting steps are optional according to ISO standard (Muralikrishna & Manickam, 2017; Rosenbaum, et al., 2018a). A deeper knowledge is required to interpret the final single index on the impacts to the environment. Moreover, normalisation might change the result of the LCA due to the change of the common unit. Thus, the conclusion drawn from the normalisation result might differ from the impact assessment result (Rosenbaum, et al., 2018a). Therefore, our research decided to omit the normalisation and weighting steps to avoid mistakes in interpreting the LCA results.

6.2.4 Interpretation

Higher value in impact assessment result indicates higher impact on the endpoints of LCA. Table 6.4 and Table 6.5 show the impact values of all endpoint categories in the integrated sulphate removal alternative are higher than in the ettringite precipitation. It can be roughly concluded that integrated sulphate removal alternative has higher environmental impact. However, further explanations on the impact of each endpoint category might give a better understanding on the comparison between the alternatives.

For human health, the impact affects the standard living years. In this case, the standard living years is taken from the life expectancy in the Netherlands, which is 82 years old (World Bank, 2019). The results from the assessment show that the loss of the healthy life years are minuscule compared to the standard living years. Therefore, the impact of chemicals used both in integrated sulphate removal and ettringite precipitation might not be critical.

On the impact of ecosystem quality, the possibility of disappearing organisms/land in a certain area and time period of integrated sulphate removal alternative is almost 7 times higher than in ettringite precipitation alternative. Based on the contribution result of the impact assessment (Appendix F), this impact on ecosystem quality is mostly affected by the sulphur dioxide emission of fuel production for both alternatives. Integrated sulphate removal alternative emitted sulphur dioxide 5 times higher than ettringite precipitation alternative. The process in integrated sulphate removal that can increase the fuel production was only the barium salt production since the energy required for ceramic NF process is similar for both alternatives. Consequently, applying chemical precipitation using barium salt would give a higher environmental impact. Unless the barium salt could be produced with more environmental-friendly energy source.

From the impact of the resource, fossil fuel extraction was the only contributing factor (Appendix F) on the integrated sulphate removal alternative and the same process contributed the most in the ettringite precipitation alternative. Referring to the description of the unit from Table 6.3, the higher the extraction energy, the lower the remaining resource amount in the nature. Therefore, it can be concluded that the integrated sulphate removal might deplete more fossil fuel resource compared to the ettringite precipitation alternative.

Based on the interpretation of the impact assessment results, fuel production can be considered as the key process that affect the impact on the environment since it contributes to the all endpoint impact categories. Nevertheless, the impact of fuel production is more important in the ecosystem quality and resource availability. Hence, changing the source of the energy in the production of the chemicals might be a way to lower the impact on the environment.

6.3 Sensitivity analysis

LCA is one kind of complex modelling systems that includes large amount of emission released to the environment. Assumptions are likely to be used on the modelling, which might lead to the uncertainty (Wei, et al., 2016). One of the sources of the uncertainty comes from the inaccuracy of the input parameter, such as non-representative data and unavailable inventory data. This is known as the parameter uncertainty (Rosenbaum, et al., 2018b). Based on the availability of the inventory data for life cycle inventory analysis, parameter uncertainty is likely to occur due to the scarcity of the data. Also, the option to use Ecoinvent database for the analysis could give uncertainty because Ecoinvent database transformed qualitative data (e.g. expert judgement, data quality indicators) to quantitative value (Wei, et al., 2016). Because of that, sensitivity analysis was performed to investigate the sensitivity of the LCA output.

Based on the result of the chemical precipitation in the IEX brine (section 4.4), NOM affected the removal of the sulphate. Hence, higher barium concentration is required to increase the removal efficacy. Local sensitivity analysis (varying one parameter at a time) was then conducted by varying the barium concentration for integrated sulphate removal whilst the ettringite precipitation was analysed by varying the calcium concentration in the first stage. However, since the changes in calcium concentration in the first stage of ettringite precipitation altered the remaining sulphate concentration, the required calcium concentration, sodium aluminate concentration, and caustic soda concentration for the second stage also changed. Therefore, all chemical concentration in the second stage of ettringite precipitation were also varied in the sensitivity analysis. For barium concentration, the analysis was conducted by varying the barium to sulphate ratio from 1 to 2, while for the ettringite precipitation, the variation of calcium to sulphate ratio was varied from 3 to 4. The results of the sensitivity analysis are shown in Table 6.6 and Table 6.7.

Table 6.6. Sensitivity analysis of LCA result of integrated sulphate removal

Ba:SO_4	**Output Change of LCA Impact Assessment**		
	Human health	**Ecosystem quality**	**Resource**
1	Reference point*		
1.2	14%	18%	17%
1.4	31%	35%	34%
1.6	47%	52%	52%
1.8	64%	70%	69%
2	81%	87%	86%

Table 6.7. Sensitivity analysis of LCA result of ettringite precipitation

$Ca:SO_4$	Output Change of LCA Impact Assessment		
	Human health	**Ecosystem quality**	**Resource**
3	Reference point*		
3.2	-1%	0%	-1%
3.4	-2%	0%	-1%
3.6	-2%	1%	-1%
3.8	-3%	1%	-2%
4	-3%	1%	-2%

**Reference point: the reference value which the change of output in higher concentration ratio was compared to. This point refers to the LCA result in section 6.2.3.*

From the result of the sensitivity analysis, LCA impact assessment in integrated sulphate removal was sensitive to the change of barium concentration since with the increase barium concentration, the output of the LCA impact assessment gave considerable changes. Therefore, an inaccurate addition of barium concentration could alter the impact to the environment.

On the contrary, the sensitivity analysis of ettringite precipitation showed that the LCA impact assessment was insensitive to the input of all chemicals involved. However, it was unclear whether all input parameters were insensitive. Hence, an additional sensitivity analysis was performed to investigate which parameter was sensitive to LCA impact assessment of ettringite precipitation. The additional analysis was made with two scenarios: 1) increasing only the calcium concentration in stage 1; and 2) changing the ratio of sodium aluminate to sulphate concentration from 0.67 to 1. The results of the additional sensitivity analysis are indicated in Table 6.8 and Table 6.9.

Table 6.8. Result of additional sensitivity analysis on ettringite precipitation (scenario 1)

$Ca:SO_4$	Output Change of LCA Impact Assessment		
	Human health	**Ecosystem quality**	**Resource**
3	Reference point*		
3.2	0%	0%	0%
3.4	1%	1%	1%
3.6	1%	1%	1%
3.8	1%	2%	2%
4	2%	2%	2%

Table 6.9. Result of additional sensitivity analysis on ettringite precipitation (scenario 2)

$Ca:SO_4$	Output Change of LCA Impact Assessment		
	Human health	**Ecosystem quality**	**Resource**
3	4%	3%	9%
3.2	3%	3%	9%
3.4	2%	1%	8%
3.6	1%	3%	7%
3.8	1%	4%	7%
4	0%	4%	6%

According to the result of the additional sensitivity analysis, the results of LCA impact assessment of ettringite precipitation were insensitive to all chemicals involved in ettringite precipitation. Therefore, the variation of the chemical might give low uncertainty on the result of LCA impact assessment.

6.4 Implementation suggestion

A suggestion for removing sulphate from IEX brine can be made by combining the information from the experiment results, ettringite precipitation, cost estimation, and LCA result. From the experiment results and ettringite precipitation modelling result, overdose of barium or calcium salts were required. Therefore, excess barium or calcium could present in the supernatant (later in feed water of ceramic NF).

Considering the LCA result of both alternatives, ettringite precipitation is thought-out to be a better option since it gives a lower impact to the environment. Furthermore, it is also supported by the lower toxicity level of calcium compared to barium. The literature regarding the toxicity of calcium is limited because calcium is categorised as a major mineral nutrient for living organisms (Rocha, et al., 2008). Meanwhile, barium has been reported to cause health effect in the case of ingestion (Tao, et al., 2016). Barium can also form complexation with the soil organic materials which could be taken up and accumulated in plants (Choudhury & Cary, 2001).

If the permeate of ceramic NF is intended to be reused as IEX regenerant, barium or calcium can accumulate in the regenerant fluid at some point. The accumulation of calcium can increase the risk of scaling in the treatment installations when the calcium is in contact with sulphate or bicarbonate. This will increase the maintenance cost. In the case of barium accumulation, further treatment will be required to remove the accumulated barium. This option might generate an issue to dispose the treated barium. However, if the NOM from the ceramic NF concentrate is intended to be reused (e.g. agriculture), barium or calcium bounded to NOM will be carried away. Calcium will be considered to be harmless in this case, while the barium is not desired to be present in the soil.

Nevertheless, based on the cost estimation comparison, the treatment of ettringite precipitation alternatinative requires an investment of more than 3 times than the integrated sulphate removal. Although the integrated sulphate removal offers a lower cost, but additional costs might follow to treat and dispose the accumulated barium. This could eventually be as high as ettringite precipitation. Therefore, ettringite precipitation should be considered as the alternative to remove the sulphate from IEX brine, considering the environmental impact of barium salt production and the possible impact of barium toxicity in living organisms. Yet, further analysis is required to obtain the optimum calcium dosage and operational parameter (e.g. mixing mechanisms), as well as the mitigation of the scaling risk to optimise the treatment cost of the brine.

7 Conclusion and Recommendation

7.1 Conclusion

This research focused on the following research questions.

1. *What are the effects of ionic strength on sulphate rejection on ceramic NF membrane?*

   Ionic strength affects the rejection of ions on ceramic NF membrane by decreasing the electrostatic effect on the membrane surface, which follows the theory of Donnan equilibrium. Investigation using different ionic strengths for binary and single salt solutions give similar results, indicating that the rejection decreases as the ionic strength increases. The decrease of the rejection is not linear as the rejection in 0.1 M brines was around 25% and in 0.5 M and 1 M were both less than 5%. Lower ion rejections are the result of a compressed double layer which can be predicted from Debye length in membrane pores. The calculated Debye length in this case are 0.97 nm, 0.43 nm, and 0.31 nm, for membrane treating 0.1 M, 0.5 M, and 1 M brines, respectively.

2. *To what extent the barium salts and calcium salts are able to remove sulphate from the brine through chemical precipitation?*

   Barium and calcium salt are able to precipitate sulphate from the brine by creating barite and gypsum. The precipitation is pH independent that it still gives the sulphate removal in non-buffered brines similar to the result from the model. However, calcium salt is not as effective as the removal of the sulphate and is around 70% when the ion concentration ratio is 1, compared to barium salt that gives 100% sulphate removal in similar ion concentration ratio. Improvement of sulphate removal using calcium can be made by precipitating the sulphate further into ettringite. Further, barium salt is preferred in the experiment due to its efficiency in removing sulphate from the brine. Sulphate removal using barium salt slightly decreased in higher ionic strength, but still in good efficacy (>95%). In addition, precipitation is hindered by NOM presence in the brine that the sulphate was removed around 16% lower.

3. *What is the result of the application of chemical precipitation and ceramic NF membrane on the NOM-rich IEX brine?*

   Chemical precipitation in the integrated approach shows similar results to the investigation of chemical precipitation in batch. On the contrary, ceramic NF gives a lower rejection both for sulphate and NOM. Sulphate us removed only by 7% while it is rejected as much as 19% by membrane filtration alone. Whilst, the NOM is rejected by 85%, which is 6% lower than rejection on membrane filtration only (91%). From precipitation stage, 27% of NOM is removed and it is assumed to contribute in lowering the rejection rate both for sulphate and NOM in the integrated approach.

4. *How can calcium salts precipitation for sulphate removal be improved?*

   Enhanced calcium precipitation though ettringite precipitation is proven to be able to increase the efficacy of sulphate removal from the brine. From the modelling result, the

amount of calcium and final pH solution are the most important parameters to promote ettringite formation. Therefore, it is not possible to have ettringite precipitation without pH conditioning. In our research, it is not possible to remove the sulphate using ettringite with the final solution pH close to the initial pH of the brine. From the model using the salt concentration of the used IEX brine, initial $Ca:SO_4$ = 3, $NaAlO_2$ concentration 67% of remaining sulphate from first stage, and final pH solution of 12 are the combination to attain the removal target.

5. *How large are the cost and the environemntal impact in implementing the sulphate removal methods ?*

   Ettringite precipitation alternative requires a quite high investment for the treatment (around 3 times higher than the integrated sulphate removal alternative). However, the result of LCA using Eco-Indicator 99 impact categories shows that ettringite precipitation gives lower environmental impact compared to the integrated sulphate removal.

7.2 Recommendation

This research has proved that chemical precipitation and ceramic membrane had a synergetic effect in removing sulphate from IEX brine. Yet, some results differ from the result when the investigations are conducted in separated approach (batch precipitation and membrane filtration only). Therefore, some improvements are needed to give better understanding of the phenomena that occurred during this research. Some recommendations that can be considered for future research are:

1. Salt dosage optimization

   From the results of the integrated sulphate removal approach, chemical precipitation has impacts in removing sulphate and NOM from brine. By adding the salt, the composition of the brine is altered that might lead to the changes of the brine property (i.e. ionic strength, pH). Therefore, optimization of the salt dosage will be useful to have an optimum dosage that can give a maximum removal performance both for precipitation and ceramic NF membranes.

2. Establishing precipitation model with NOM
   The modelling part in this research excludes the NOM due to the complexity of the mixture, thus, determining the parameter in the database is not easy. However, including NOM in the model will give a better prediction of the salt behavior in the precipitation process. So that, it will give better perspective in the subsequent membrane filtration stage.

3. NOM fractionation after chemical precipitation

   The composition is NOM is complex, therefore, when the chemical precipitation is applied to the NOM-rich brine, the precipitated compound of the brine is still uncertain. Some theories have been found that predict which fraction of NOM that are affected by the precipitation. Hence, NOM fractionation of the brine after the precipitation will validate the theories and give better insight of the possible NOM fouling in the membrane filtration step.

4. Experiment duration of integrated sulphate removal approach

   This research only observes the removal of sulphate during a short period (3 hours), however, the implementation in the field will require a continuous operation. Observation of this approach in longer duration is important to investigate the possibility of the NOM fouling and colloidal fouling caused by particles carried from the precipitation stage.

Furthermore, a longer duration will help to understand the possibility of metastable conditions in the mixture of brine and salt. If metastable conditions occur, the precipitation of the sulphate can be enhanced by adjusting other involving parameters (i.e. temperature).

5. Scaling up the integrated sulphate removal approach

   All the experiments are conducted in laboratory scale by using a small tubular membrane. Some experiments on a larger scale are fruitful to consider the feasibility of applying this approach in full-scale. At larger scale, operational parameters can be analysed further, such as mixing method (i.e. mixing rate, mixing basin), flow, and pressure, whether it influences the efficiency of the approach. Besides, the upgraded research scale will enable to determine the economic feasibility of this approach in full scale.

6. Deeper analysis of LCA

   LCA is a complex analysis system that requires a deep understanding to produce a comprehensive and more accurate analysis of the environmental burden caused by the sulphate removal alternatives. More knowledge is required to investigate and fill the unavailable inventory data since the inventory stage is the crucial part of LCA. In addition, performing the LCA until normalisation and weighting steps might give a better interpretation once the accuracy of inventory data is higher. Therefore, a separate research on the LCA of the sulphate removal alternatives might be required if a high accuracy of the impact assessment is needed.

Bibliography

Ahlroth, S. (2014). The use of valuation and weighting sets in environmental impact assessment. *Resource, Conservation, and Recycling, 85*, 34-41. doi:10.1016/j.resconrec.2013.11.012

Akinwekomi, V., Maree, J. P., & Wolkersdorfer, C. (2017). Using calcium carbonate/hydroxide and barium carbonate to remove sulphate from mine water. *Mine Water Environment, 36*, 264-272. doi:10.1007/s10230-017-0451-7

Almasri, D., Mahmoud, K. A., & Abdel-Wahab, A. (2015). Two-stage sulfate removal from reject brine in inland desalination with zero-liquid discharge. *Desalination, 362*, 52-58. doi:10.1016/j.desal.2015.02.008

Althaus, H.-J., Hischier, R., Osses, M., Primas, A., Hellweg, S., Jungbluth, N., & Chudacoff, M. (2007). *Life Cycle Inventories of Chemicals. Ecoinvent Report No. 8 v2.0.* Dübendorf: Swiss Centre for Life Cycle Inventories. Retrieved from www.ecoinvent.org

Appelo, C. A. (2015). Principles, caveats and improvements in databases for calculating hydrogeochemical reactions in saline waters from 0 to 200°C and 1 to 1000 atm. *Applied Geochemistry, 55*, 62-71. doi:10.1016/j.apgeochem.2014.11.007

Appelo, C., & Postma, D. (2010). *Geochemistry, Groundwater and Pollution* (2 ed.). Amsterdam: A.A. Balkema Publisher.

Azaza, H., Mechi, L., Doggaz, A., Optasanu, V., Tlili, M., & Amor, M. B. (2017). Calcite and barite precipitation in CaCO3-BaSO4-NaCl and BaSO4-NaCl-CaCl2 aqueous systems: kinetic and microstructural study. *Arabian Journal of Geoscience, 10*, 220. doi:10.1007/s12517-017-3005-1

Bargerman, G., Westerink, J., Manuhut, C., & ten Kate, A. (2015). The effect of membrane characteristics on nanofiltration membrane performance during proessing of practically saturated salt solutions. *Journal of Membrane Science, 485*, 112-122. doi:10.1016/j.memsci.2015.03.039

Benatti, C. T., Tavares, C. R., & Lenzi, E. (2009). Sulfate removal from waste chemicals by precipitation. *Journal of Environmental Management, 90*, 504-511. doi:10.1016/j.jenvman.2007.12.006

Benedetti, M. F., Milne, C. J., Kinniburgh, D. G., van Riemsdijk, W. H., & Koopal, L. K. (1995). Metal ion binding to humic substances: Application of the non-ideal competitive adsorption model. *Environmental Science & Technology, 29*, 446-457.

Benedetti, M. F., van Riemsdijk, W. H., Koopal, L. K., Kinniburgh, D. G., Gooddy, D. C., & Milne, C. J. (1996). Metal ion binding by natural organic matter: From the model to the field. *Geochimica et Cosmochimica Acta, 60*(14), 2503-2513.

Bjørn, A., Owsianiak, M., Laurent, A., Olsen, S. I., Corona, A., & Hauschild, M. Z. (2018). Scope Definition. In M. Z. Hauschild, R. K. Rosenbaum, & S. I. Olsen (Eds.), *Life Cycle Analysis Theory and Practice.* Cham: Springer. doi:10.1007/978-3-319-56475-3

Boerlage, Ś. F., Kennedy, M. D., Bremere, I., Witkamp, G. J., van der Hoek, J. P., & Schippers, J. C. (2000). Stable barium sulphate supersaturation in reverse osmosis. *Journal of Membrane Science, 179*, 53-68.

Boerlage, Ś. F., Kennedy, M. D., Witkamp, G. J., van der Hoek, J. P., & Schippers, J. C. (1999). BaSO4 solubility prediction in reverse osmosis membrane system. *Journal of Membrane Science, 159*, 47-59.

Brady, J. E., & Humiston, G. E. (1986). *General Chemistry Principles and Structure* (4th ed.). John Wiley & Sons, Inc.

Calmon, C. (1986). Recent developments in water treatment by ion exchange. *Reactive Polymers, 4*, 131-146.

Causserand, C., & Aimar, P. (2010). Characterization of Filtration Membranes. In E. Drioli, & L. Giorno (Eds.), *Comprehensive Membrane Science and Engineering* (Vol. I, pp. 311-335). Elsevier.

Chen, H., Jia, X., Wei, M., & Wang, Y. (2017). Ceramic tubular nanofiltration membranes with tunable performances by atomic layer deposition and calcination. *Journal of Membrane Science, 528*, 95-102. doi:10.1016/j.memsci.2017.01.020

Chen, P., Ma, X., Zhong, Z., Zhang, F., Xing, W., & Fan, Y. (2017). Performance of ceramic nanofiltration membrane for desalination of dye solutions containing NaCl and Na2SO4. *Desalination, 404*, 102-111. doi:10.1016/j.desal.2016.11.014

Chen, X., Lin, Y., Lu, Y., Qiu, M., Jing, W., & Fan, Y. (2015). A facile nanoparticle doping sol-gel method for the fabrication of defect-free nanoporous ceramic membrane. *Colloids and Interface Science Communications, 5*, 12-15. doi:10.1016/j.colcom.2015.05.003

Choi, S., Yun, Z., Hong, S., & Ahn, K. (2001). The effect of co-existing ions and surface characteristics of nanomembranes on the removal of nitrate and flouride. *Desalination, 133*, 53-64.

Choudhury, H., & Cary, R. (2001). *Concise Internation Chemical Assessment Document 33: Barium and Barium Compounds.* Geneva: World Health Organization.

Clark, B., & Brown, P. (1999). The formation of calcium sulfoaluminate hydrate compounds, Part I. *Cement and Concrete Research, 29*, 1943-1948.

Combe, C., Gizard, C., Aimar, P., & Sanchez, V. (1997). Experimental determination of four characteristics used to predict the retention of a ceramic nanofiltration membrane. *Journal of Membrane Science, 129*, 147-160.

Comerton, A. M., Andrews, R. C., & Bagley, D. M. (2009). The influence of natural organic matter and cations on fouled nanofiltrtaion membrane effective molecular weight cut-off. *Journal of Membrane Science, 327*, 155-163. doi:10.1016/j.memsci.2008.11.013

Cowan, J., & Weintritt, D. (1976). *Water-Formed Scale Deposits.* Houston: Gulf Publication Co. Retrieved from https://app.knovel.com/hotlink/toc/id:kpWFSD0001/water-formed-scale-deposits/water-formed-scale-deposits

Croué, J., Violleau, D., Bodaire, C., & Lagube, B. (1999). Removal of hydrophobic and hydrophilic constituents by anion exchange resin. *Water Science & Technology, 40*(9), 207-214.

da Silva Biron, D., dos Santos, V., & Zeni, M. (2018). *Ceramic Membranes Applied in Separation Processes.* (C. P. Bergmann, Ed.) Springer. doi:10.1007/978-3-319-58604-5

Davies, J. W., & Collins, A. G. (1971). Solubility of barium and strontium sulfates in strong electrolyte solutions. *Environmental Science & Technology, 5*(10), 1039-1043.

Déon, S., Dutournié, P., Limousy, L., & Bourseau, P. (2009). Transport of salt mixtures through nanofiltration membranes: Numerical identification of electric and dielectric contributions. *Separation and Purification Technology, 69*, 225-233. doi:10.1016/j.seppur.2009.07.022

Dudal, Y., & Gérard, F. (2004). Accounting for natural organic matter in aqueous chemical equilibirum models: A review of the theoris and applications. *Earth-Science Review, 66*, 199-216. doi:10.1016/j.earsciev.2004.01.002

Epsztein, R., Shaulsky, E., Dizge, N., Warsinger, D. M., & Elimelech, M. (2018). Role of ionic charge density in Donnan exclusion of monovalent anions by nanofiltration. *Environmental Science & Technology, 52*, 4108-4116. doi:10.1021/acs.est.7b06400

Fane, A., Awang, A., Bolko, M., Macoun, R., Schofield, R., Shen, Y., & Zha, F. (1992). Metal recovery from wastewater using membranes. *Water Science & Technology, 25*(10), 5-18. doi:10.2166/wst.1992.0233

Fang, P., Tang, Z.-j., Chen, X.-b., Huang, J.-h., Tang, Z.-x., & Cen, C.-p. (2018). Removal of high-concentration sulfate ions from the sodium alkali FGD wastewater using ettringite precipitation method: Factor assessment, feasilibility, and prospect. *Journal of Chemistry*. doi:10.1155/2018/1265168

Feng, L. (2018). *Ceramic nanofiltrtaion membranes: Rejection of salts and NOM at high ionic strength and modification of pore size by atomic layer deposition.* Master thesis. Retrieved from http://resolver.tudelft.nl/uuid:35caa895-45a1-484a-8e57-cbf5e0b8cd51

Finkbeiner, P., Redman, J., Patriarca, V., Moore, G., Jefferson, B., & Jarvis, P. (2018). Understanding the potential for selective natural organic matter removal by ion exchange. *Water Research, 146*, 256-263. doi:10.1016/j.watres.2018.09.042

Galjaard, G., & Koreman, E. (2015). SIX® A New Resin Treatment Technology for NOM-removal. *IWA NOM6.* Malmo.

Germishuizen, C., Franzen, S., Grobler, H., Simate, G., & Sheridan, C. (2018). Case study modelling for an ettringite treatment process. *Water SA, 44*(1), 86-92. doi:10.4314/wsa.v44i1.10

Gitis, V., & Gadi. (2016). *Ceramic Membranes - New Opportunities and Practical Applications.* John Wiley & Sons. Retrieved February 13, 2019, from https://app.knovel.com/hotlink/toc/id:kpCMNOPA01/ceramic-membranes-new/ceramic-membranes-new

Goedkoop, M., & Spriensma, R. (2001). *The Eco-indicator 99 A Damage Oriented Method for Life Cycle Impact Assessment Methodology Report.* Amersfoort: PRé Consultants B.V.

He, S., Oddo, J. E., & Tomson, M. B. (1994a). The nucleation kinetics of calcium sulfate dihydrate in NaCl solutions up to 6 M and 90°C. *Journal of Colloid and Interface Science, 162*, 297-303.

He, S., Oddo, J. E., & Tomson, M. B. (1994b). The inhibition of gyspum and barite nucleation in NaCl brines at temperature from 25 to 90°C. *Applied Geochemistry, 9*, 561-567.

He, Y., Li, G.-M., Wang, H., Jiang, Z.-W., Zhao, J.-F., Su, H.-X., & Huang, Q.-Y. (2009). Experimental study on the rejection of salt and dye with cellulose acetate nanofiltration membrane. *Journal of the Taiwan Institute of Chemical Engineers, 40*, 289-295. doi:10.1016/j.jtice.2008.09.008

Hendricks, D. (2006). *Water Treatment Unit Processes Physical and Chemical.* Boca Raton, Florida, United States: CRC Press.

Huber, S. A., Baiz, A., Abert, M., & Pronk, W. (2011). Characterisation of aquatic humic and non-humic matter with size-exclusion chromatography - organic carbon detection - organic nitrogen detection (LC-OCD-OND). *Water Research, 45*(2), 879-885. doi:10.1016/j.watres.2010.09.023

Jarusutthirak, C., Mattaraj, S., & Jiraratananon, R. (2007). Factors affecting nanofiltrtaion performances in natural organic matter rejection and flux decline. *Separation and Purification Technology, 58*, 68-75. doi:10.1016/j.seppur.2007.07.010

Kabdaşli, I., Bilgin, A., & Tünay, O. (2016). Sulphate control by ettringite precipitation in textile industry wastewaters. *Environmental Technology, 37*(4), 446-451. doi:10.1080/09593330.2015.1026245

Kim, J., Buckau, G., Li, G., Duschner, H., & Psarros, N. (1990). Characterization of humic and fulvic acids from Gorleben groundwater. *Fresenius' Journal of Analytical Chemistry, 338*, 245-252.

Kinniburgh, D. G., van Riemsdijk, W. H., Koopal, L. K., Borkovec, M., Benedetti, M. F., & Avena, M. J. (1999). Ion binding to natural organic matter: competition, heterogeneity, stoichiometry and therodynamic consistency. *Colloids and Surfaces, 151*, 147-166.

Kramer, F., Shang, R., Scherrenberg, S., Rietveld, L., & Heijman, S. (2019). Quantifying defects in ceramic tight ultra- and nanofiltration membranes and investigating their robustness. *Separation and Purification Technology, 219*, 159-168. doi:10.1016/j.seppur.2019.03.019

Krieg, H., Modise, S., Keizer, K., & Neomagus, H. (2004). Salt rejection in nanofiltration for single and binary salt mixtures in view of sulphate removal. *Desalination, 171*, 205-215. doi:10.1016/j.desal.2004.05.005

Kucher, M., Babic, D., & Kind, M. (2006). Precipitation of barium sulfate: Experimental investigation about the influence of supersaturation and free latice ion ratio on particle formation. *Chemical Engineering and Processing, 45*, 900-907. doi:10.1016/j.cep.2005.12.006

Lanteri, Y., Fievet, P., & Szymczyk, A. (2009). Evaluation of the steric, electric, and dielectric exclusion model on the basis of salt rejection rate and membrane potential measurement. *Journal of Colloid and Interface Science, 331*, 148-155. doi:10.1016/j.cis.2008.11.014

Lee, M., Wu, Z., & Li, K. (2015). Advances in ceramic membranes for water treatment. In A. Basile, A. Cassano, & N. K. Rastogi, *Advances in Membrane Technologies for Water Treatment Materials, Processes and Applications* (Vol. 75, pp. 43-82). Woodhead Publishing (Elsevier). doi:10.1016/B978-1-78242-121-4.01001-7

Lee, S., Cho, J., & Elimelech, M. (2005). Combined influence of natural organic matter (NOM) and colloidal particles on nanofiltration membrane fouling. *Journal of Membrane Science, 262*, 27-41. doi:10.1016/j.memsci.2005.03.043

Lu, H., Kan, A., Zhang, P., Yu, J., Fan, C., Work, S., & Tomson, M. B. (2012). Phase stability and inhibition of calcium sulfate in the system NaCl/Monoethylene glycol/H2O. *SPE Journal, 17*(01). doi:10.2118/130697-PA

MacAdam, J., & Jarvis, P. (2015). Water-Formed Scales and Deposits: Types, Characteristics, and Relevant Industries. In Z. Amjad, & K. Demadis (Eds.), *Mineral Scales and Deposits* (pp. 3-23). Elsevier. doi:10.1016/B978-0-444-63228-9.00001-2

Marchetti, P., Butté, A., & Livingston, A. G. (2012). An improved phenomenological model for prediction of solven permeation through ceramic NF and UF membranes. *Journal of Membrane Science, 415-416*, 444-458. doi:10.1016/j.memsci.2012.05.030

Mazzoni, C., Orlandini, F., & Bandini, S. (2009). Role of electrolyte type on TiO2-ZrO2 nanofiltration membranes performances. *Desalination, 240*, 227-235. doi:10.1016/j.desal.2007.11.074

Metcalfe, D., Jarvis, P., Rockey, C., & Judd, S. (2016). Pre-treatment of surface waters for ceramic microfiltration. *Separation and Purification Technology, 163*, 173-180. doi:10.1016/j.seppur.2016.02.046

Mullin, J. (2001). *Crystallization* (4th ed.). Oxford: Butterworth-Heinemann.

Muralikrishna, I. V., & Manickam, V. (2017). *Environmental Management.* Oxford: Elsevier. doi:10.1016/B978-0-12-811989-1.00005-1

Nancollas, G., & Purdie, N. (1963). Crystallization of barium sulphate in aqueous solution. *Transactions of the Faraday Society, 59*, 735-740. doi:10.1039/TF9635900735

Nicolini, J. V., Borger, C. P., & Ferrza, H. C. (2016). Selective rejection of ions and correlation with surface propoerties of nanofiltration membranes. *Separation and Purification Technology, 171*, 238-247. doi:10.1016/j.seppur.2016.07.042

Ortiz-Albo, P., Ibañez, R., Urtiaga, A., & Ortiz, I. (2019). Phenomenological prediction of desalination brines nanofiltration through the indirect determination of zeta potential. *Separation and Purification Technology, 210*, 746-753. doi:10.1016/j.seppur/2018.08.066

Park, S.-J., & Seo, M.-K. (2011). *Interface Science and Technology* (Vol. 18). Academic Press.

Peeters, J., Boom, J., Mulder, M., & Strathmann, H. (1998). Retention measurements of nanofiltration membranes with electrolyte solutions. *Journal of Membrane Science, 145*, 199-209.

Pera-Titus, M., & Llorens, J. (2007). Characterization of meso- and macroporous ceramic membranes in terms of flux measurement: A moment-based analysis. *Journal of Membrane Science, 302*, 218-234. doi:10.1016/j.memsci.2007.06.057

Pérez-González, A., Ibáñez, R., Gómez, P., Urtiaga, A., Ortiz, I., & Irabien, J. (2015). Nanofiltration separation of polyvalent and monovalent anions in desalination brines. *Journal of Membrane Science, 473*, 16-27. doi:10.1016/j.memsci.2014.08.045

Perkins, R. B. (2000). *The Solubility and Thermodynamic Properties of Ettringite, Its Chromium Analogs, and Calcium Aluminum Monochromate (3CaO.Al2O3.CaCrO4.nH2O).* Doctoral Dissertation, Portland State University.

Puhlfürβ, P., Voigt, A., Weber, R., & Morbé, M. (2000). Microporous TiO_2 membranes with a cut off <500 Da. *Journal of Membrane Science, 174*, 123-133.

Qiu, M., Chen, X., Fan, Y., & Xing, W. (2017). Ceramic Membranes. In E. Drioli, L. Giorno, & E. Fontananova (Eds.), *Comprehensive Membrane Science and Engineering* (2nd ed., Vol. I, pp. 270-297). Oxford: Elsevier. doi:10.1016/B978-0-12-409547-2.12243-7

Rentizelas, A., & Georgakellos, D. (2014). Incorporating life cycle external cost in optimization of the electricity generation mix. *Energy Policy, 65*, 134-149. doi:10.1016/j.enpol.2013.10.023

Risthaus, P., Bosbach, D., Becker, U., & Putnis, A. (2001). Barite scale formation and dissolution at high ionic strength sutdied with atomic force microscopy. *Colloids and Surfaces, 191*, 201-214.

Ritchie, J. D., & Perdue, E. M. (2003). Proton-binding study of standard and reference fulvic acids, humic acids, and natural organic matter. *Geochimica et Cosmochimica Acta, 67*(1), 85-96.

Rocha, C. D., Hoff, C., & Bryce, J. (2008). Calcium Cycle. In S. E. Jørgensen (Ed.), *Global Ecology.* Academic Press.

Ronquim, F. M., Cotrim, M. E., Guilhen, S. N., & Bernardo, A. (2018). Improved barium removal and supersaturation depletion in wastewater by precipitation with excess sulfate. *Journal of Water Process Engineering, 23*, 265-276. doi:10.1016/j.jwpe.2018.04.007

Rosenbaum, R. K., Georgiadis, S., & Fantke, P. (2018b). Uncertainty Management and Sensitivity Analysis. In M. Z. Hauschild, R. K. Rosenbaum, & S. I. Olsen (Eds.), *Life Cycle Assessment Theory and Practice.* Cham: Springer. doi:10.1007/978-3-319-56475-3

Rosenbaum, R. K., Hauschild, M. Z., Boulay, A.-M., Fantke, P., Laurent, A., Núñez, M., & Vieira, M. (2018a). Life Cycle Impact Assessment. In M. Z. Hauschild, R. K. Rosenbaum, & S. I. Olsen (Eds.), *Life Cycle Assessment Theory and Practice.* Cham: Springer. doi:10.1007/978-3-319-56475-3

Saar, R. A., & Weber, J. H. (1982). Fulvic acid: modifier of metal-ion chemistry. *Environmental Science & Technology, 16*(9), 510A.

Salehi, F., Razavi, S. M., & Elahi, M. (2011). Purifying anion exchange resin regeneration effluent using polyamide nanofiltration membrane. *Desalination, 278*, 31-35. doi:10.1016/j.desal.2011.04.067

Schäfer, A., Fane, A., & Waite, T. (1998). Nanofiltration of natural organic matter: Removal, fouling and the influence of multivalent ions. *Desalination, 118*, 109-122.

Shammas, N. K., & Wang, L. K. (2016). *Water Engineering Hydraulics, Distribution and Treatment.* Hoboken: John Wiley & Sons, Inc.

Shang, R., Goulas, A., Tang, C., de Frias Serra, X., Rietveld, L., & Heijman, S. (2017). Atmospheric pressure atomic layer deposition for tight ceramic nanofiltration membranes: Systhesis and application in water purification. *Journal of Membrane Science, 528*, 163-170. doi:10.1016/j.memsci.2017.01.023

Shang, R., Verliefde, A. R., Hu, J., Heijman, S. G., & Rietveld, L. C. (2014a). The impact of EfOM, NOM and cations on phosphate rejection by tight ceramic ultrafiltration. *Separation and Purification Technology, 132*, 289-294. doi:10.1016/j.seppur.2014.05.024

Shang, R., Verliefde, A. R., Hu, J., Zeng, Z., Lu, J., Antoine, K. J., . . . Rietveld, L. C. (2014b). Tight ceramic UF membranes as RO pre-treatment: The role of electrostatic interactions on phosphate rejection. *Water Research, 48*, 498-507. doi:10.1016/j.watres.2013.10.008

Shim, Y., Lee, H.-J., Lee, S., Moon, S.-H., & Cho, J. (2002). Effects of natural organic matter and ionic species on membrane surface charge. *Environmental Science Technology, 36*(17), 3864-3871. doi:10.1021/es015880b

Singh, R., & Hankins, N. P. (2016). Introduction to Membrane Processes for Water Treatment. In N. P. Hankins, & R. Singh, *Emerging Membrane Technology for Sustainable Water Treatment* (pp. 15-52). Elsevier. doi:10.1016/B978-0-444-63312-5.00002-4

Song, Z., Fathizadeh, M., Huang, Y., Chu, K., Yoon, Y., Wang, L., . . . Yu, M. (2016). TiO2 nanofiltration membranes pepared by molecular layer deposition for water purification. *Journal of Membrane Science, 510*, 72-78. doi:10.1016/j.memsci.2016.03.011

Swanepoel, H., de Beer, M., & Liebenberg, L. (2012). Complete sulphate removal from neutralised acidic mine drainage with barium carbonate. *Water Practice & Technology, 7*(1). doi:10.2166/wpt.2012.003

Tait, S., Clarke, W. P., Keller, J., & Batstone, D. J. (2009). Removal of sulfate from high-strength wastewater by crystallisation. *Water Research, 43*, 762-772. doi:10.1016/j.watres.2008.11.008

Tansel, B. (2012). Significance of themodynamic and physical characteristics on permeation of ions during membrane separation: Hydrated radius, hydration free energy and viscous effects. *Separation and Purification Technology, 86*, 119-126. doi:10.1016/jseppur.2011.10.033

Tansel, B., Sager, J., Rector, T., Garland, J., Strayer, R., Levine, L., . . . Bauer, J. (2006). Significance of hydrated radius and hydration shells on ionic permeability during nanofiltration in dead

end and cross flow modes. *Separation and Purification Technology, 51*, 40-47. doi:10.1016/j.seppur/2005.12.020

Tao, H., Man, Y., Shi, X., Zhu, J., Pan, H., Qin, Q., & Liu, S. (2016). Inconceivable Hypokalemia: A case report of acute severe barium chloride poisoning. *Case Reports in Medicine*. doi:10.1155/2016/2743134

Thannimalay, L., Yusof, S., & Zawawi, N. Z. (2013). Life cycle assessment of sodium hydroxide. *Austalian Journal of Basic and Applied Sciences, 7*(2), 421-431.

van der Bruggen, B., Koninckx, A., & Vandecasteele, C. (2004). Separation of monovalent and divalent ions from aqueous solution by electrodialysis and nanofiltrtaion. *Water Research, 38*, 1347-1353. doi:10.1016/j.watres.2003.11.008

van Gestel, T., Vandecasteele, C., Buekenhoudt, A., Dotremont, C., Luyten, J., Leysen, R., . . . Maes, G. (2002). Salt retention in nanofiltration with multilayer ceramic TiO_2 membranes. *Journal of Membrane Science, 209*, 379-389.

van Oers, L. (2016, September 5). *CML-IA Characterisation Factors.* Retrieved August 2019, from http://www.cml.leiden.edu/software/data-cmlia.html

Vaudevire, E., Koreman, E., Galjaard, G., Trommel, R., & Visser, M. (2012). Further treatment of ion exchange brine with dynamic vapour recompression. *Water Practice & Technology, 7*(4). doi:10.2166/wpt.2012.074

Vezzani, D., & Bandini, S. (2002). Donnan equilibrium and dielectric exclusion for characterization of nanofiltration membranes. *Desalination, 149*, 477-483.

Volk, C., Wood, L., Johnson, B., Robinson, J., Zhu, H. W., & Kaplan, L. (2002). Monitoring dissolved organic carbon in surface and drinking waters. *Journal of Environmental Monitoring, 4*, 43-47. doi:10.1039/b107768f

Wang, D.-X., Su, M., Yu, Z.-Y., Wang, X.-L., Ando, M., & Shintani, T. (2005). Separation performance of nanofiltration membrane influenced by species and concentration of ions. *Desalination, 175*, 219-225. doi:10.1016/j.desal.2004.10.009

Wang, Z., Xiao, K., & Wang, X.-m. (2018). Role of coexistence of negative and positive membrane surface charges in electrostatic effect for salt rejection by nanofiltration. *Desalination, 444*, 75-83. doi:10.1016/j.desal.2018.07.010

Weber, R., Chmiel, H., & Mavrov, V. (2003). Characteristics and application of new ceramic nanofiltration membranes. *Desalination, 157*, 113-125.

Wei, W., Larrey-Lassalle, P., Faure, T., Dumoulin, N., Roux, P., & Mathias, J.-D. (2016). Using the reability theory for assessing the decision confidence probability for comparative life cycle assessments. *Environmental Science & Technology, 50*, 2272-2280. doi:10.1021/acs.est.5b03683

White, F. M. (2011). *Fluid Mechanics* (7th ed.). New York: McGraw-Hill.

World Bank. (2019). *World Bank Open Data*. Retrieved August 11, 2019, from Life expectancy at birth, total (years): https://data.worldbank.org/indicator/SP.DYN.LE00.IN?locations=EU-NL

Xu, Y., Liao, Y., Lin, Z., Lin, J., Li, Q., Lin, J., & Jin, Z. (2019). Precipitation of calcium sulfate dihydrate in the presence of fulvic acid and magnesium ion. *Chemical Engineering Journal, 361*, 1078-1088. doi:10.1016/j.cej.2019.01.003

Yan, Z.-Q., Zeng, L.-M., Li, Q., Liu, T.-Y., Matsuyama, H., & Wang, X.-L. (2016). Selective separation of chloride and sulfate by nanofiltration for high saline wastewater recycling. *Separation and Purification Technology, 166*, 135-141. doi:10.1016/j.seppur.2016.04.009

Appendix

Appendix A. Retention curve of PEG analysis

Membrane: C01

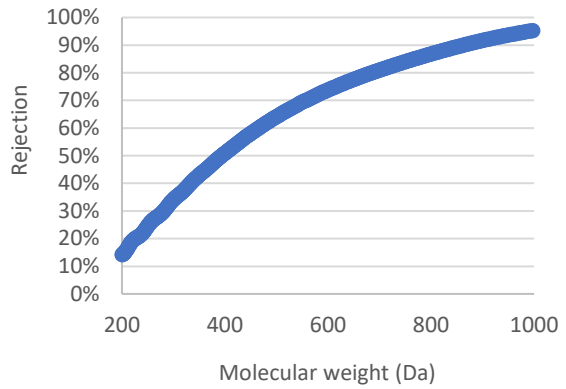

Membrane: M1

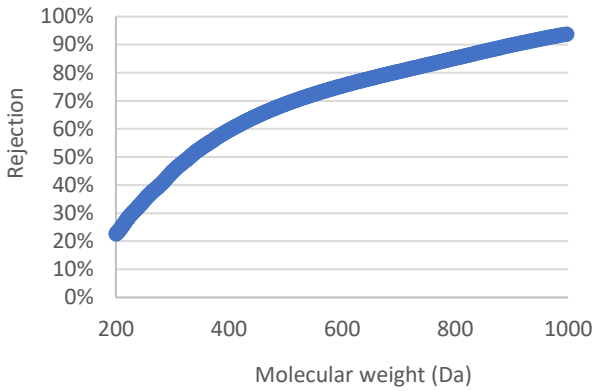

Membrane: M2

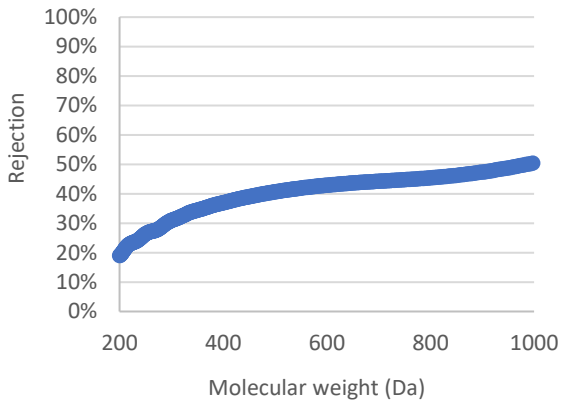

Membrane: M3

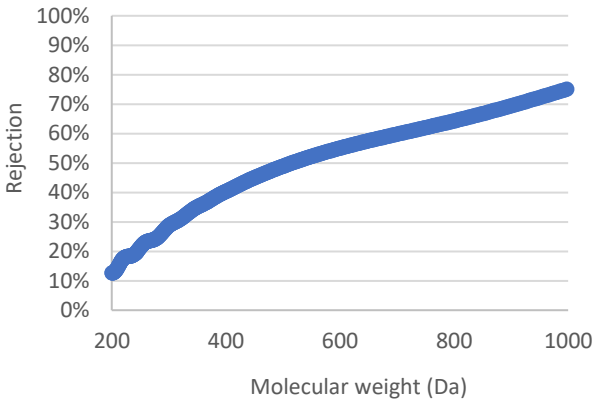

Membrane: M4

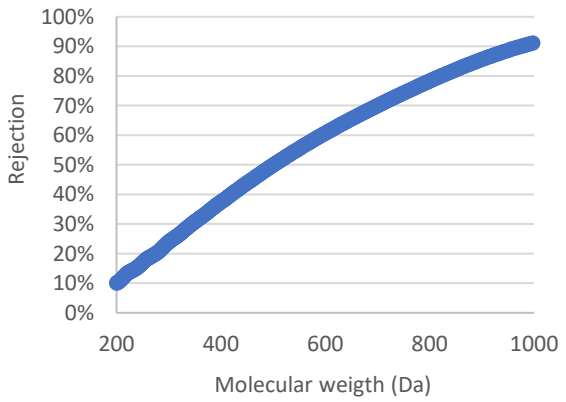

Membrane: M6

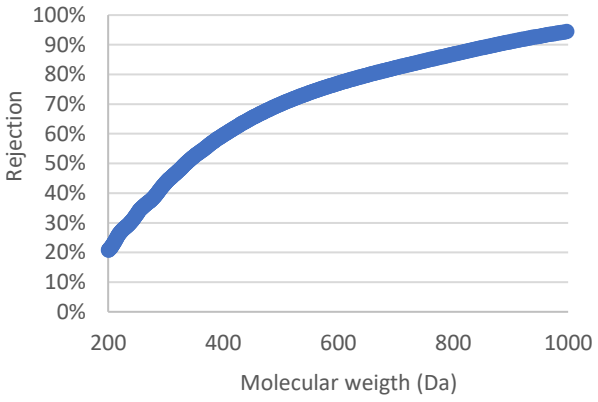

Membrane: T3

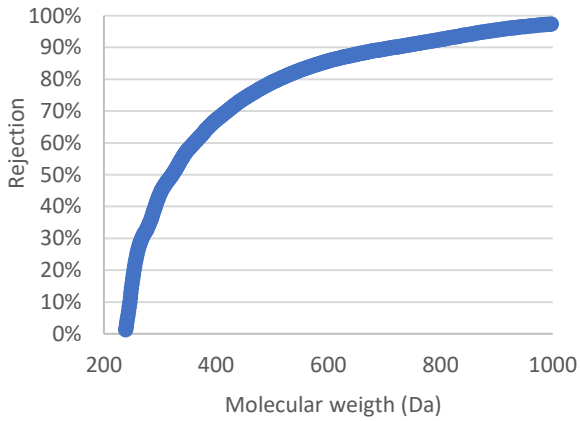

Membrane: T4

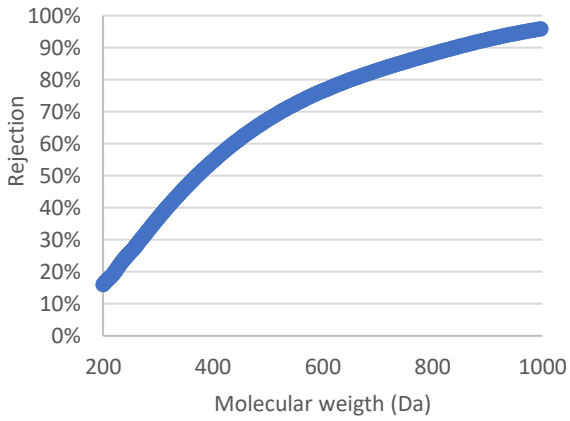

Membrane: T5

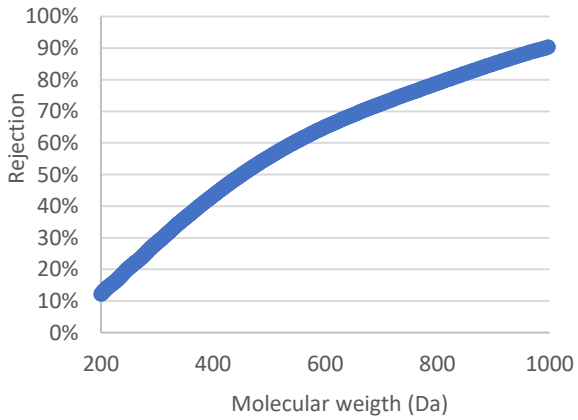

Membrane: T6

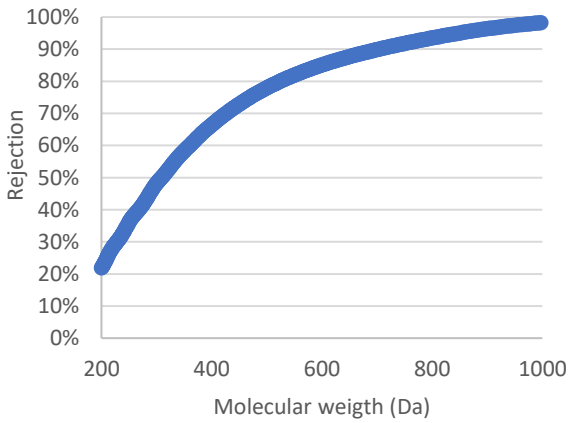

Membrane: T8

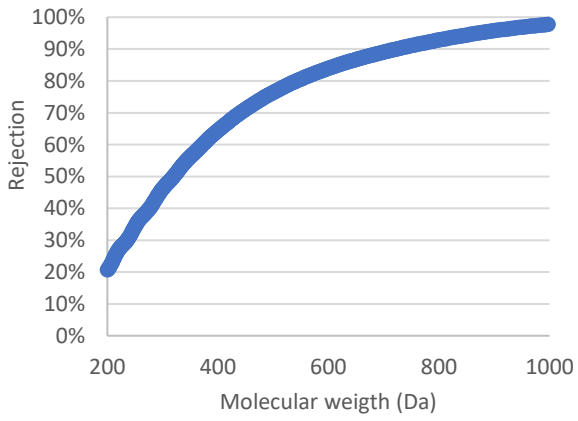

Membrane: T9

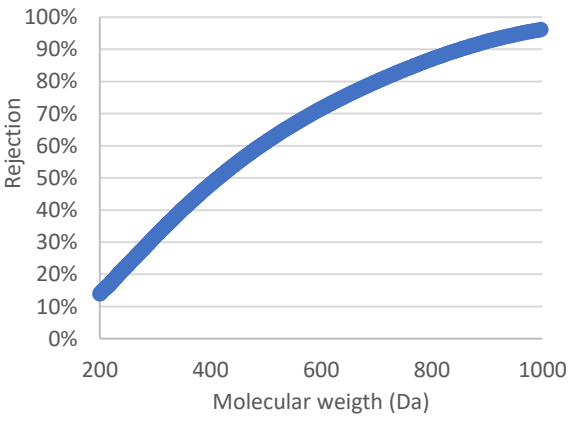

Appendix B. Permeability and flux of membrane filtration

1. Permeability of M6 during salt rejection experiment

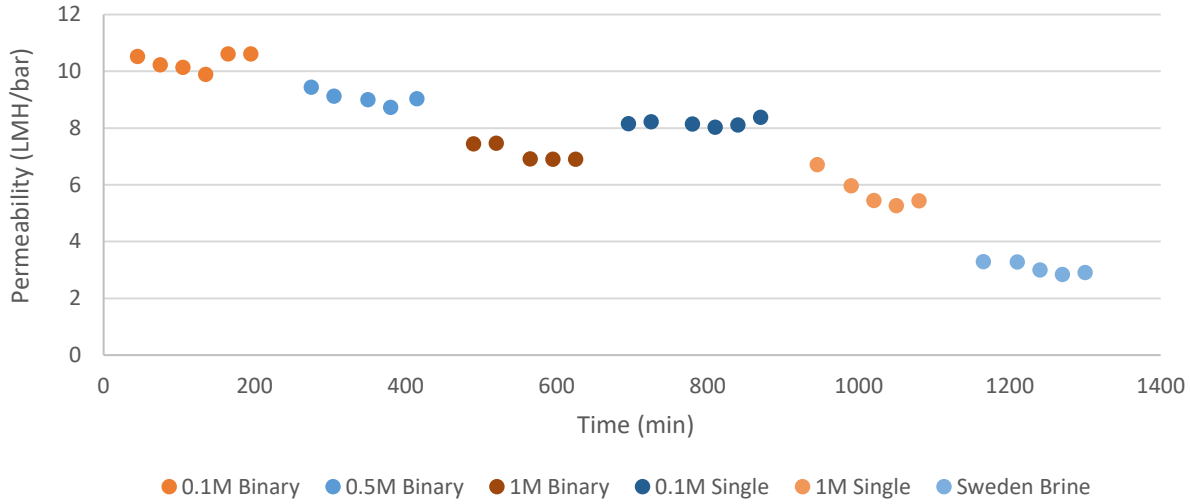

2. Permeability of C01 during salt rejection experiment

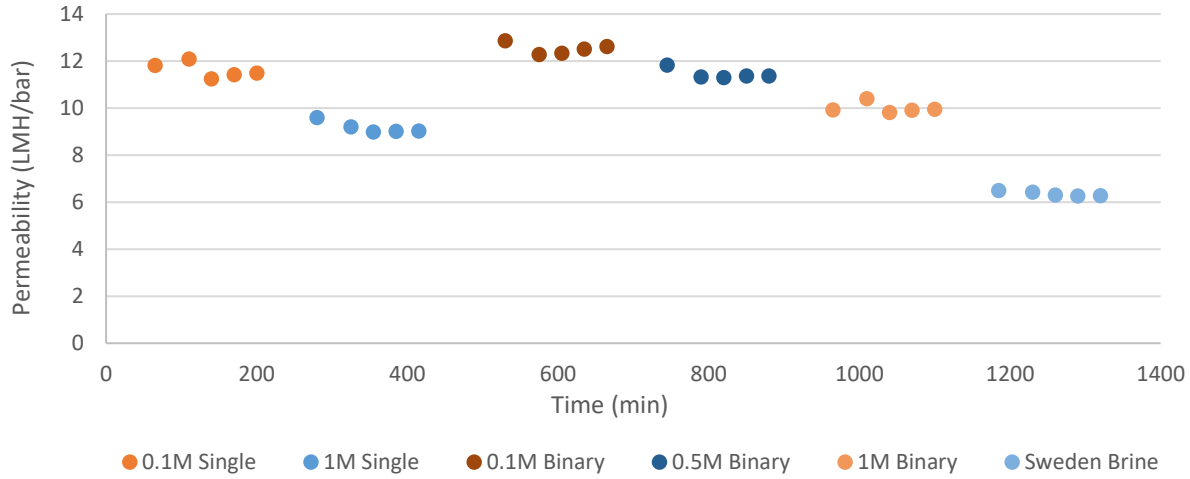

3. Permeability of C01 during integrated sulphate removal experiment

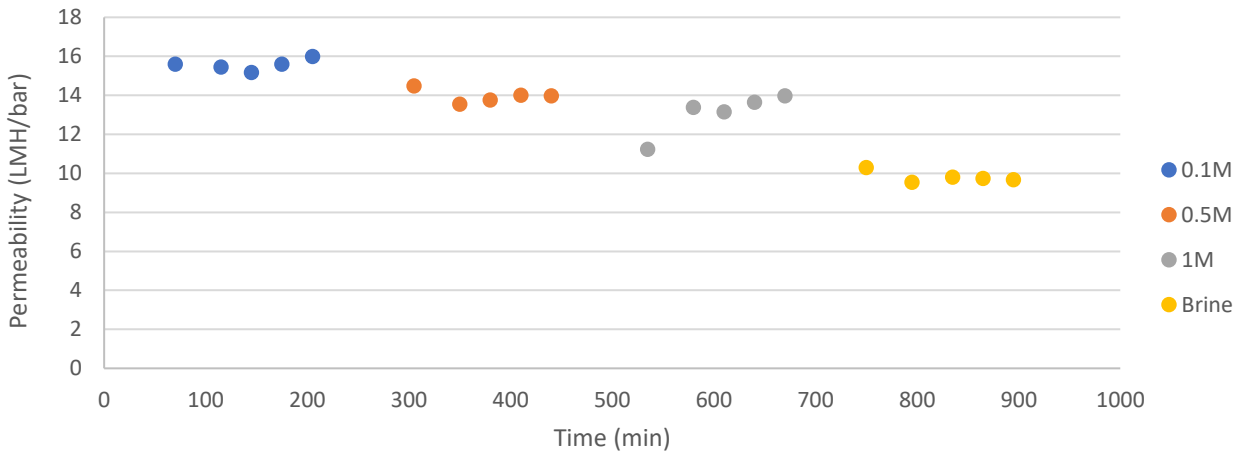

4. Flux of M6 during salt rejection experiment

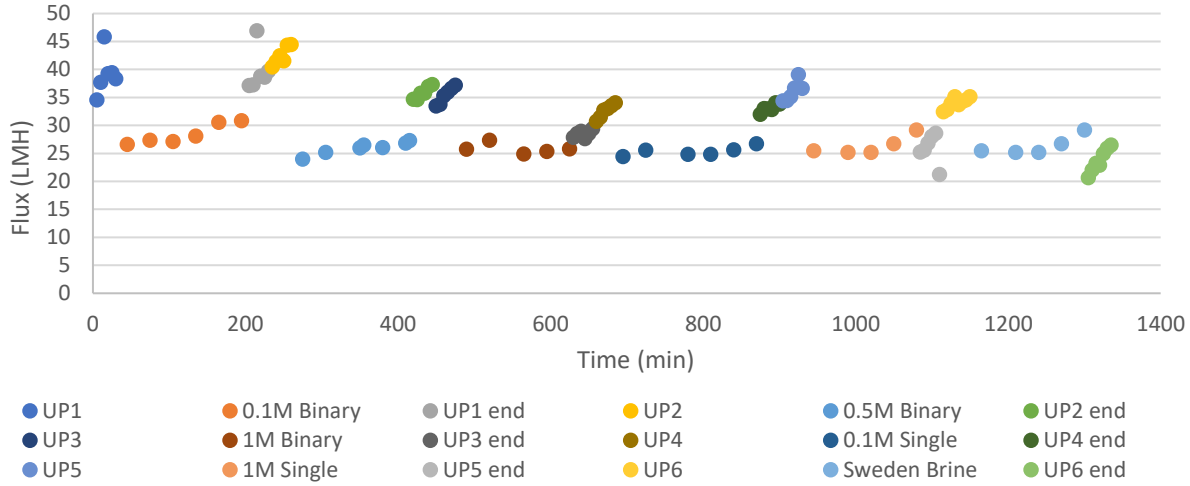

5. Flux of C01 during salt rejection experiment

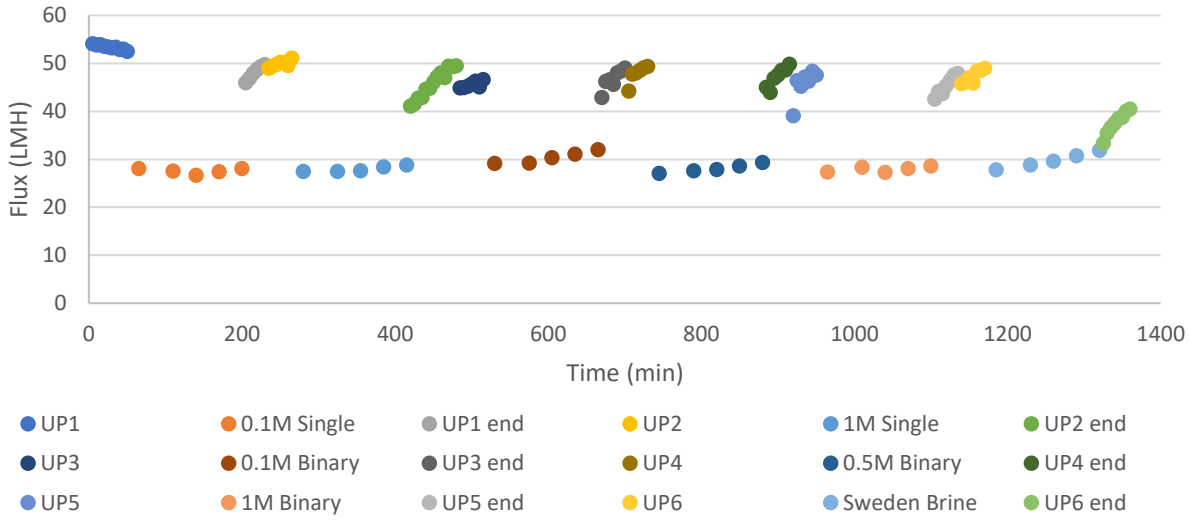

6. Flux of C01 during integrated sulphate removal experiment

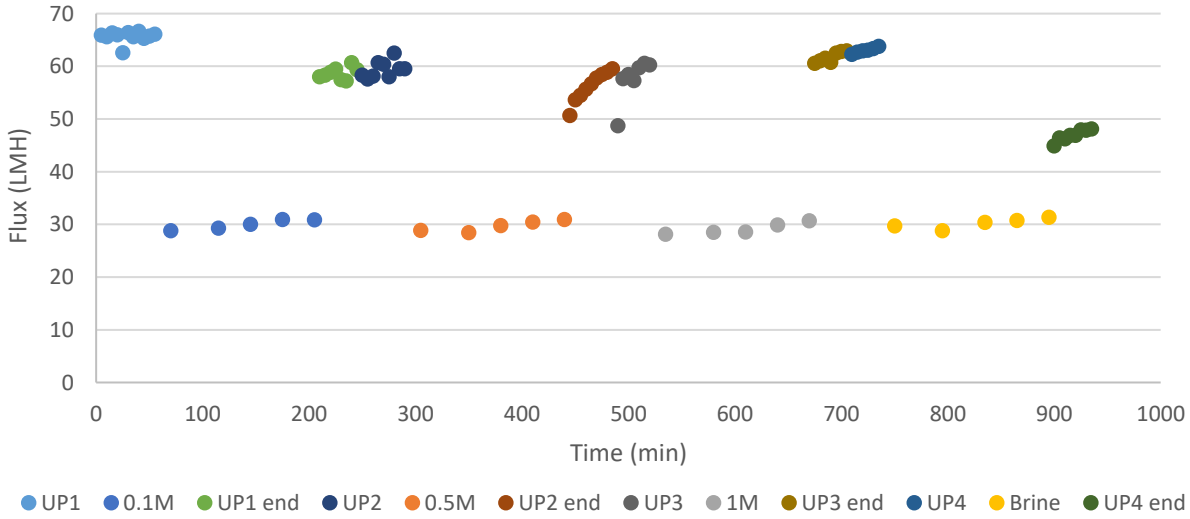

Appendix C. PhreeqC modelling manuscripts

1. Sulphate removal efficacy using barium salt

```
DATABASE PITZER.DAT

SOLUTION 1
-units mg/L
pH 8
S(6) 10000
Na 4786.791
END

USE SOLUTION 1
EQUILIBRIUM_PHASES 1
Barite 0 0
REACTION 1
BaCl2:2H2O 1
9.37e-2 9.58e-2 9.79e-2 9.99e-2 1.02e-1 1.04e-1 1.06e-1 1.08e-1
1.1e-1 1.12e-1 1.15e-1
REACTION_TEMPERATURE 1
20

SELECTED_OUTPUT
-file so4concentration.txt
-molalities SO4-2
END
```

2. Sulphate removal efficacy using calcium salt

```
DATABASE PITZER.DAT

SOLUTION 1
-units mg/L
pH 8
S(6) 10000
Na 4786.791
END

USE SOLUTION 1
EQUILIBRIUM_PHASES 1
Gypsum 0 0
REACTION 1
CaCl2:2H2O 1
9.37e-2 9.58e-2 9.79e-2 9.99e-2 1.02e-1 1.04e-1 1.06e-1 1.08e-1
1.1e-1 1.12e-1 1.15e-1 1.17e-1 1.19e-1 1.21e-1 1.23e-1 1.25e-1
1.27e-1 1.29e-1 1.31e-1 1.33e-1 1.35e-1
REACTION_TEMPERATURE 1
20

SELECTED_OUTPUT
-file so4+ca_concentration.txt
-molalities SO4-2 Ca+2
```

```
END
```

3. Sulphate removal using barium salt in solution of 0.01 M ionic strength

```
DATABASE PHREEQC.DAT

SOLUTION 1
pH 8
temp 20
-units mg/L
Na 191.58
S(6) 160
Cl 177.26
END

USE SOLUTION 1
EQUILIBRIUM_PHASES 1
Barite 0 0
REACTION 1
BaCl2:2H2O 1
1.667e-3
END
```

4. Sulphate removal using barium salt in solution of 0.1 M ionic strength

```
DATABASE PITZER.DAT

SOLUTION 1
pH 8
temp 20
-units mg/L
Na 1915.81
S(6) 1600.7
Cl 1772.64
END

USE SOLUTION 1
EQUILIBRIUM_PHASES 1
Barite 0 0
REACTION 1
BaCl2:2H2O 1
1.667e-2
END
```

5. Sulphate removal using barium salt in solution of 0.5 M ionic strength

```
DATABASE PITZER.DAT

SOLUTION 1
pH 8
temp 20
-units mg/L
Na 9496.26
S(6) 9000
Cl 8000
END

USE SOLUTION 1
EQUILIBRIUM_PHASES 1
Barite 0 0
REACTION 1
BaCl2:2H2O 1
9.369e-2
END
```

6. Sulphate removal using barium salt in solution of 1 M ionic strength

```
DATABASE PITZER.DAT

SOLUTION 1
pH 8
temp 20
-units mg/L
Na 19158.16
S(6) 16007
Cl 17726.35
END

USE SOLUTION 1
EQUILIBRIUM_PHASES 1
Barite 0 0
REACTION 1
BaCl2:2H2O 1
1.667e-1
END
```

Appendix D. Additional data, calculation, and manuscript for Ettringite modelling

1. Additional data for Pitzer database

```
SOLUTION_MASTER_SPECIES

Al      Al+3  0.0   Al          26.9815

SOLUTION_SPECIES

Al+3 = Al+3
   log_k 0.0
   -gamma     9.0   0.0
   -dw   0.559e-9

#aqueous speciesAl+3 + H2O = AlOH+2 + H+
   log_k -5.0
   delta_h 11.49    kcal
   -analytic  -38.253 0.0      -656.27 14.327
Al+3 + 2 H2O = Al(OH)2+ + 2 H+
   log_k -10.1
   delta_h 26.90    kcal
   -analytic  88.50 0.0   -9391.6 -27.121
Al+3 + 3 H2O = Al(OH)3 + 3 H+
   log_k -16.9
   delta_h 39.89    kcal
   -analytic  226.374 0.0      -18247.8   -73.597
Al+3 + 4 H2O = Al(OH)4- + 4 H+
   log_k -22.7
   delta_h 42.30    kcal
   -analytic  51.578     0.0   -11168.9   -14.865

PHASES
Ettringite
   Ca6(Al(OH)6)2(SO4)3:26 H2O + 12 H+ = 2 Al+3 + 3 SO4-2 + 6 Ca+2
+ 38 H2O
   log_k           62.5362
   -delta_H   -382.451   kJ/mol     # Calculated enthalpy of
reaction Ettringite
#  Enthalpy of formation:      -4193 kcal/mol
        -analytic -1.0576e+003 -1.1585e-001 5.9580e+004
3.8585e+002 1.0121e+003
#       -Range:  0-200
```

2. Manuscript for model validation

```
DATABASE PITZER.DAT

SOLUTION 1
-units mmol/L
pH 7
S(6) 97
Na 194
END

PHASES
        Fix_H+
        H+ = H+
        log_k  0.0
END

USE SOLUTION 1
EQUILIBRIUM_PHASES 1
Gypsum 0 0
REACTION 1
CaCl2 1
1.94e-01
REACTION_TEMPERATURE 1
23
SAVE SOLUTION 2
END

USE SOLUTION 2
EQUILIBRIUM_PHASES 2
Ettringite 0 0
Fix_H+ -10.9 NaOH 1.0
REACTION 2
Ca(OH)2 1.13e-02
NaAlO2 7.57e-03
REACTION_TEMPERATURE 1
END
```

3. Input data of sulphate removal improvement using ettringite precipitation

$Ca:SO_4$	Concentration (mol/L)		
	$CaCl_2$	$Ca(OH)_2$	$NaAlO_2$
0.9	0.0937	0.0332	0.0223
0.92	0.0958	0.0320	0.0214
0.94	0.0979	0.0307	0.0206
0.96	0.0999	0.0296	0.0198
0.98	0.1020	0.0285	0.0191
1	0.1041	0.0275	0.0184
1.02	0.1062	0.0265	0.0178
1.04	0.1083	0.0256	0.0171
1.06	0.1104	0.0247	0.0166
1.08	0.1124	0.0239	0.0160
1.1	0.1145	0.0228	0.0152
1.12	0.1166	0.0221	0.0148
1.14	0.1187	0.0214	0.0143
1.16	0.1208	0.0208	0.0139
1.18	0.1228	0.0202	0.0135
1.2	0.1249	0.0196	0.0132
1.22	0.1270	0.0191	0.0128
1.24	0.1291	0.0186	0.0125
1.26	0.1312	0.0182	0.0122
1.28	0.1333	0.0178	0.0119
1.3	0.1353	0.0174	0.0116

4. Manuscript sulphate removal improvement by ettringite precipitation

```
DATABASE PITZER.DAT

SOLUTION 1
-units mmol/L
pH 8
S(6) 104
Na 208
END

USE SOLUTION 1
EQUILIBRIUM_PHASES 1
Gypsum 0 0
REACTION 1
CaCl2:2H2O 1
1.35e-01 #input based on lattice ion ratio between calcium and
sulphate in stage 1
REACTION_TEMPERATURE 1
23
SAVE SOLUTION 2
END

USE SOLUTION 2
EQUILIBRIUM_PHASES 2
Ettringite 0 0
REACTION 2
Ca(OH)2 1.74e-02 #input based on remaining sulphate in stage 1
(100% of sulphate)
NaAlO2 1.74e-02 #input based on remaining sulphate in stage 1
(67% of sulphate)
REACTION_TEMPERATURE 1
END
```

5. Input data for sulphate removal in IEX brine by ettringite precipitation

Composition/Parameter	Value
Initial pH	8.8
Working temperature	23°C
SO_4^{2-}	23.63 mmol/L (2.279 g/L)
Na	259.7 mmol/L (5.971 g/L)
Cl^-	165.9 mmol/L (5.879 g/L)
Ca:SO_4 (Stage 1)	1 and 1.3
$CaCl_2$ (Stage 2)	100%
$NaAlO_2$ (Stage 2)	67%
Final pH	8.8-10.5

6. Manuscript sulphate removal in IEX brine by ettringite precipitation

```
DATABASE PITZER.DAT

SOLUTION 1
-units mmol/L
pH 8.8
S(6) 23.63
Na 259.7
Cl 165.9
END

PHASES
        Fix_H+
        H+ = H+
        log_k  0.0
END

USE SOLUTION 1
EQUILIBRIUM_PHASES 1
Gypsum 0 0
REACTION 1
CaCl2:2H2O 1
7.09e-02 #input based on desired lattice ion ratio
REACTION_TEMPERATURE 1
23
SAVE SOLUTION 2
END

USE SOLUTION 2
EQUILIBRIUM_PHASES 2
Ettringite 0 0
Fix_H+ -12 NaOH 1.0 #input based on desired final pH
REACTION 2
CaCl2 1.563e-02 #input based on desired concentration
NaAlO2 1.05e-02 #input based on remaining sulphate (67%)
REACTION_TEMPERATURE 1
END
```

Appendix E. Cost estimation data

1. Cost estimation for integrated sulphate removal treatment method

   a) Experimental data for integrated sulphate removal treatment method

Component	Unit	Value
Chemical precipitation		
Sulphate concentration	mol/L	0.024
	g/L	2.27
Barium concentration	mol/L	0.024
	g/L	5.77
Brine volume	m^3	1
	L	1000
Barium consumption	g	5772
Stirring machine energy	kWh	4
Mixing duration	min	10
Membrane filtration		
Flux	L/m^2h	30
Pressure	Bar	3
Cross flow velocity	m/s	1.3
Pump energy	kWh	0.55
Flowmeter energy	kWh	0.006
Filtration duration	hours	5.6
Membrane cleaning		
Sodium hypochlorite	%	0.2
	mL/L	12.5
Solution volume	L	0.3

   b) Cost calculation for integrated sulphate removal treatment method

Material	Unit cost (€)	Unit	Amount	Unit	Total cost (€)	Source
Chemical precipitation						
Barium salt	30.20	/kg	5.77	kg	174.32	https://www.rightpricechemicals.com/buy-barium-chloride-dihydrate-reagent-acs.html
Electricity	0.23	/kWh	0.67	kWh	0.15	https://www.dutchnews.nl/features/2019/05/after-a-e30-rise-in-january-dutch-energy-prices-among-highest-in-eu/
Ceramic NF						
Electricity	0.23	/kWh	3.11	kWh	0.72	https://www.dutchnews.nl/features/2019/05/after-a-e30-rise-in-january-dutch-energy-prices-among-highest-in-eu/
Membrane cleaning						
Sodium hypochlorite	2.02	/L	0.00375	L	0.01	https://www.rightpricechemicals.com/buy-sodium-hypochlorite-12-5-percent-solution.html
TOTAL					**175.20**	

2. Cost estimation for ettringite precipitation treatment method

a) Experimental data for ettringite precipitation treatment method

Component	Unit	Value
Chemical precipitation – Stage 1		
Sulphate concentration	mol/L	0.024
	g/L	2.27
Calcium concentration	mol/L	0.031
	g/L	4.52
Brine volume	m^3	1
	L	1000
Barium consumption	g	4516
Stirring machine energy	kWh	4
Mixing duration	min	10
Chemical precipitation – Stage 2		
Sulphate concentration	mol/L	0.0066
	g/L	0.636
Calcium concentration	mol/L	0.0066
	g/L	0.73
Sodium aluminate ($NaAlO_2$) concentration	mol/L	0.004
	g/L	0.339
NaOH concentration	mol/L	0.011
	mL/L	0.21
Brine volume	m^3	1
	L	1000
Calcium consumption	g	734
$NaAlO_2$ consumption	g	339
NaOH consumption	mL	214
Stirring machine energy	kWh	4
Mixing duration	min	10
Membrane filtration		
Flux	L/m^2h	30
Pressure	Bar	3
Cross flow velocity	m/s	1.3
Pump energy	kWh	0.55
Flowmeter energy	kWh	0.006
Filtration duration	hours	5.6
Membrane cleaning		
Sodium hypochlorite	%	0.2
	mL/L	12.5
Solution volume	L	0.3

b) Cost calculation for ettringite precipitation treatment method

Material	Unit cost (€)	Unit	Amount	Unit	Total cost (€)	Source
Chemical precipitation						
Calcium salt Stage 1	50.26	/kg	10.42	kg	523.86	https://www.rightpricechemicals.com/buy-calcium-chloride-dihydrate-reagent-acs.html
Calcium salt Stage 2	50.89	/kg	1.73	kg	88.10	https://www.rightpricechemicals.com/buy-calcium-chloride-dihydrate-reagent-acs.html
$NaAlO_2$	23.2	/kg	0.86	Kg	19.91	https://www.sigmaaldrich.com/catalog/product/sial/13404?lang=en&region=NL
NaOH	4.91	/L	4.11	L	20.17	https://www.rightpricechemicals.com/sodium-hydroxide-0-1n-solution.html
Electricity	0.23	/kWh	1.33	kWh	0.31	https://www.dutchnews.nl/features/2019/05/after-a-e30-rise-in-january-dutch-energy-prices-among-highest-in-eu/
Ceramic NF						
Electricity	0.23	/kWh	3.11	kWh	0.72	https://www.dutchnews.nl/features/2019/05/after-a-e30-rise-in-january-dutch-energy-prices-among-highest-in-eu/
Membrane cleaning						
Sodium hypochlorite	2.02	/L	0.00375	L	0.01	https://www.rightpricechemicals.com/buy-sodium-hypochlorite-12-5-percent-solution.html
TOTAL					**653.08**	

Appendix F. Life cycle assessment data

1. Data inventory for integrated sulphate removal

Processes	Product		Extention		Source
	In	Out	In	Out	
Production of electricity	Fuel: 0.32 liter	Electricity: 1 kWh		NOx: 6.43 x 10^{-3} kg SO_2: 6.16 x 10^{-4} kg CO_2: 0.674 kg	Rentizelas & Georgakellos (2014)
Production of fuel		Fuel: 100 liter	Crude oil: 50 liter	SO_2: 2 kg CO_2" 10 kg	Cooper (2003)
Chemical precipitation	Electricity: 0.67 kWh Barium chloride: 8.25 kg	Supernatant: 1.43 m^3	IEX brine: 1.43 m^3		Calculation
Production of barium chloride	Electricity: 2.63 kWh Barium sulphide: 0.81 kg Hydrochloric acid: 0.35 kg	Barium chloride: 1 kg	Barite: 1.12 kg Carbon monoxide: 0.54 kg	Sulphur dioxide: 0.002 kg	Ecoinvent database
Productin of hydrochloric acid	Electricity: 0.33 kWh	Hydrochloric acid: 1 kg	Hydrogen: 0.027 kg Chlorine: 0.973 kg		Ecoinvent database
Ceramic nanofitration	Electricity: 3.11 kWh Supernatant: 1.43 m^3	Permeate: 1 m^3		Concentrate: 0.43 m^3	Calculation

2. Data inventory for ettringite precipitation

Processes	Product		Extention		Source
	In	Out	In	Out	
Production of electricity	Fuel: 0.32 liter	Electricity: 1 kWh		NOx: 6.43 x 10^{-3} kg SO_2: 6.16 x 10^{-4} kg CO_2: 0.674 kg	Rentizelas & Georgakellos (2014)
Production of fuel		Fuel: 100 liter	Crude oil: 50 liter	SO_2: 2 kg CO_2" 10 kg	Cooper (2003)
Calcium chloride addition	Electricity: 0.67 kWh Calcium chloride: 6.46 kg	Supernatan 1t: 1.43 m^3	IEX brine: 1.43 m^3		Calculation
Production of calcium chloride	Electricity: 0.025 kWh	Calcium chloride: 1 kg	Calcium carbonate: 1.2 kg Sodium chloride: 1.5 kg	Heat: 0.09 MJ Ammonia: 0.001 kg	Ecoinvent database
Ettringite precipitation	Electricity: 0.67 kWh Supernatant 1: 1.43 m^3 Calcium chloride: 1.05 kg Sodium aluminate: 0.48 kg Sodium hydroxide: 0.31 kg	Supernatant 2: 1 kg			Calciulation
Production of sodium alumiante	Sodium hydroxide: 0.49 kg Aluminium hydroxide: 0.95 kg	Sodium aluminate: 1 kg			Calculation
Production of aluminium hydroxide	Electricity: 0.068 kWh Sodium hydroxide: 0.052 kg Heat: 1.71 MJ	Aluminium hydroxide: 1 kg	Aluminium: 0.39 kg	Sulphur dioxide: 1.63 x 10^{-3} kg Carbon dioxide: 0.06 kg	Ecoinvent database
Ceramic nanofitration	Electricity: 3.11 kWh Supernatan 2t: 1.43 m^3	Permeate: 1 m^3		Concentrate: 0.43 m^3	Calculation

3. Result of emission in LCA of integrated sulphate removal

Emission	Process	Value	Contribution
Nitrogen oxide	Production of electricity	0.17 kg	100%
Sulphur dioxide	Production of electricity	0.0163 kg	8%
	Production of fuel	0.169 kg	84%
	Production of barium chloride	0.0165 kg	8%
Carbon dioxide	Production of electricity	17.8 kg	95%
	Production of fuel	0.846 kg	5%
Crude oil	Production of fuel	-4.23 liter	100%
IEX brine	Chemical precipitation	-1.43 m^3	100%
Barite	Production of barium chloride	-9.24 kg	100%
Carbon monoxide	Production of barium chloride	-4.46 kg	100%
Hydrogen	Production of hydrochloric acid	-0.078 kg	100%
Chlorine	Production of hydrochloric acid	-2.81 kg	100%
NF concentrate	Ceramic NF	0.43 m^3	100%

4. Result of emission in LCA of ettringite precipitation

Emission	Process	Value	Contribution
Nitrogen oxide	Production of electricity	0.0319 kg	68%
	Production of sodium hydroxide	0.0151 kg	32%
Sulphur dioxide	Production of electricity	0.00306 kg	8%
	Production of fuel	0.0318 kg	86%
	Production of aluminum hydroxide	0.0019 kg	5%
Carbon dioxide	Production of electricity	3.35 kg	28%
	Production of fuel	0.159 kg	1%
	Production of sodium hydroxide	8.23 kg	70%
Crude oil	Production of fuel	-0.794 liter	90%
	Production of sodium hydroxide	-0.0922 liter	10%
IEX brine	Chemical precipitation	-1.43 m^3	100%
Heat	Production of calcium chloride	1.57 MJ	100%
Ammonia	Production of calcium chloride	0.0174 kg	100%
NF concentrate	Ceramic NF	0.43 m^3	100%
Aluminum	Production of aluminum hydroxide	-0.456 kg	100%
Calcium carbonate	Production of calcium chloride	-20.9 kg	100%
Sodium chloride	Production of calcium chloride	-26.1 kg	100%